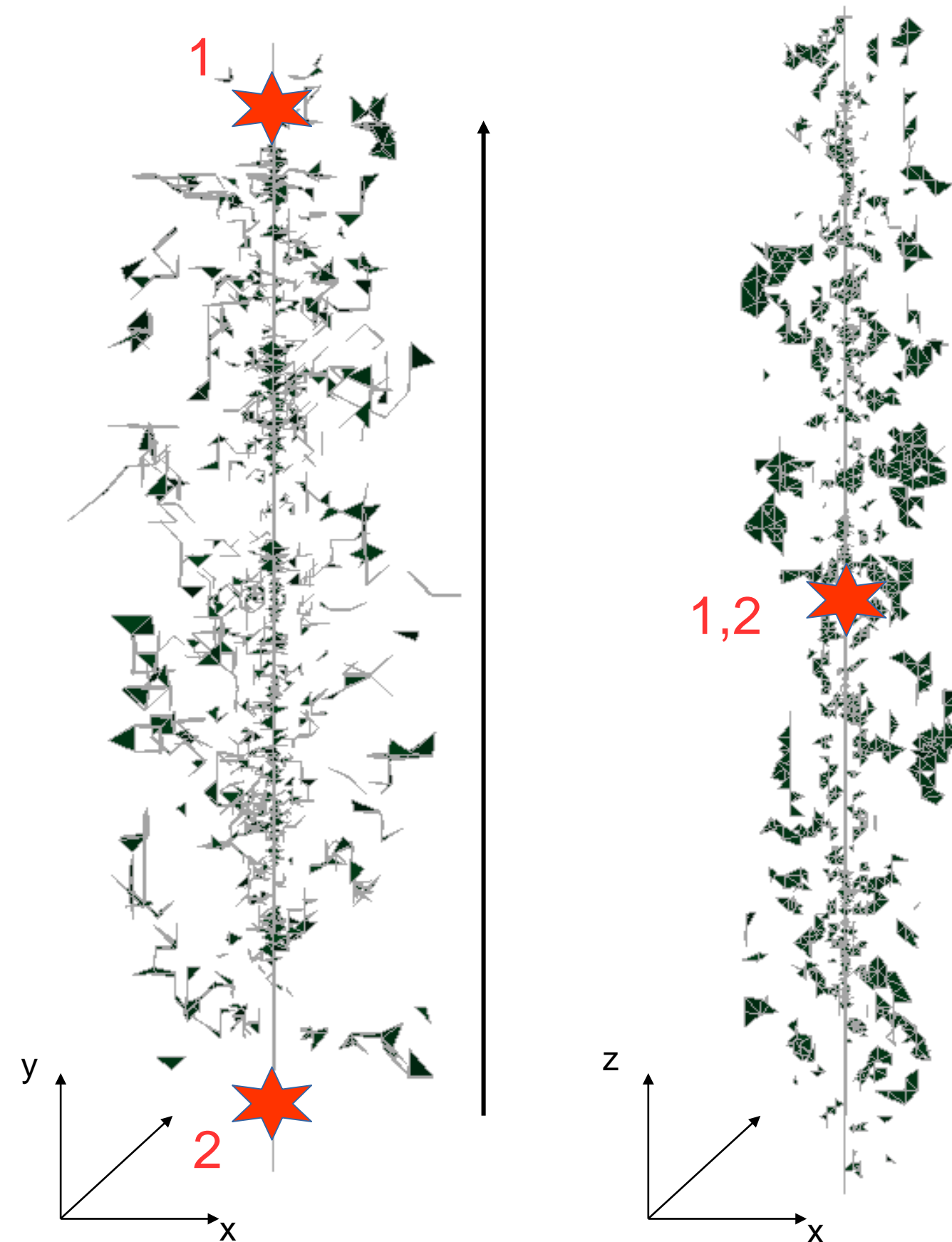


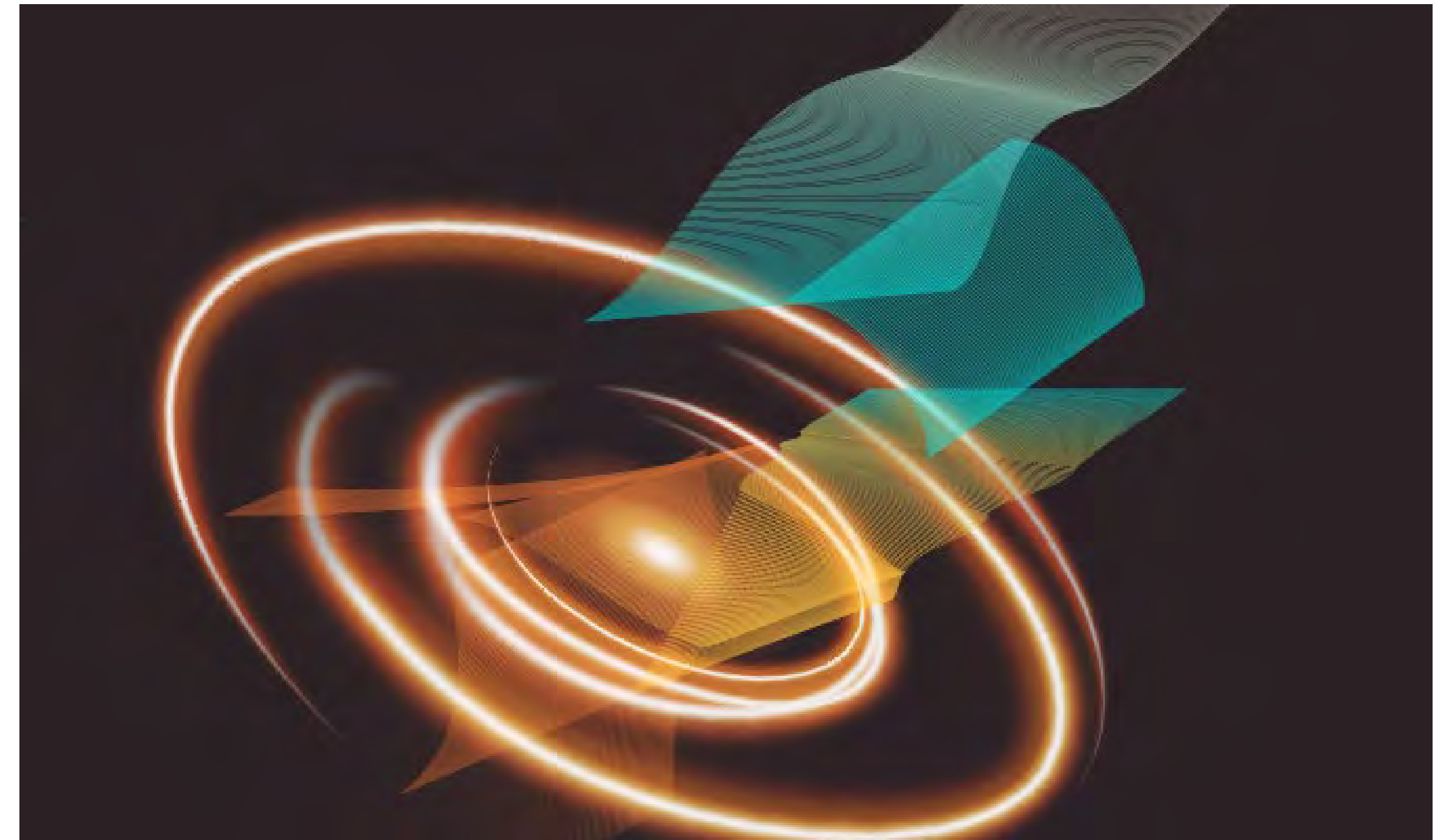
Multi-physics earthquake simulations on complex fault networks across scales

Alice-Agnes Gabriel

T. Ulrich, S. Wollherr, S. Anger, J. A. Lopez-Comino, K. Palgunadi, M. Galis, P. M. Mai



Statistical fracture network for dynamic rupture simulations from physics-based Markov Chain Monte Carlo approach (Sebastian Anger, POSTER P2-10 3320)

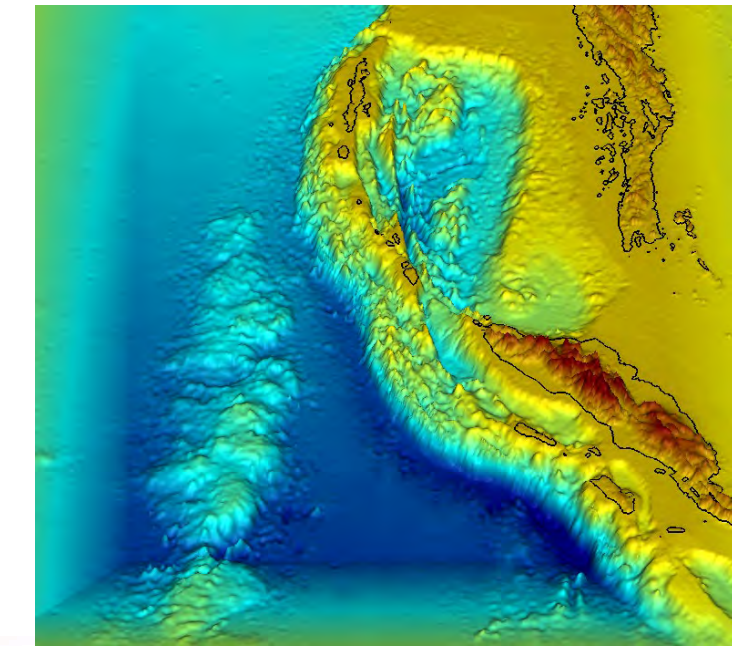
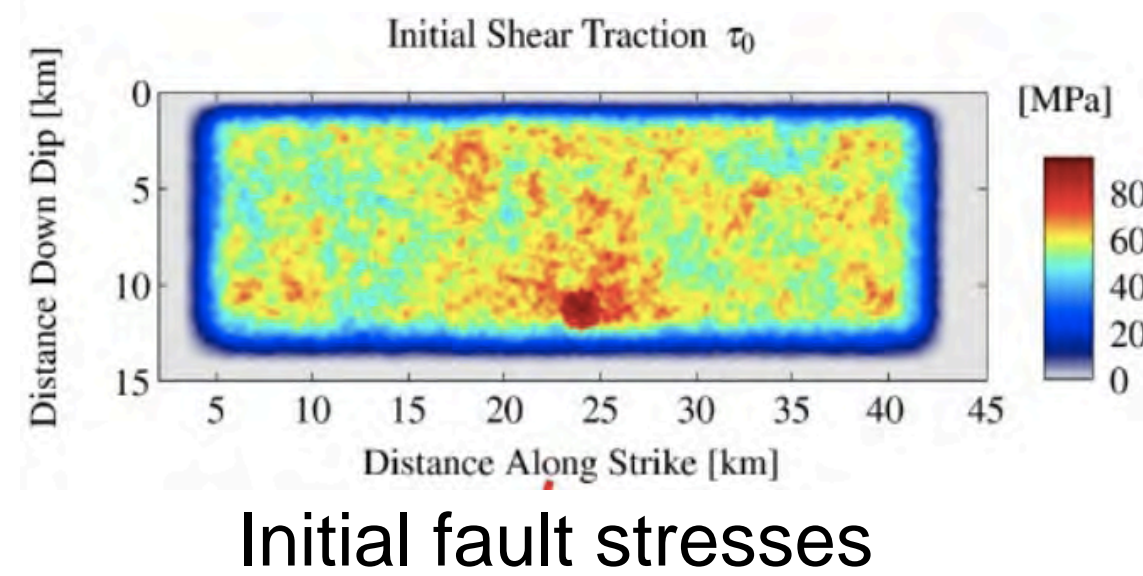


Artist impression of our complex dynamic rupture scenario of the 2016, Kaikōura Earthquake (Ulrich et al., Nature Comm. 2019)

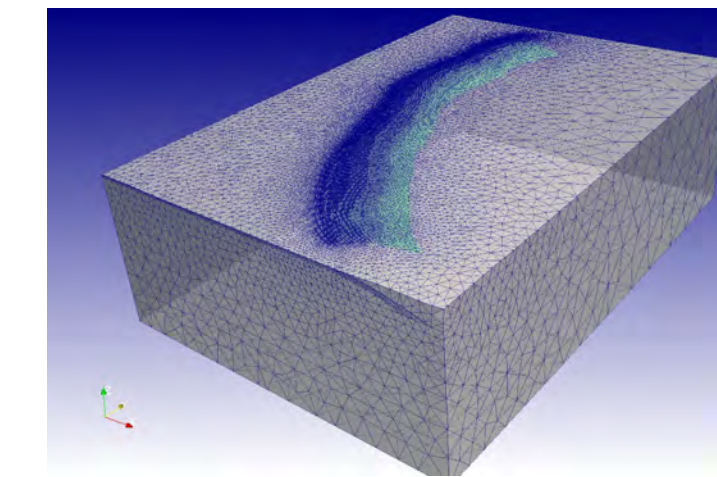
Dynamic rupture earthquake simulation

- **Physics-based approach:** Solving for spontaneous dynamic earthquake rupture as non-linear interaction of frictional failure and seismic wave propagation

“Input”



Geological structure



CAD & mesh generation



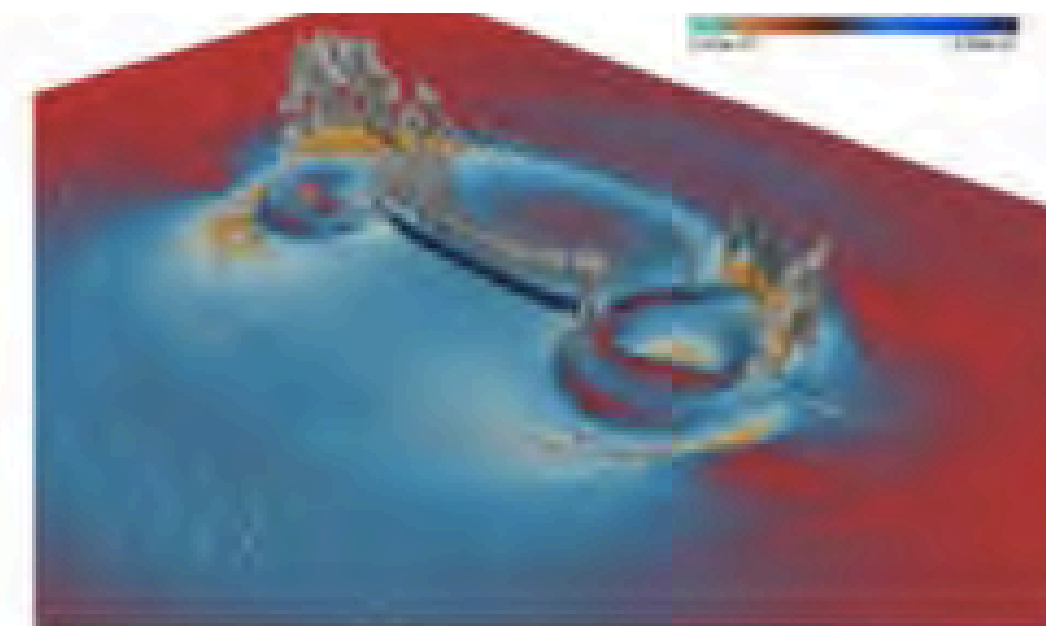
Failure Criterion

SOLVER

Ground motion

Synthetic seismograms

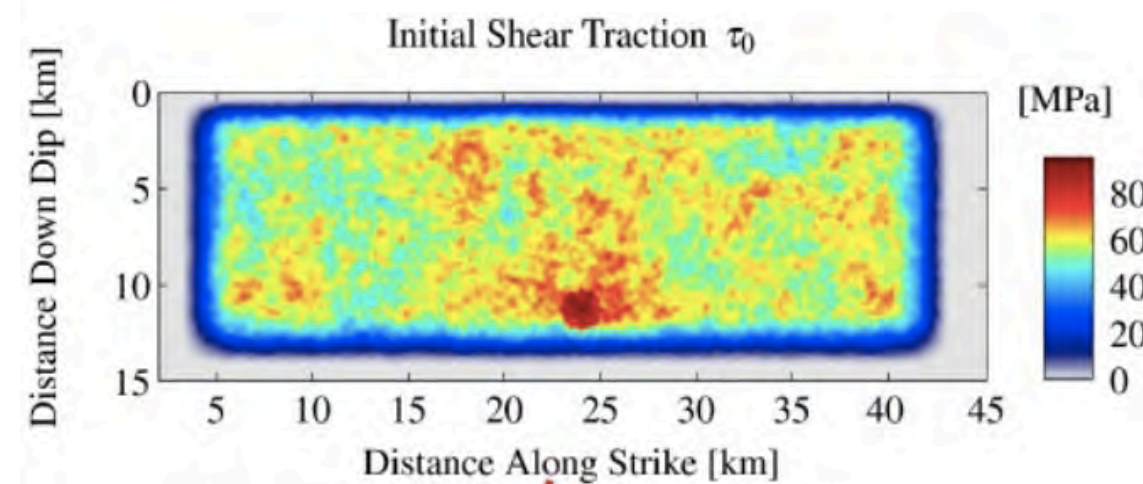
“Output”



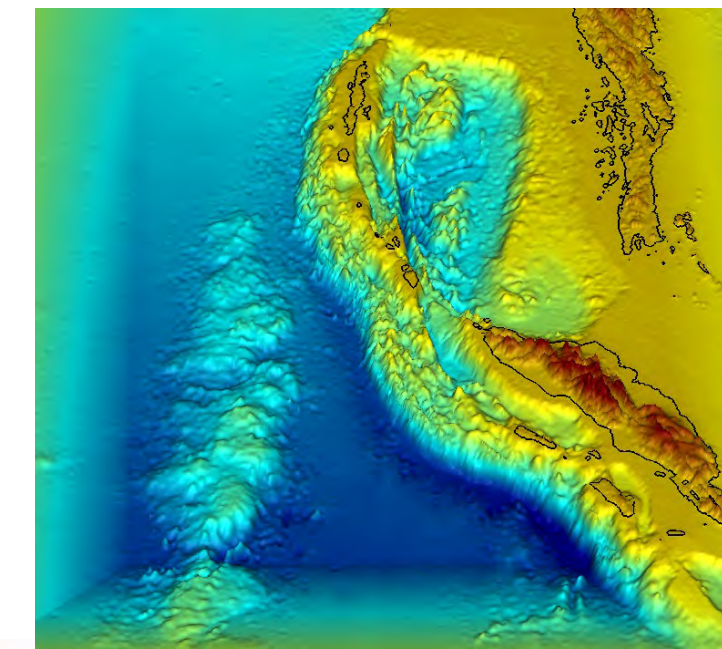
Dynamic rupture earthquake simulation

- **Physics-based approach:** Solving for spontaneous dynamic earthquake rupture as non-linear interaction of frictional failure and seismic wave propagation

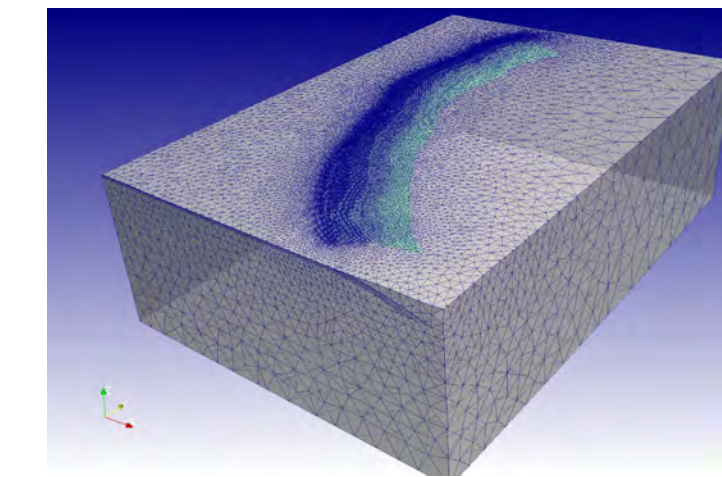
“Input”



Initial fault stresses



Geological structure



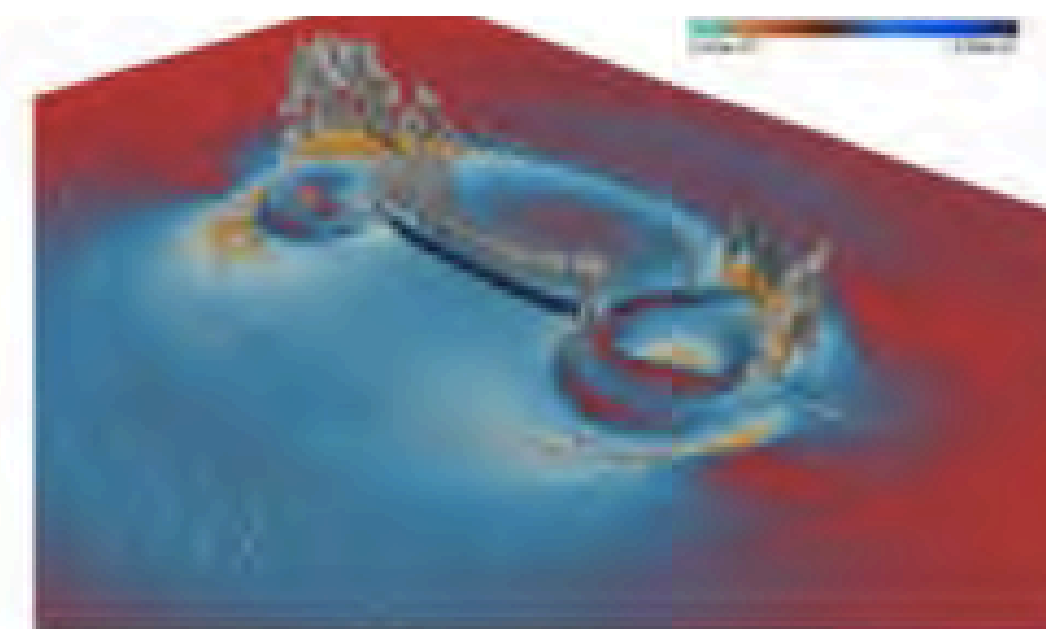
CAD & mesh generation



Failure Criterion

SOLVER

Ground motion



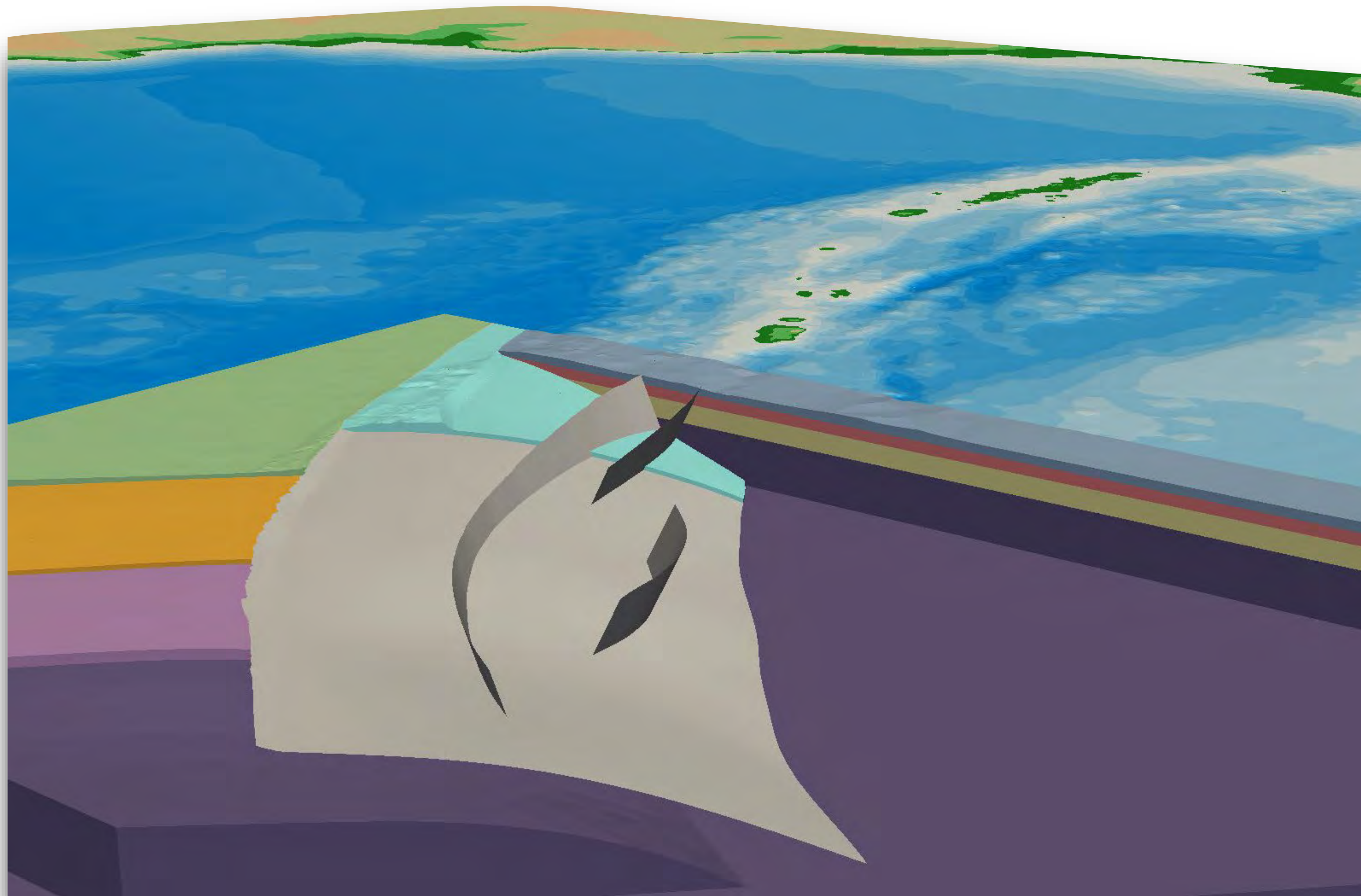
Synthetic seismograms



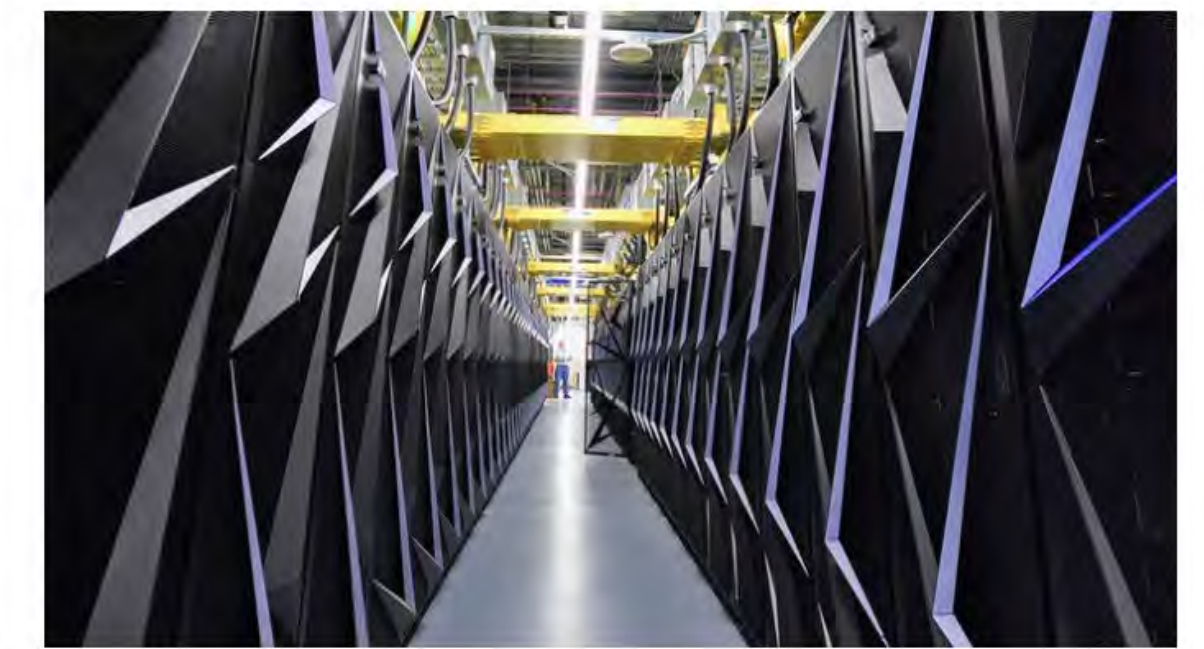
“Output”

- **Requires:** Integrative view of multi-scale physics of **rock fracture**, **dynamic rupture propagation**, and emanated **seismic radiation** in complex 3D environments
- **Enables:** In-scale analysis of **which physical processes are dominant and relevant at a given spatio-temporal scale** (and in real earthquakes)?

Large-scale dynamic rupture earthquake scenarios shedding light on the physical conditions that allow rupture cascades on complex fault systems



Computational model for **large-scale megathrust, splay faults and tsunami scenarios of the 2004 Sumatra-Andaman event** (Uphoff et al., Best Paper, SC 2017). **High-performance computing empowered simulations**, 1500 km of fault zones and 2,5 Hz wave propagation, 111 billion Degrees of Freedom, 3,300,000 time steps



Nearly complete, the 200-petaflop Summit will be a prelude to A21, the first U.S. exaflop computer. LYNN FREENY/DEPARTMENT OF ENERGY VIA FLICKR

Racing to match China's growing computer power, U.S. outlines design for exascale computer

By **Robert F. Service** | Feb. 7, 2018, 11:00 AM

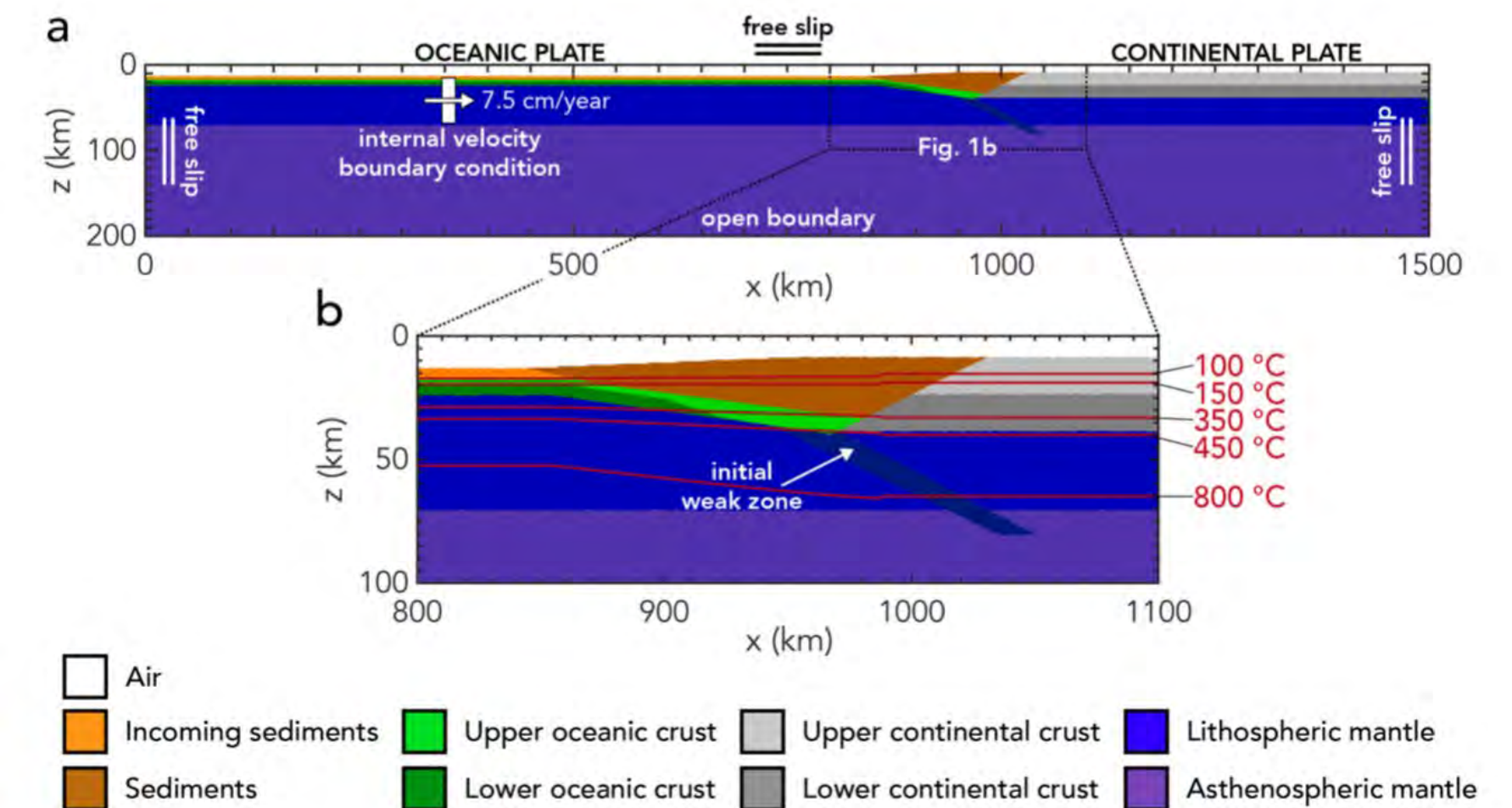


Figure 1. Complete (a) and zoomed (b) model setup of the geodynamic seismic cycle model with lithology (in colour, see key), isotherms (red), and boundary conditions (white).

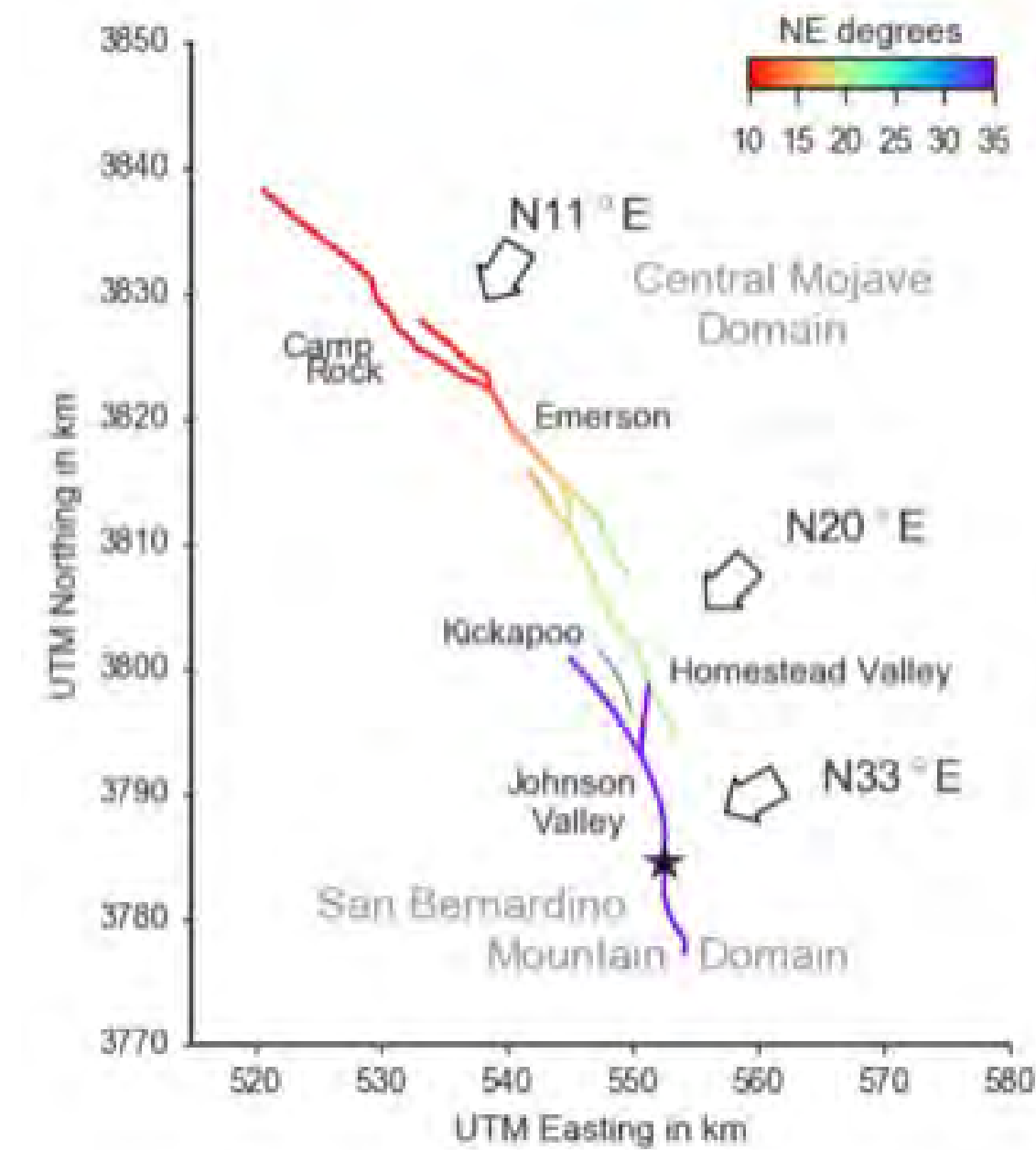
Coupling with geodynamic thermo-mechanical models to provide constraints on fault rheology and the state of stress for subduction zones, Van Zelst et al., 2019, [eartharxiv.org/f6ng5](https://arxiv.org/abs/1902.08055)

The 1992 Mw 7.3 Landers earthquake

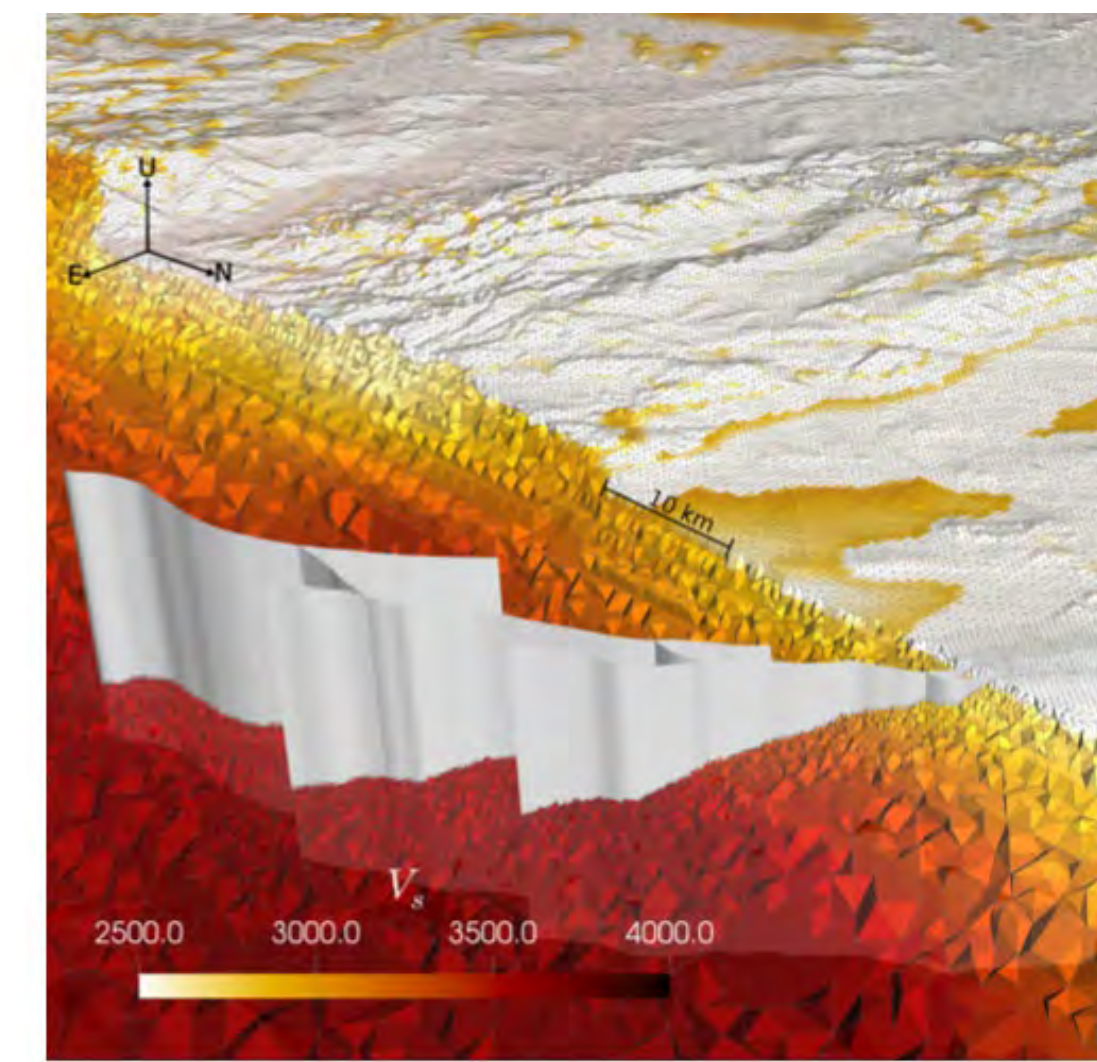
“reloaded” (Wollherr et al., preprint [doi:10.31223/osf.io/kh6j9](https://doi.org/10.31223/osf.io/kh6j9))

Geometry (fault morphology) matters!

- **Large-scale dynamic rupture simulation** aiming to understand on “natural-scale” which of the earthquake source “complexities” provides **first order influences**
- **A high degree of realism** leads in turn to a **high degree of uniqueness**



Mapped fault traces (Fleming et al., 1998) and assumed orientation of maximum compressional principal stress.



Computational model feat. 3D Community Velocity Model-Harvard (CVM-H, Shaw et al., 2015). Local refinement is applied in the vicinity of the faults (200 m) and the Earth's topography (500 m) (Farr et al., 2007)

The 1992 Mw 7.3 Landers earthquake

“reloaded” (Wollherr et al., preprint [doi:10.31223/osf.io/kh6j9](https://doi.org/10.31223/osf.io/kh6j9))

Geometry (fault morphology) matters!

- Large-scale dynamic rupture simulation aiming to understand on “natural-scale” which of the earthquake source “complexities” provides **first order influences**
- A high degree of realism leads in turn to a high degree of uniqueness

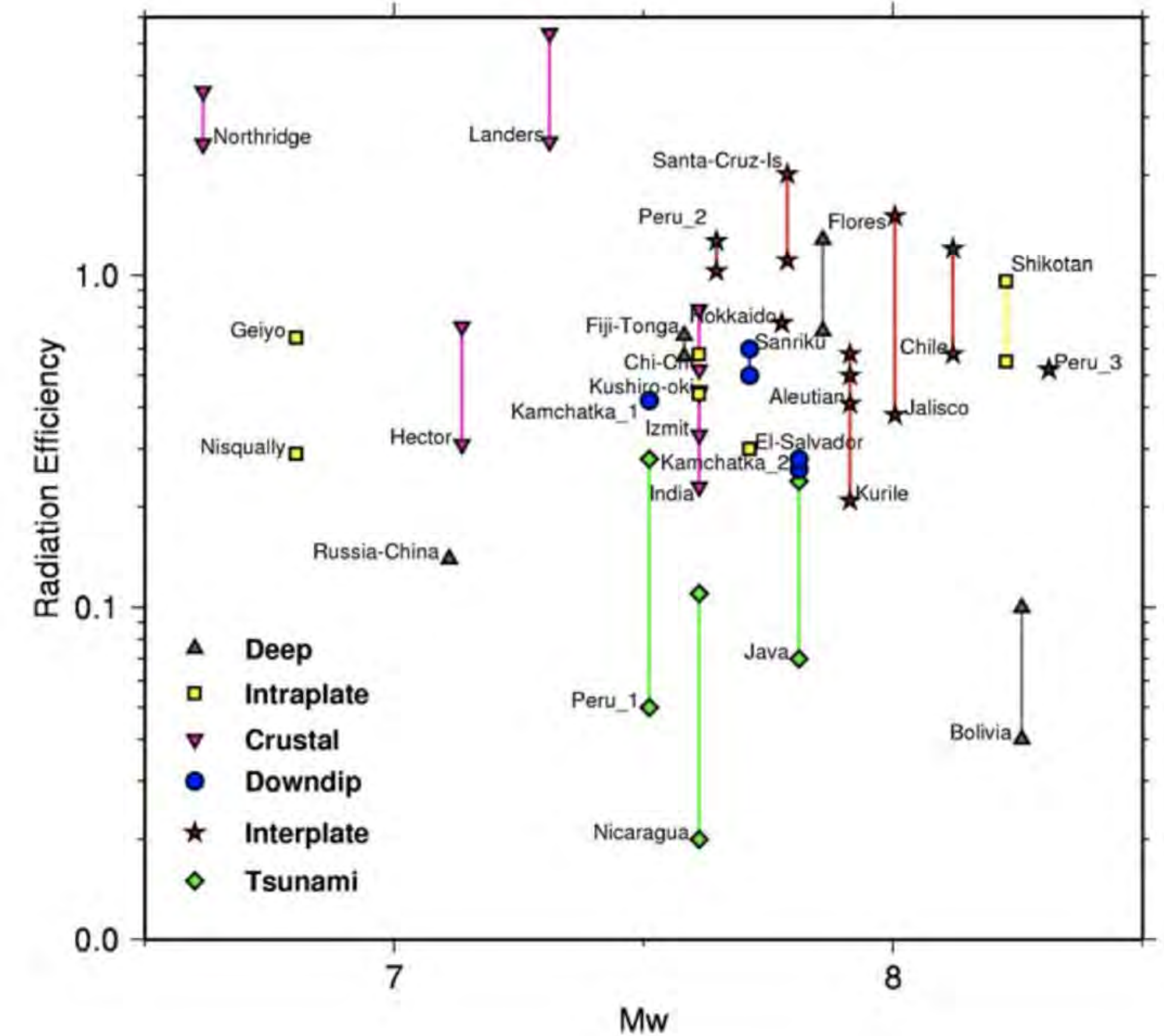


Figure 4. Radiation efficiency $\eta_R = E_R / (E_R + E_G)$ as a function of M_w . The different symbols show different types of earthquakes as described in the legend. Most

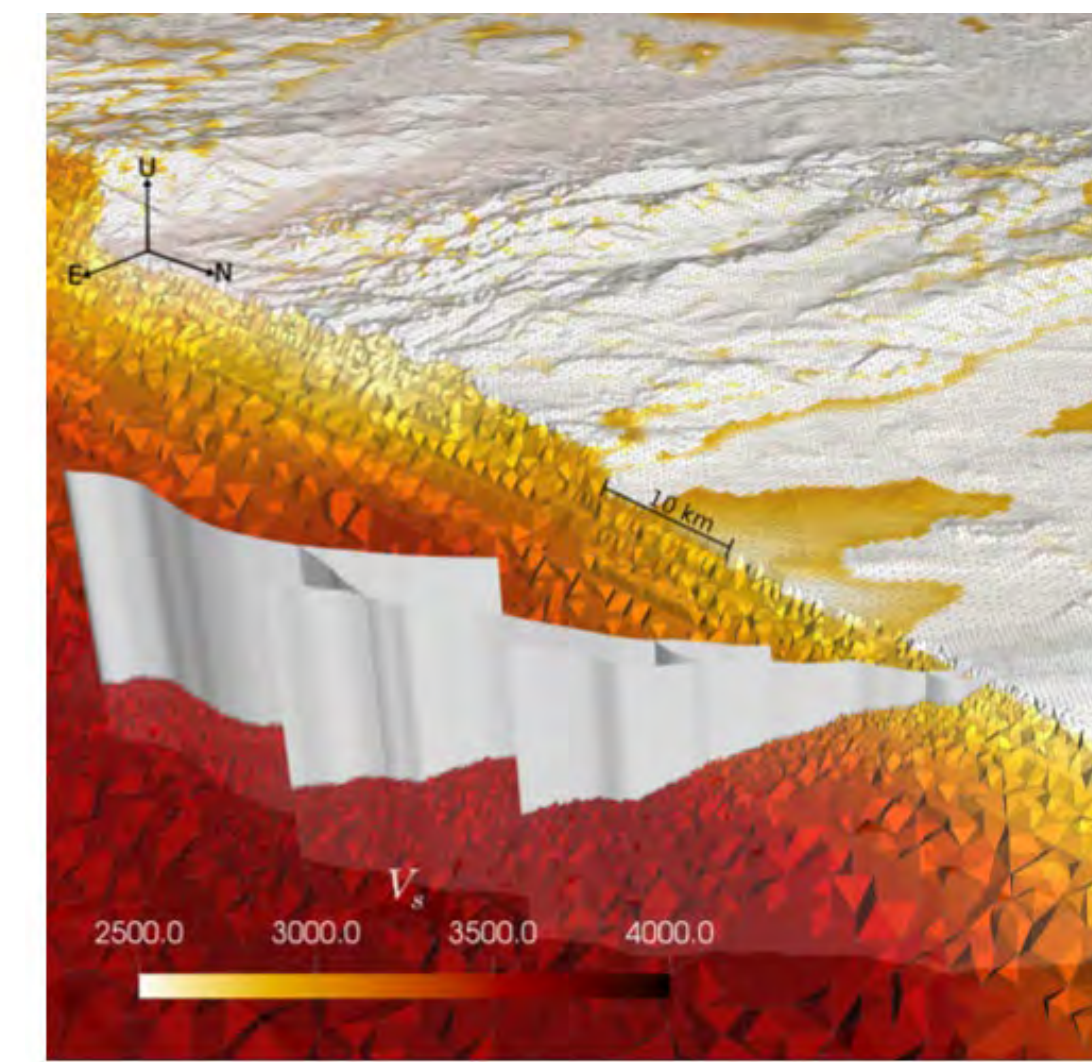
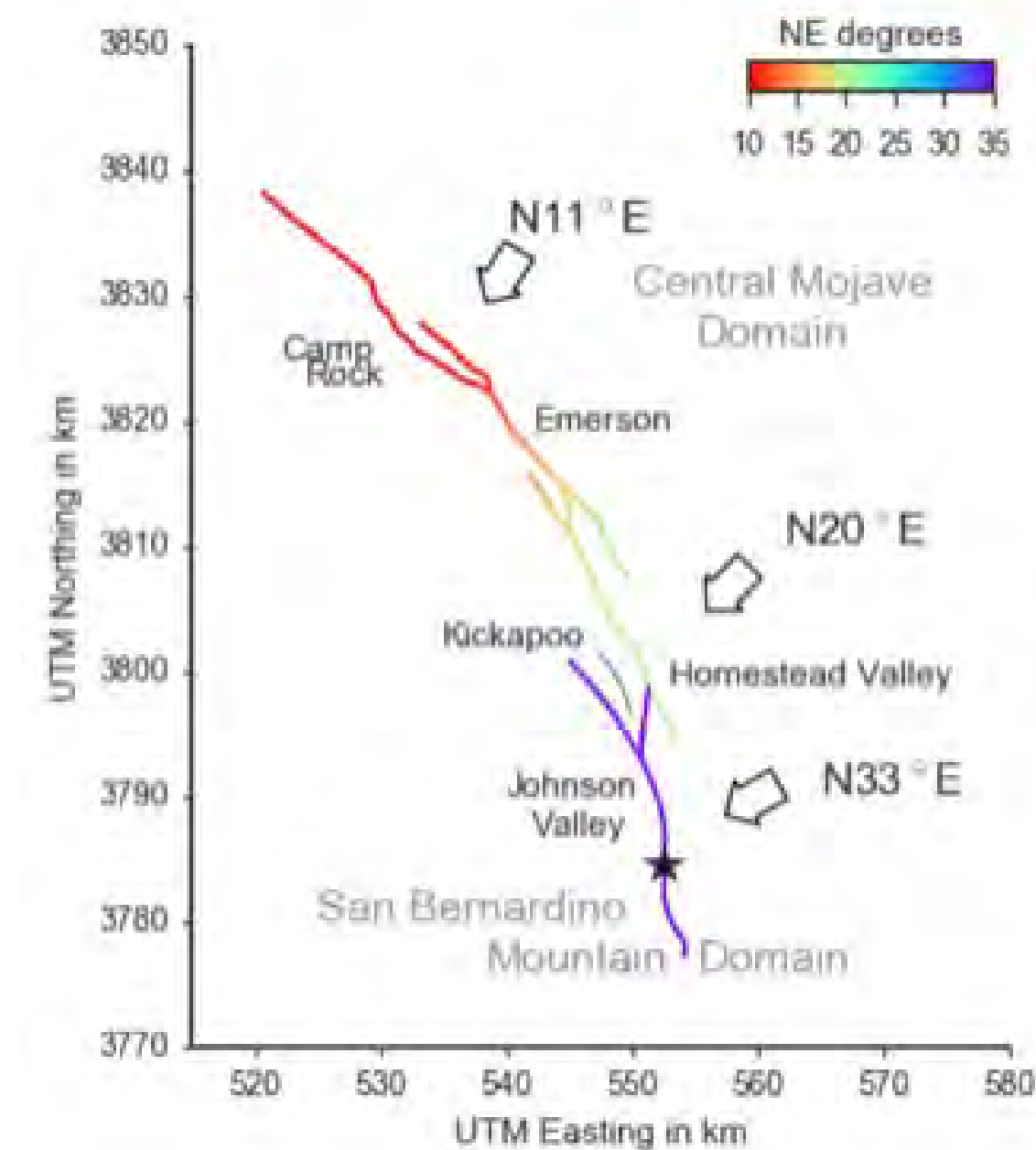
Kanamori, Hiroo. "The diversity of the physics of earthquakes." *Proceedings of the Japan Academy, Series B* 80.7 (2004): 297-316.

The 1992 Mw 7.3 Landers earthquake

“reloaded” (Wollherr et al., preprint [doi:10.31223/osf.io/kh6j9](https://doi.org/10.31223/osf.io/kh6j9))

Geometry (fault morphology) matters!

- Large-scale dynamic rupture simulation aiming to understand on “natural-scale” which of the earthquake source “complexities” provides first order influences
- A high degree of realism leads in turn to a high degree of uniqueness
- **Sustained** dynamic rupture interconnecting fault segments **constraints pre-stress and fault strength**
- Complex rupture transfers as combination of direct branching and dynamic triggering over **large distances** due to simultaneous failure of segments and **affected by viscoelastic wave attenuation**



failure on-fault coupled to seismic wave propagation accounting for off-fault plasticity

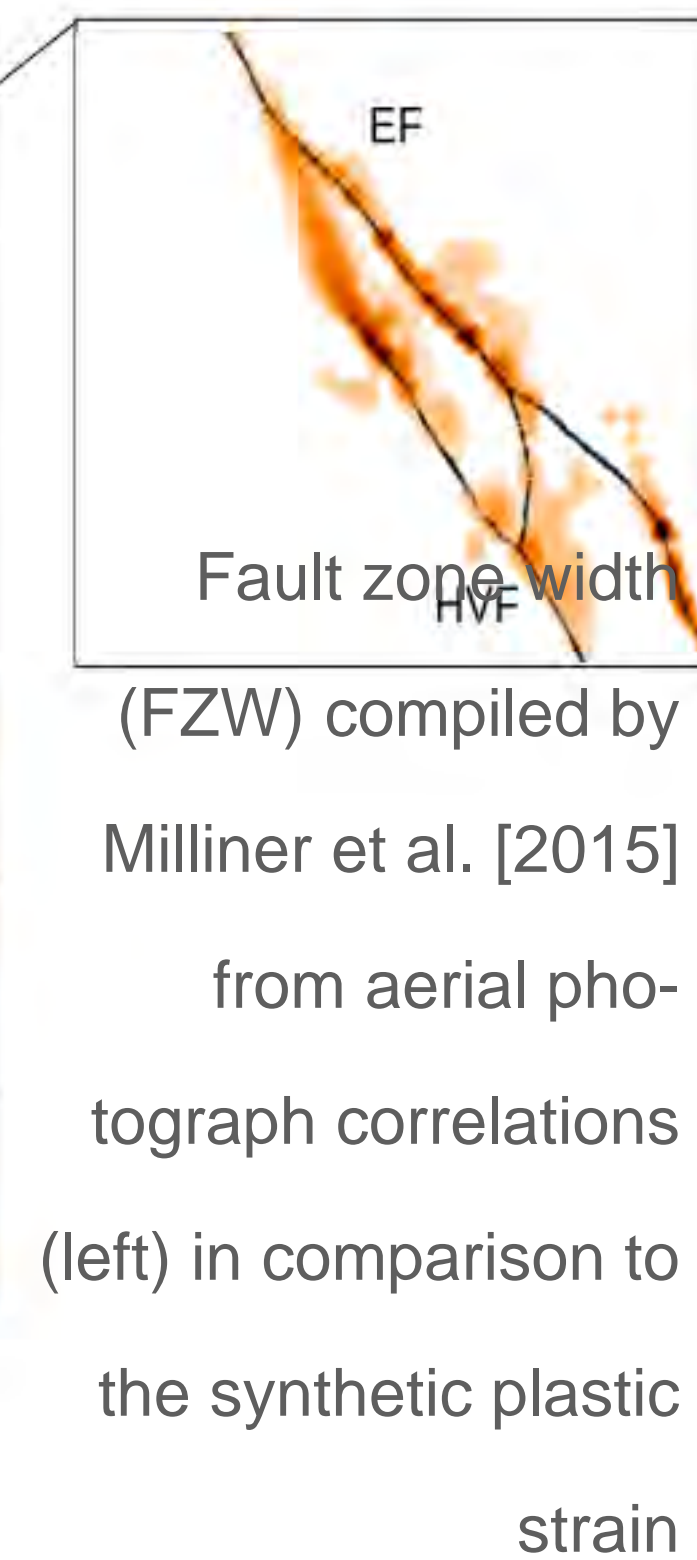
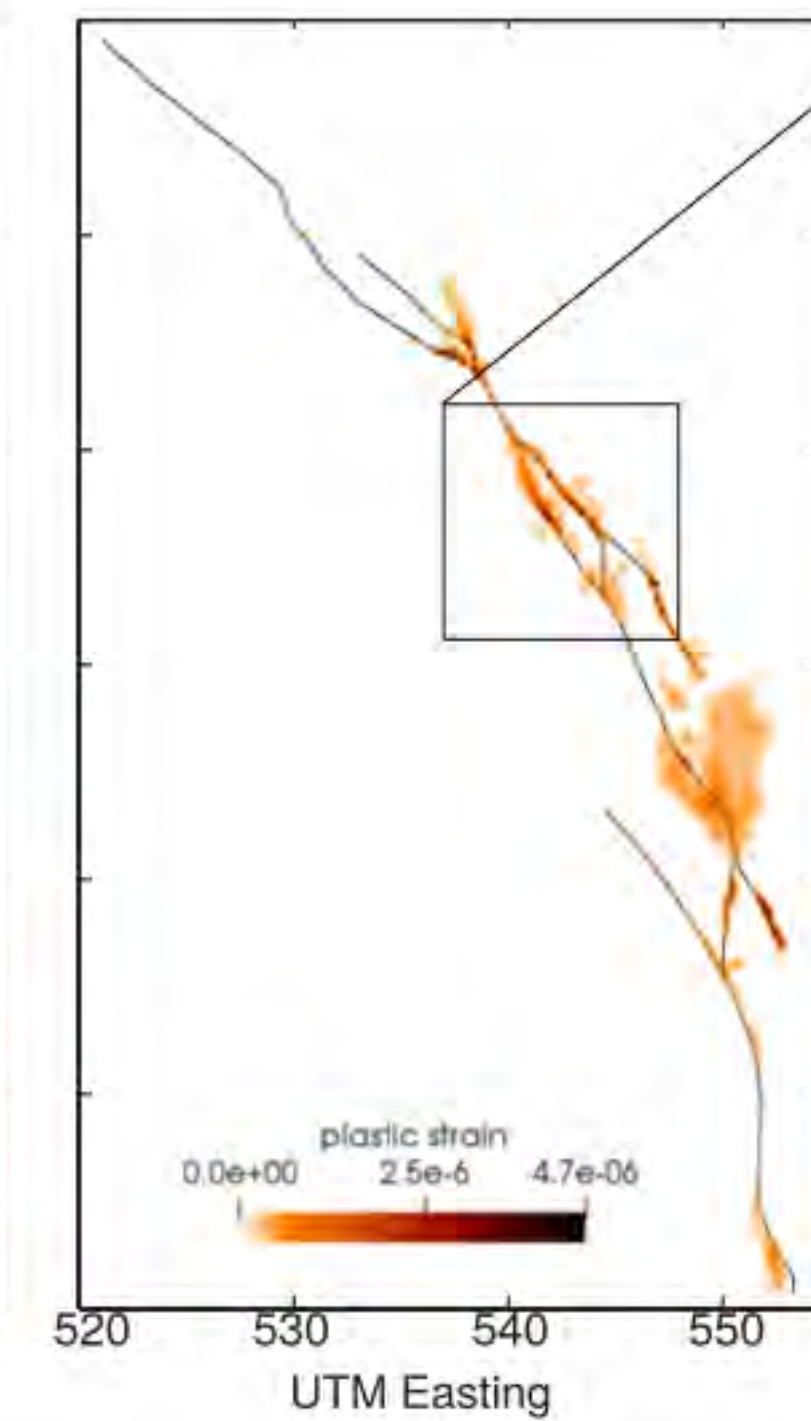
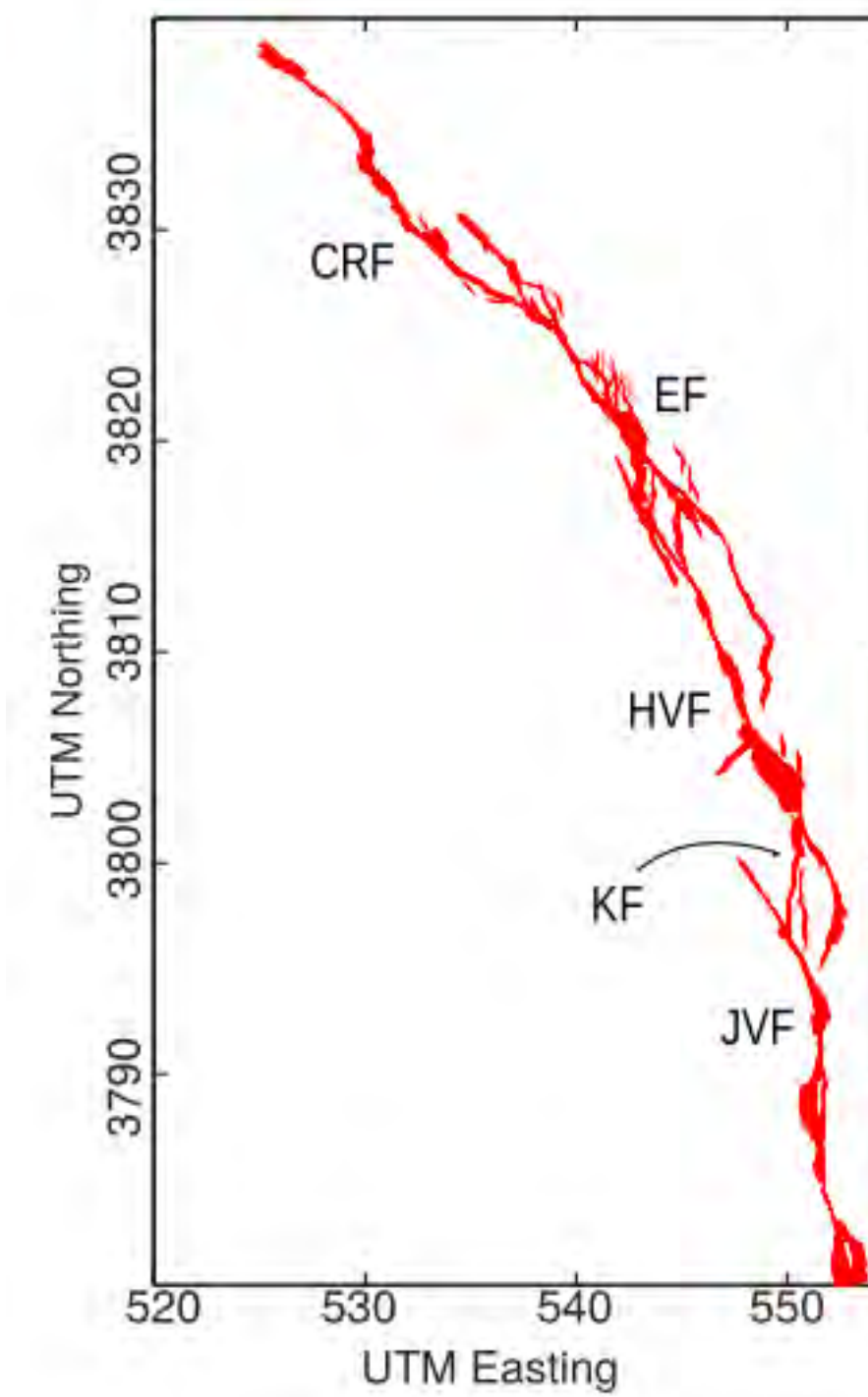
(Wollherr et al., 2019) and (Wollherr et al., 2019) (Wollherr et al., 2019)

The 1992 Mw 7.3 Landers earthquake

“reloaded” (Wollherr et al., preprint [doi:10.31223/osf.io/kh6j9](https://doi.org/10.31223/osf.io/kh6j9))

Multi-physics, such as off-fault plasticity, matters!

- **Drastic increase of off-fault deformation in geometrically complex fault regions** enhancing geometric barriers, hindering rupture transfers and matching newly available mapping
- **Strain localisation** forming non-prescribed ‘faults’

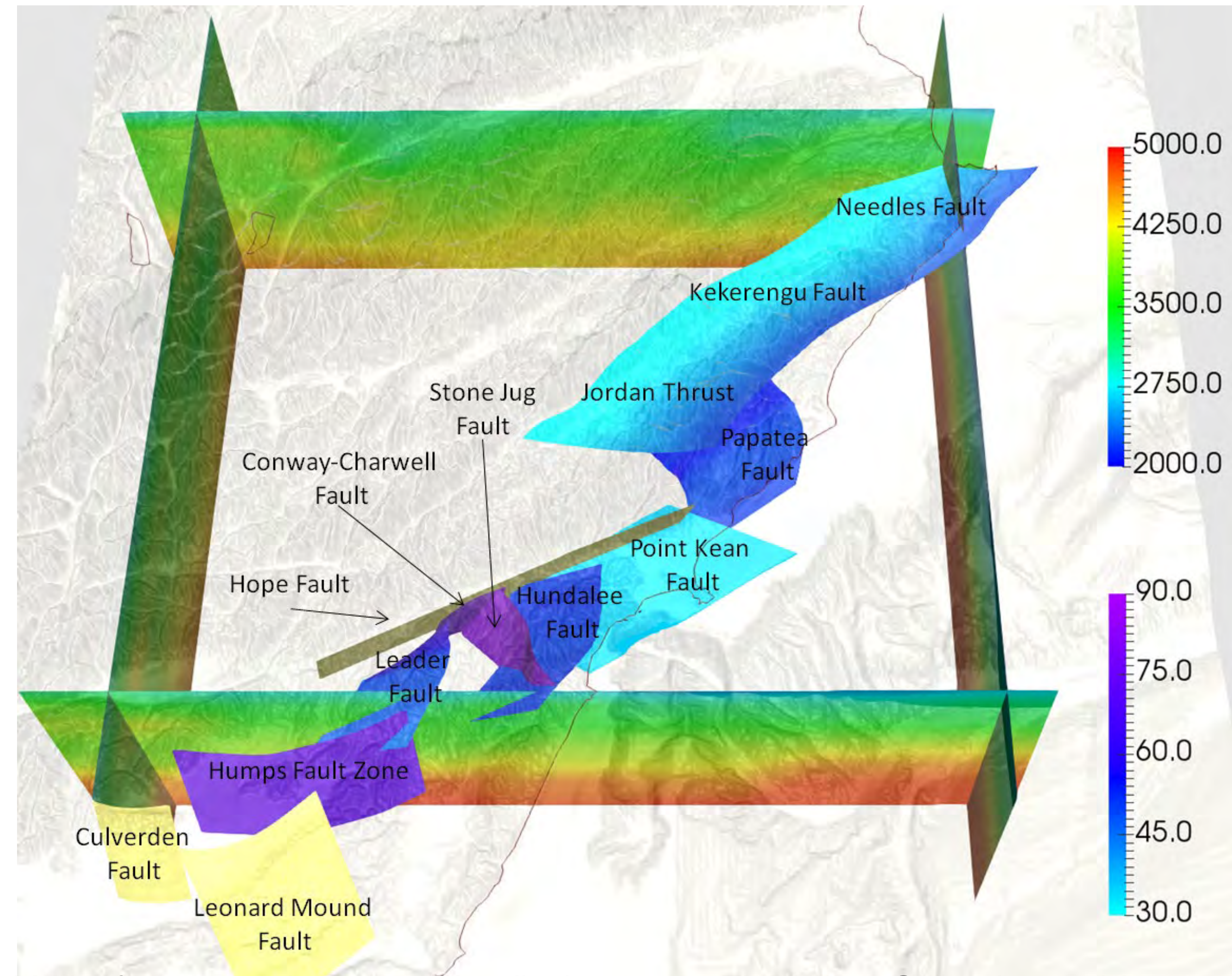


The 2016 Mw 7.8 Kaikōura earthquake - a rupture cascade on weak crustal faults

(Ulrich et al., 2019, <https://eartharxiv.org/aed4b/>)

→ Mechanical viability of a complex rupture cascade linking the crustal fault system only when operating at low apparent friction

- Rupture propagation across **highly segmented fault system with diverse orientations and faulting mechanisms** (strike-slip, thrusting)
- Most of the modeled faults are relatively **well oriented with respect to the regional stress field**

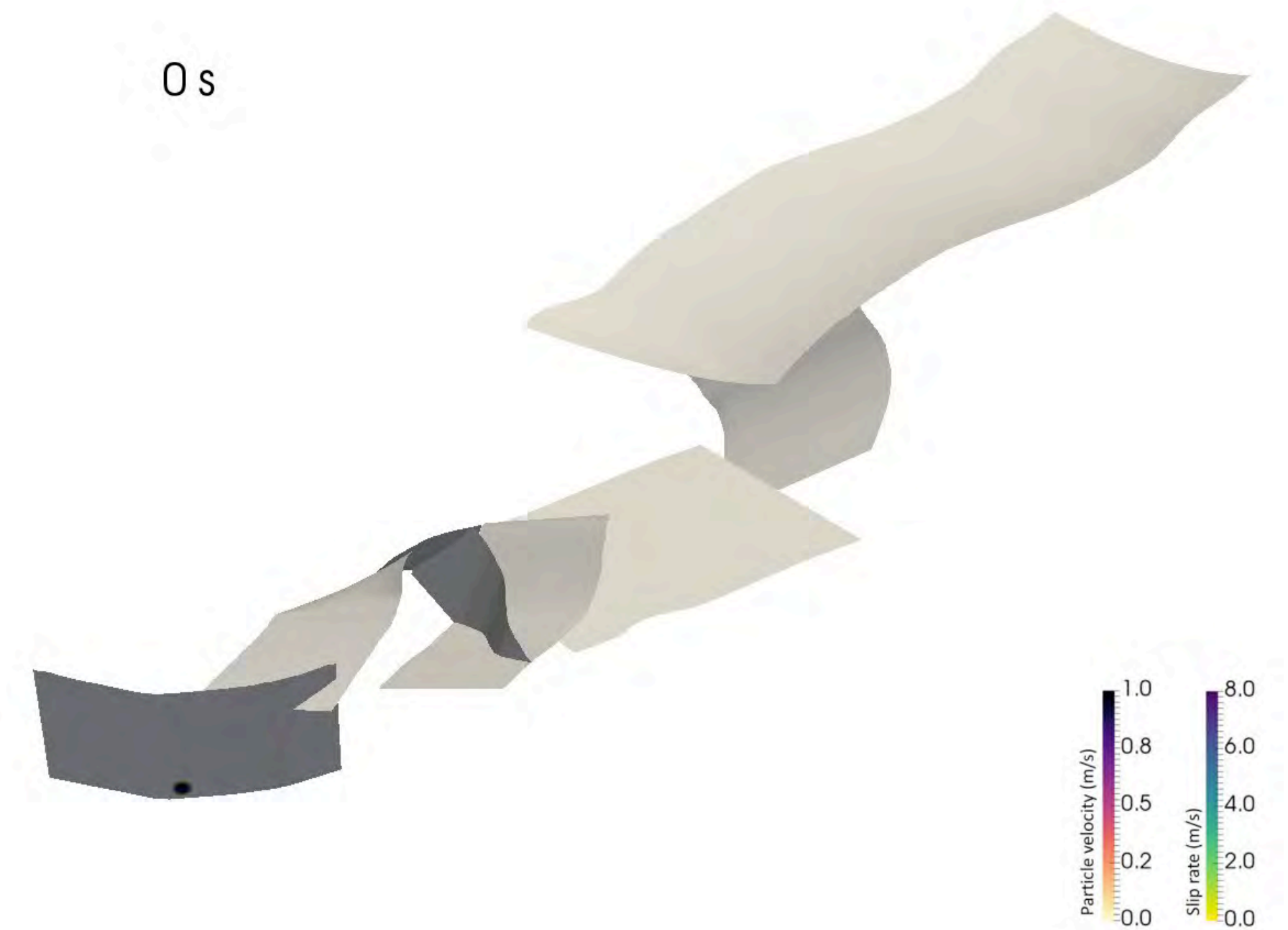


Model fault network coloured by dipping angle. The Hope, Culverden and Leonard Mound faults are included but do not rupture. Faults are embedded in high-resolution topography and bathymetry (Mitchell et al., 2012) and 3D subsurface structure

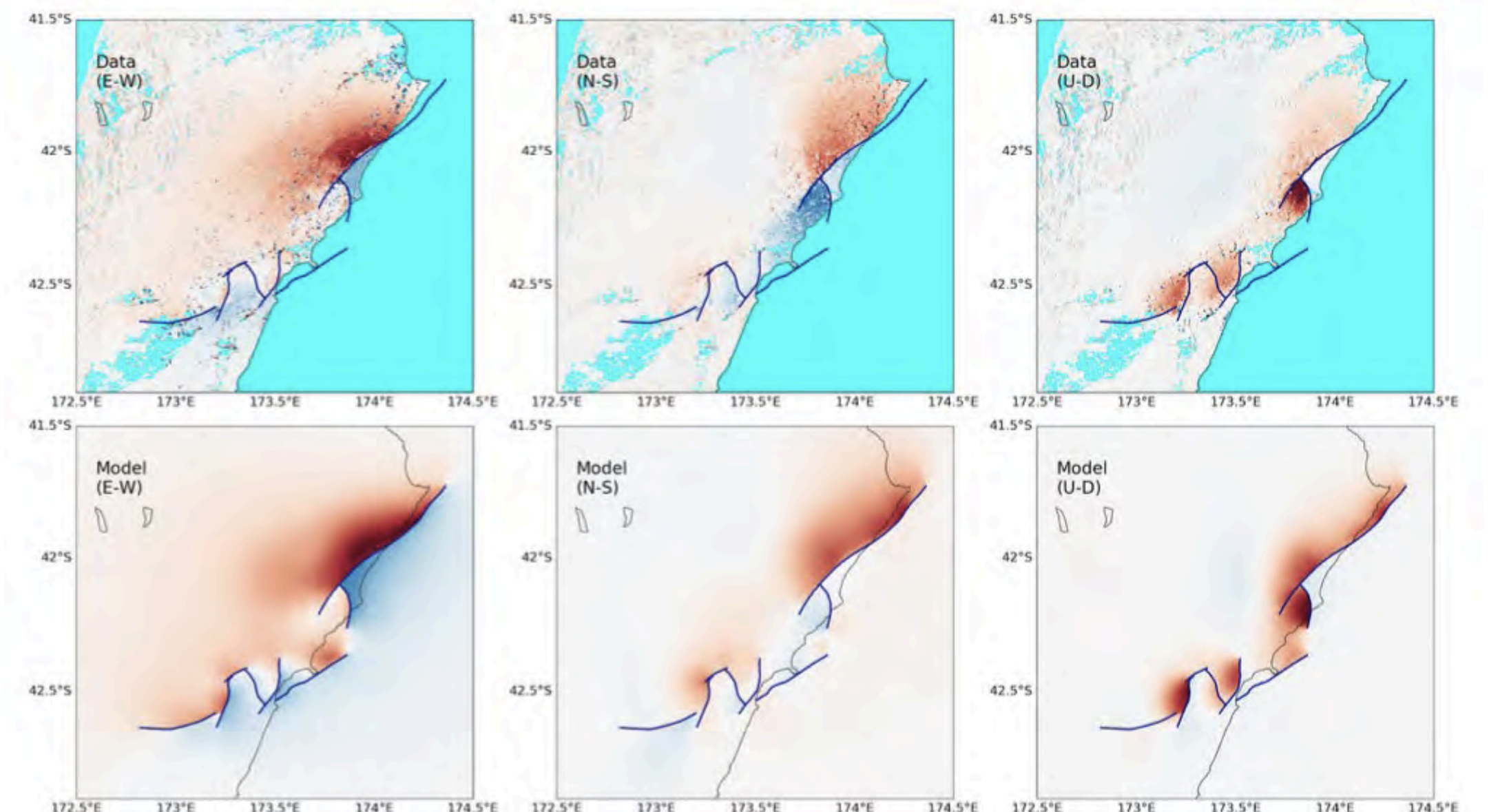
The 2016 Mw 7.8 Kaikōura earthquake - a rupture cascade on weak crustal faults

→ Reproducing observations and
constraining competing views

- Rupture propagation across fault segments with diverse orientations and faulting mechanisms does **not** require slip on the underlying subduction interface
- **Slow** apparent rupture velocity from **zigzagging** rupture path
- **Point Kean fault** (Clark et al., 2017) acted as a **crucial link** between the Hundalee fault and the Northern faults
- **Non-rupture of the Hope fault** due to unfavourable dynamic stresses on the restraining step-over formed by the Conway-Charwell and Hope faults



On-fault slip rate and wave speed. Multiple rupture fronts, Point Kean, Papatea and Kekerengu segments slip more than once.



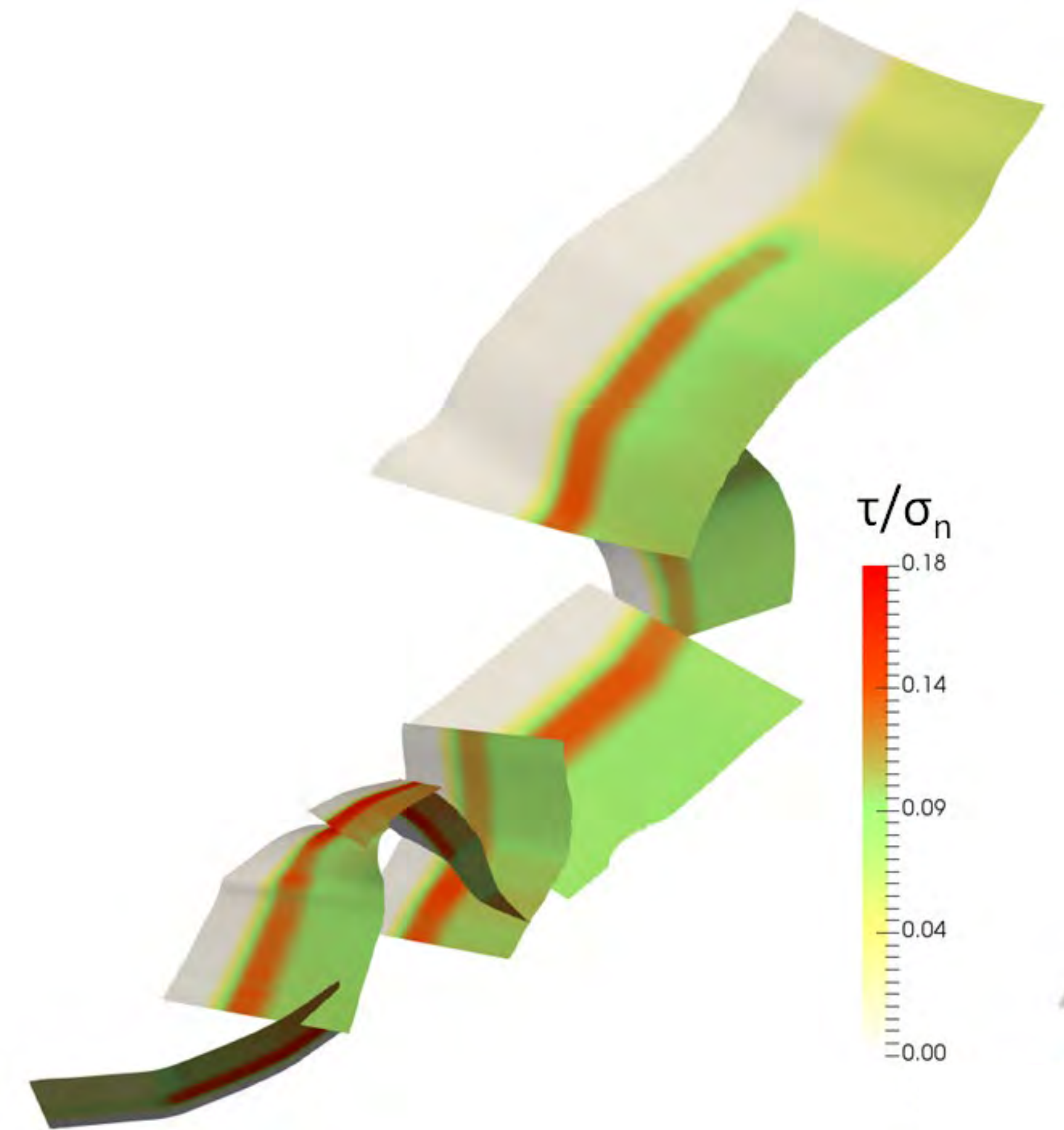
3D ground displacement cf. inferred by space geodetic data (Xu et al. 2018)

The 2016 Mw 7.8 Kaikōura earthquake - a rupture cascade on weak crustal faults

→ Fault weakness across time scales
restores dynamic triggering potential

- Fault weakness (I) - **low dynamic friction**
- Fault weakness (II) - **overpressurized fluids**
- Fault weakness (III) - **deep stress concentration induced by deep fault creep**

(Ulrich et al., preprint <https://eartharxiv.org/aed4b/>)



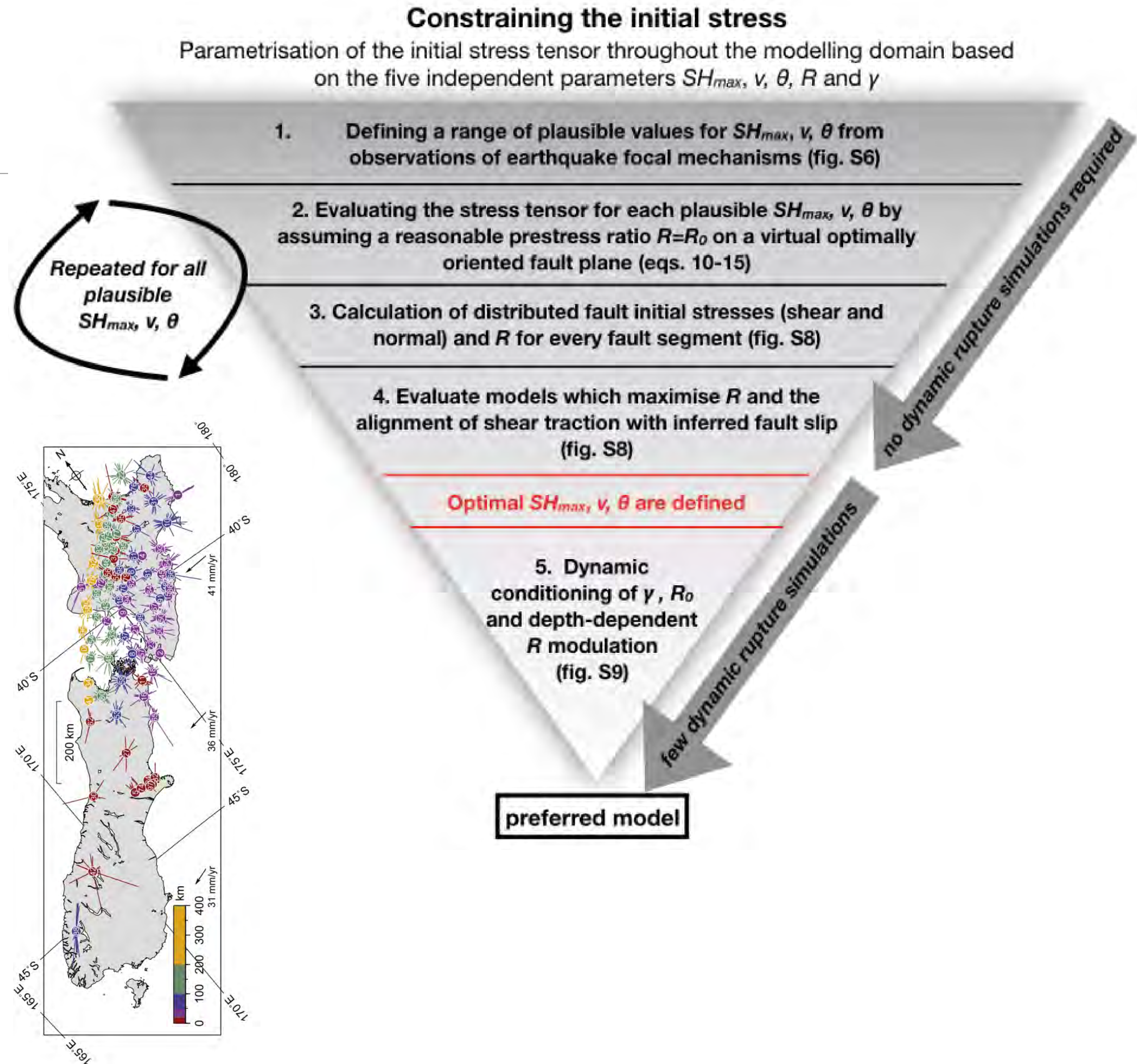
“Optimal stress algorithm” - all faults are overall stressed well below failure and yet break spontaneously.

Initial fault stress and strength

We systematically search for a **smoothly varying regional stress** parametrized by:

- **3 angles (principal stress orientations)**
- **Deviatoric stress** given by relative fault strength and the ratio between fluid-pressure and lithostatic confining stress
- Of those 7 parameters, 4 are directly constrained by regional stress and seismogenic depth, **3 are unknown: fluid pressure, background shear stress and intensity of deep stress concentration**

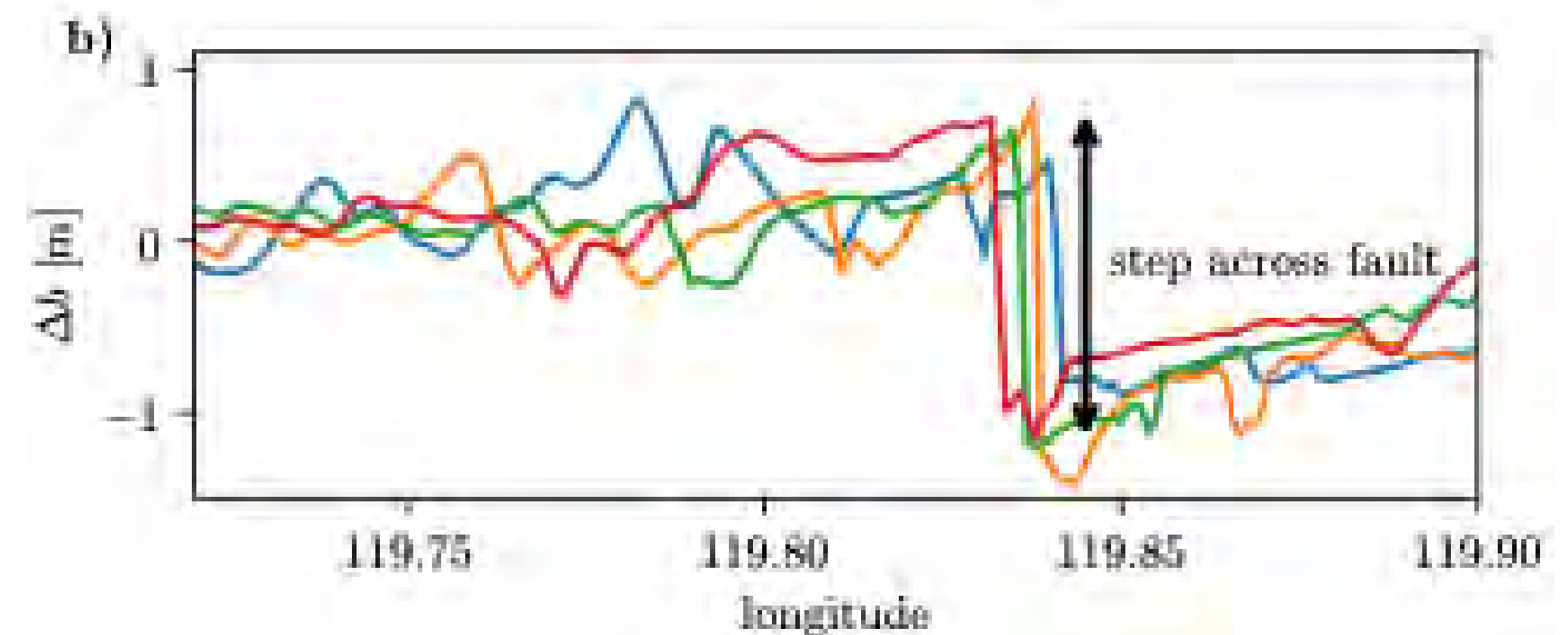
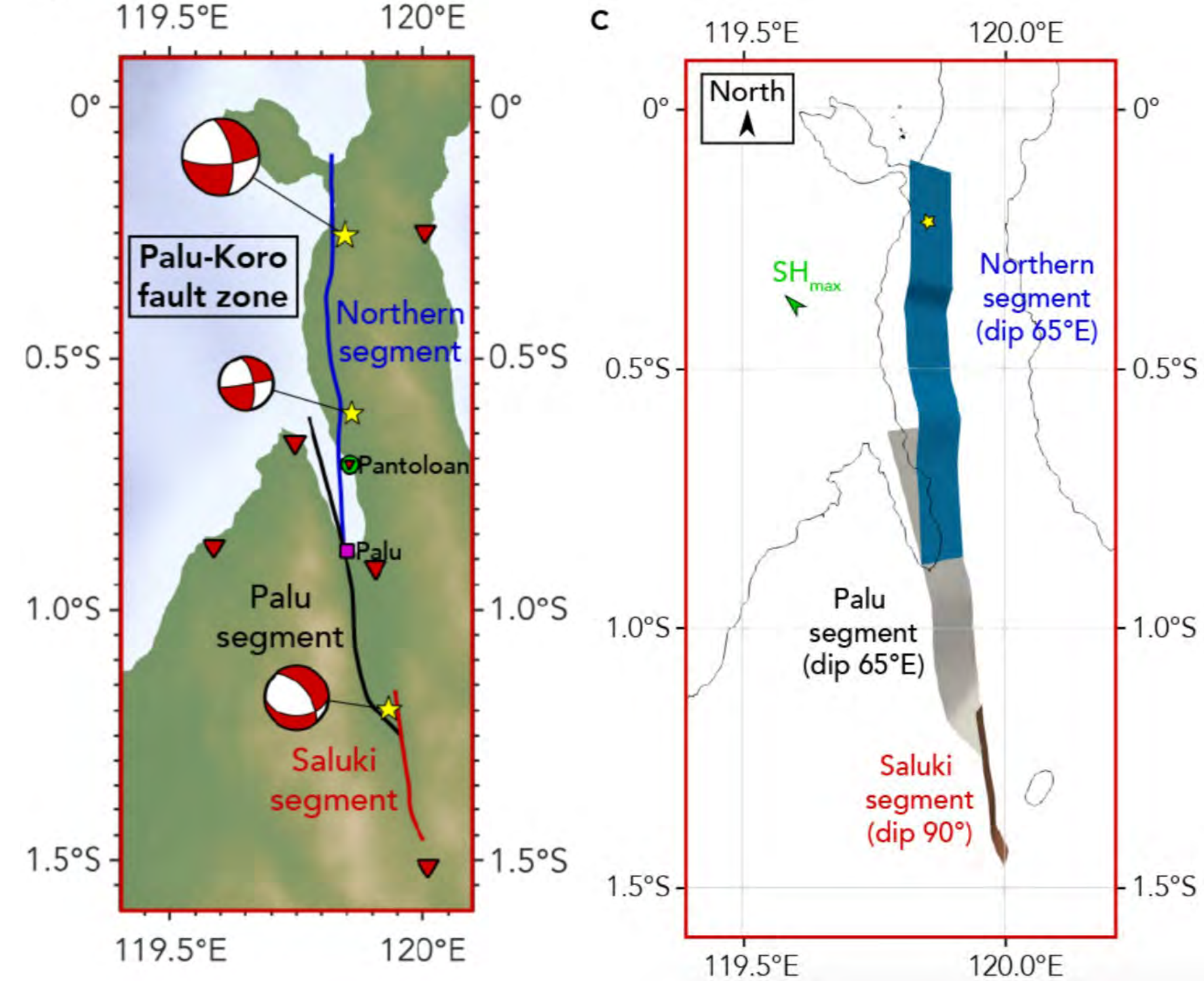
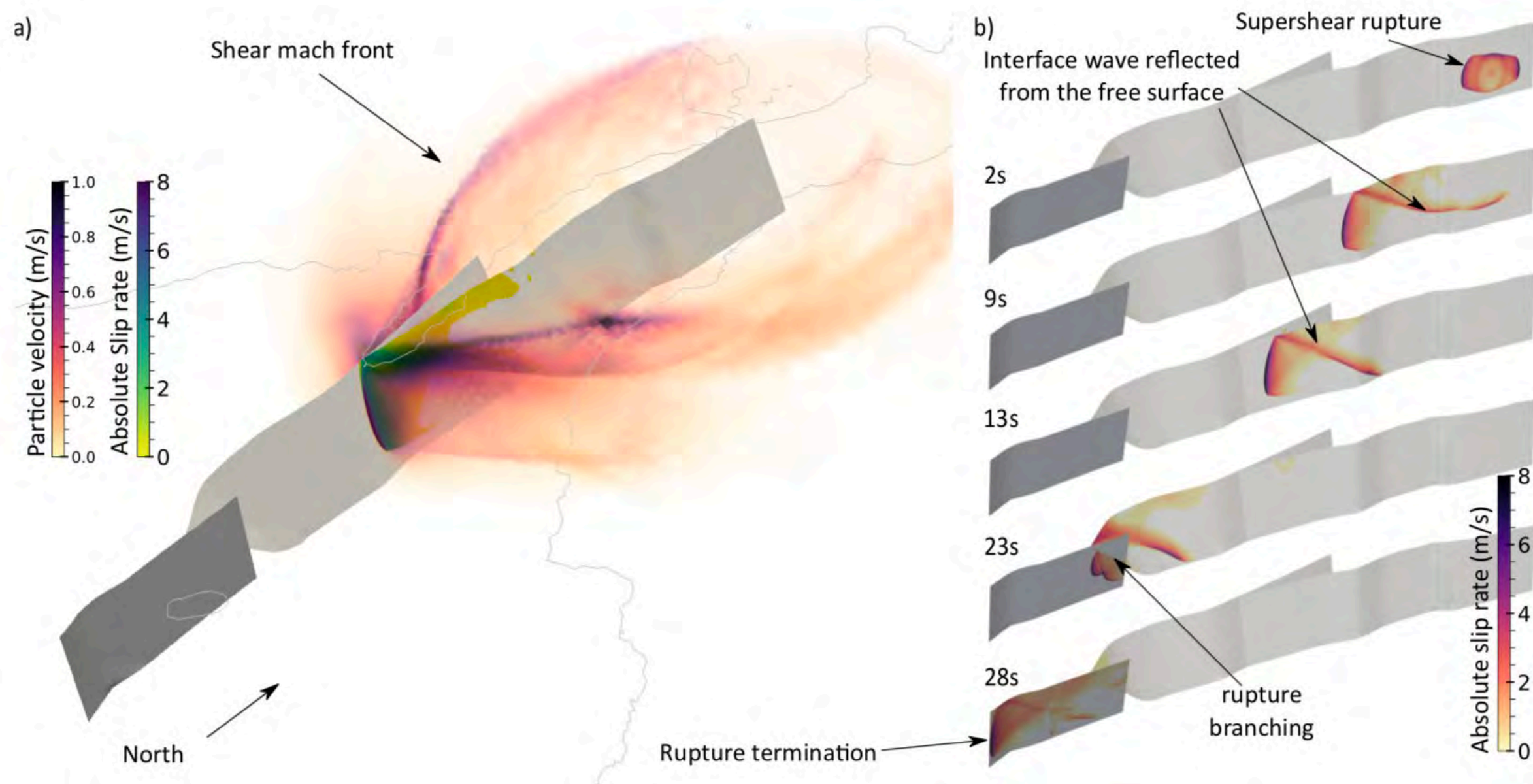
Townend et al., 2012



Dynamic rupture earthquake simulation

Physics-based complement to empirical seismic hazard assessment

For example: Few weeks after the Sept. 2018 Palu-Koro earthquake and tsunami dynamic rupture earthquake ground displacements alone are shown to be sufficient to generate the observed tsunami within Palu Bay, Sulawesi, Indonesia

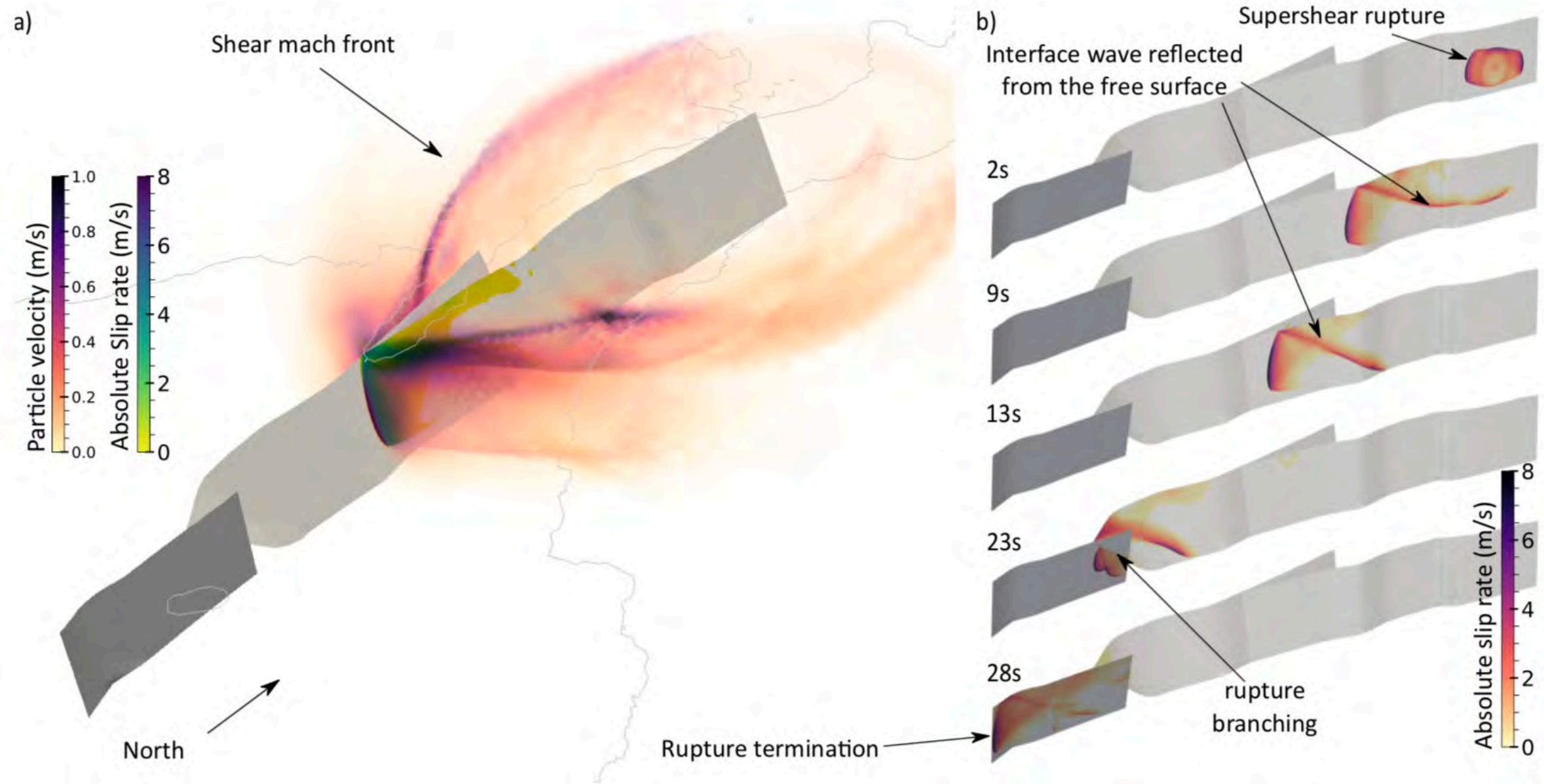


(Ulrich et al., 2019,
<https://eartharxiv.org/3bwqa/>)

Dynamic rupture earthquake simulation

Physics-based complement to empirical seismic hazard assessment

For example: Few weeks after the Sept. 2018 Palu-Koro earthquake and tsunami dynamic rupture earthquake ground displacements alone are shown to be sufficient to generate the observed tsunami within Palu Bay, Sulawesi, Indonesia



(Ulrich et al., 2019, <https://eartharxiv.org/3bwqa/>)

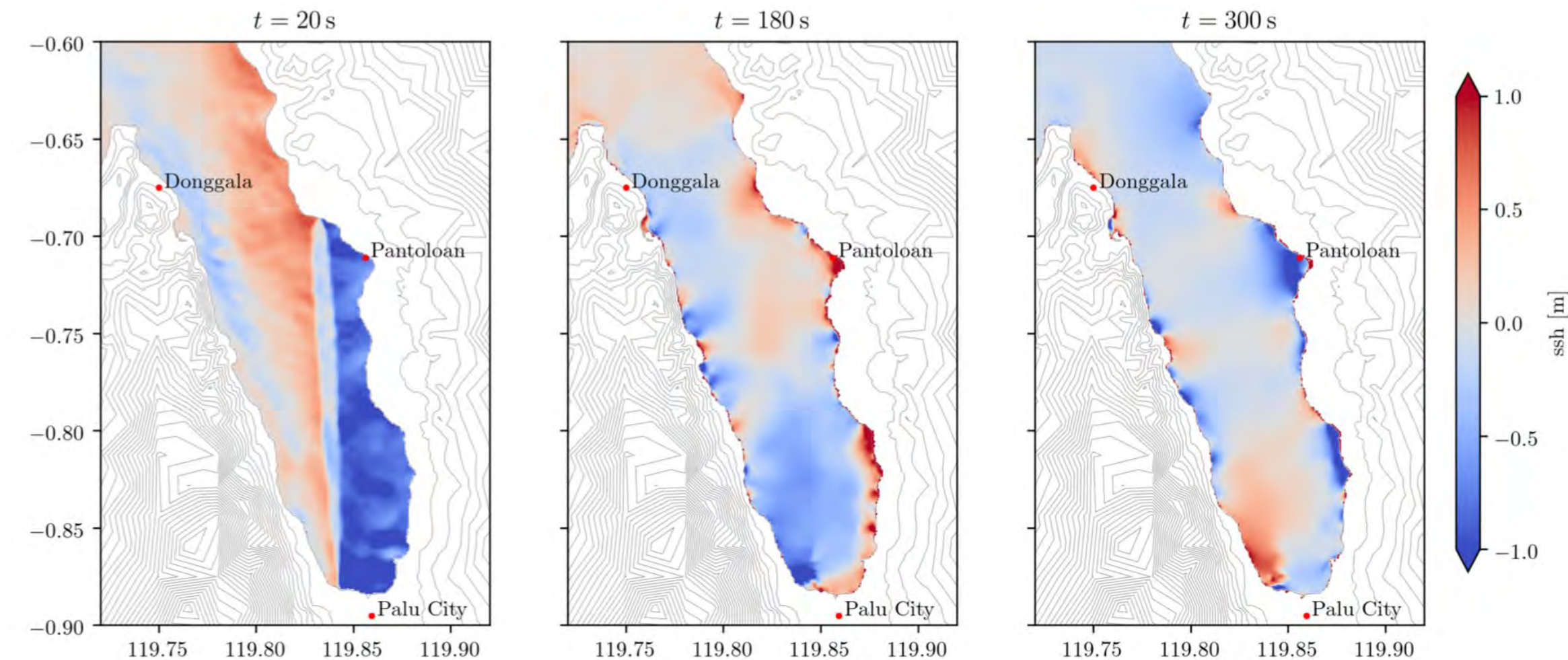
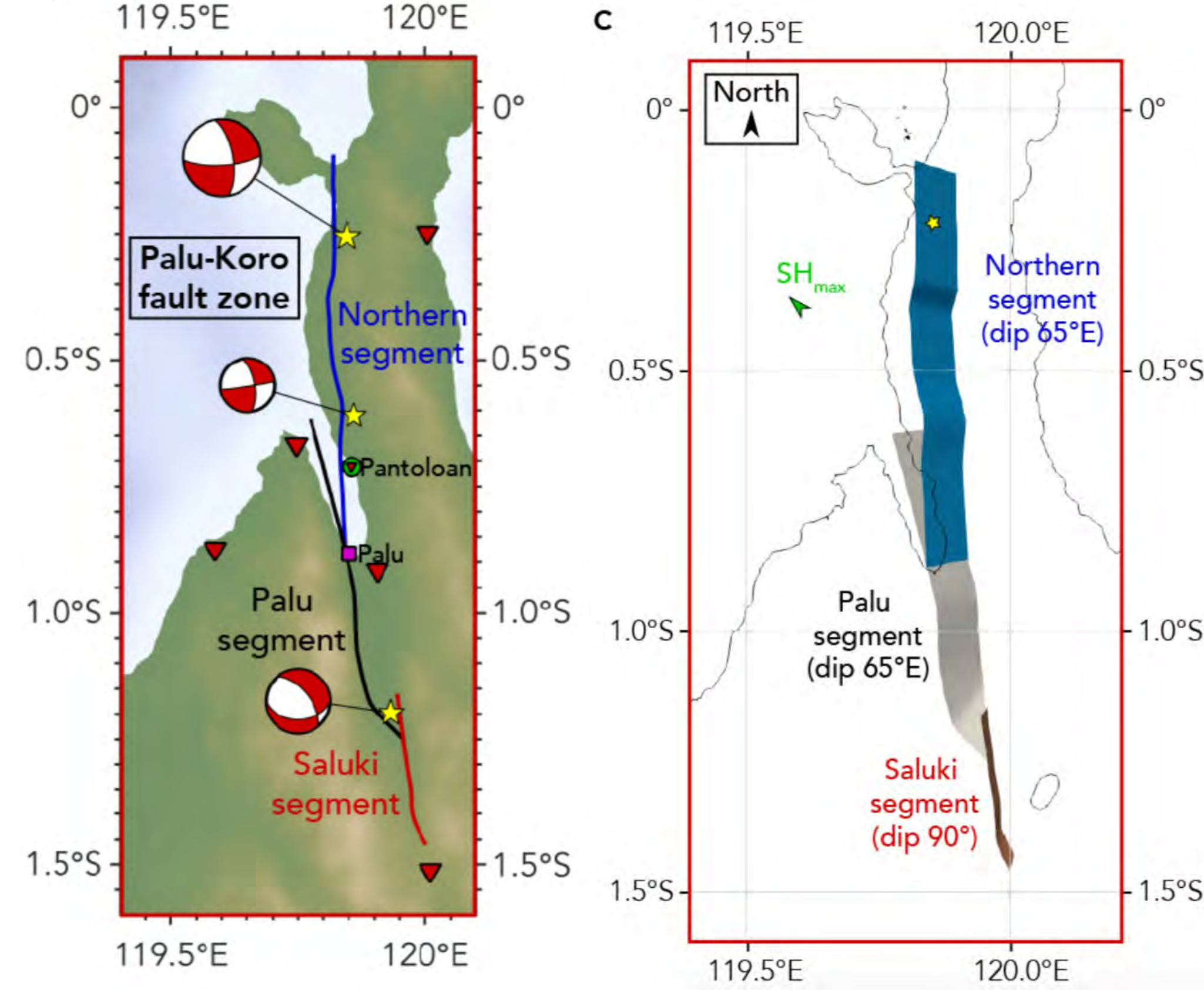
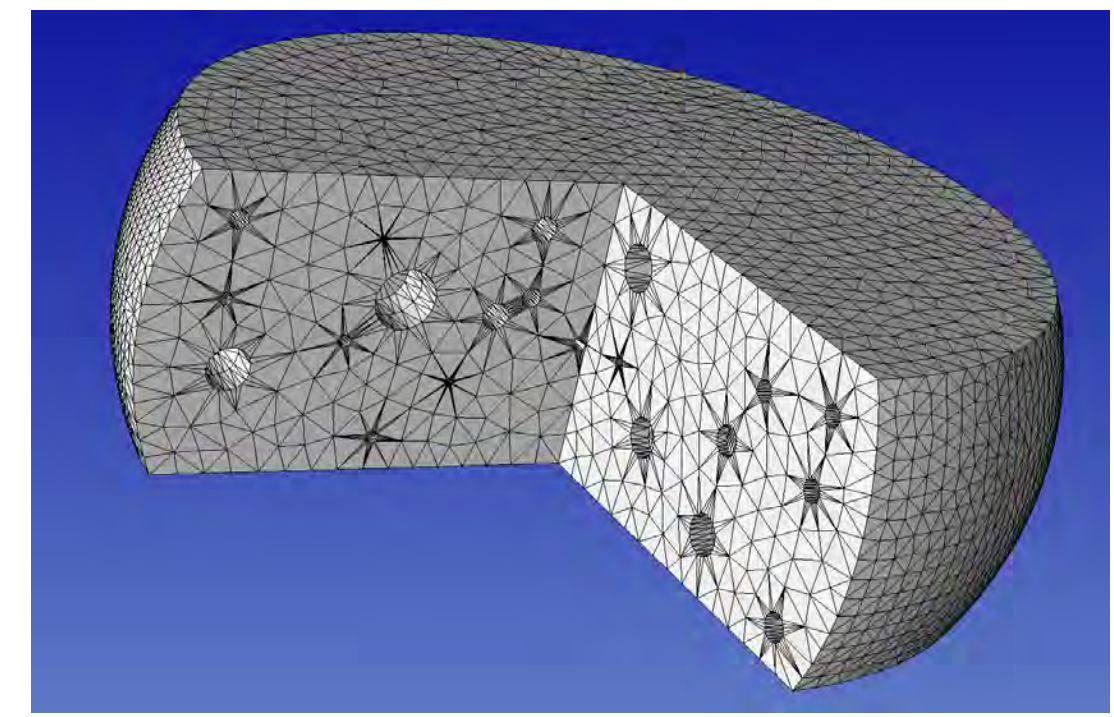
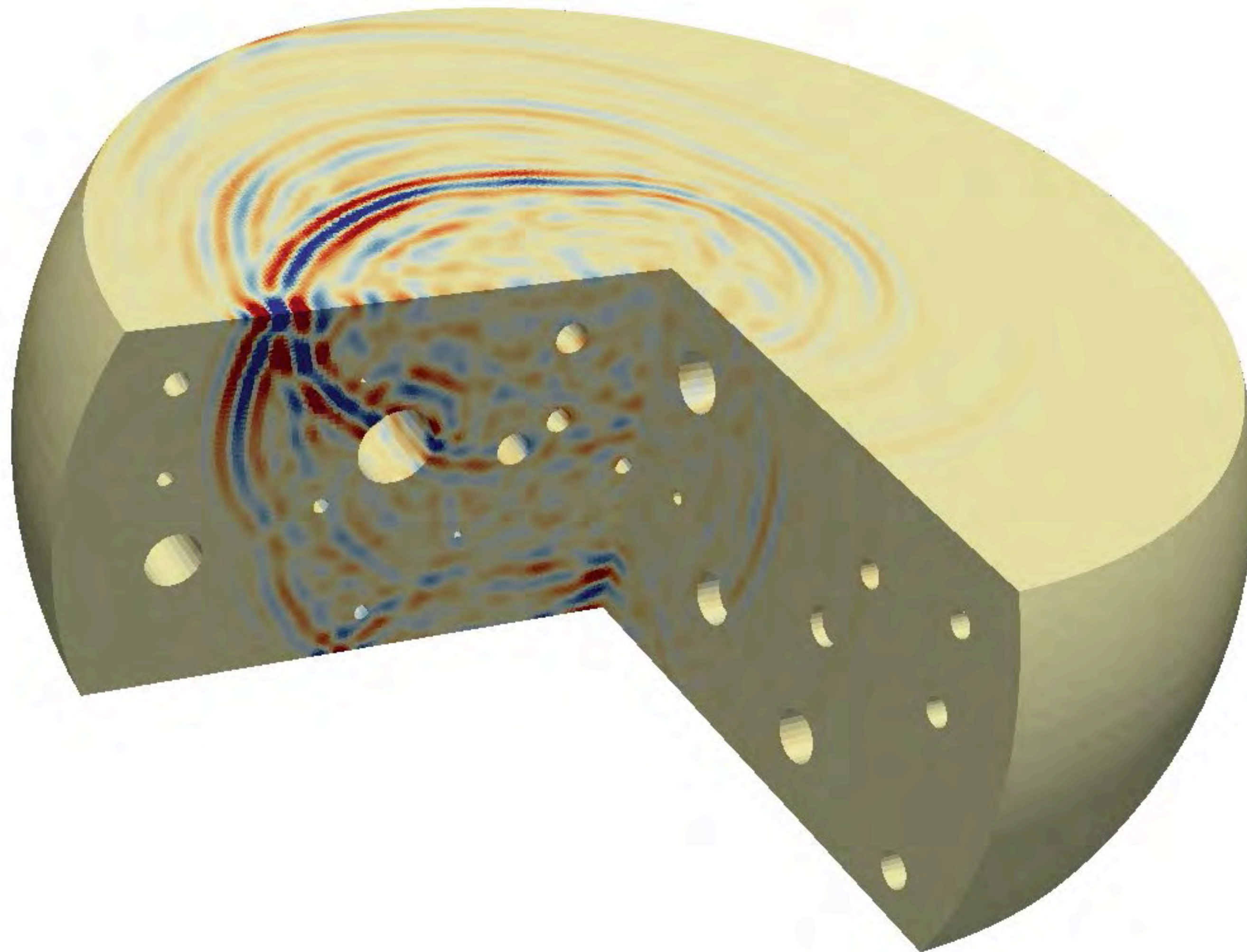
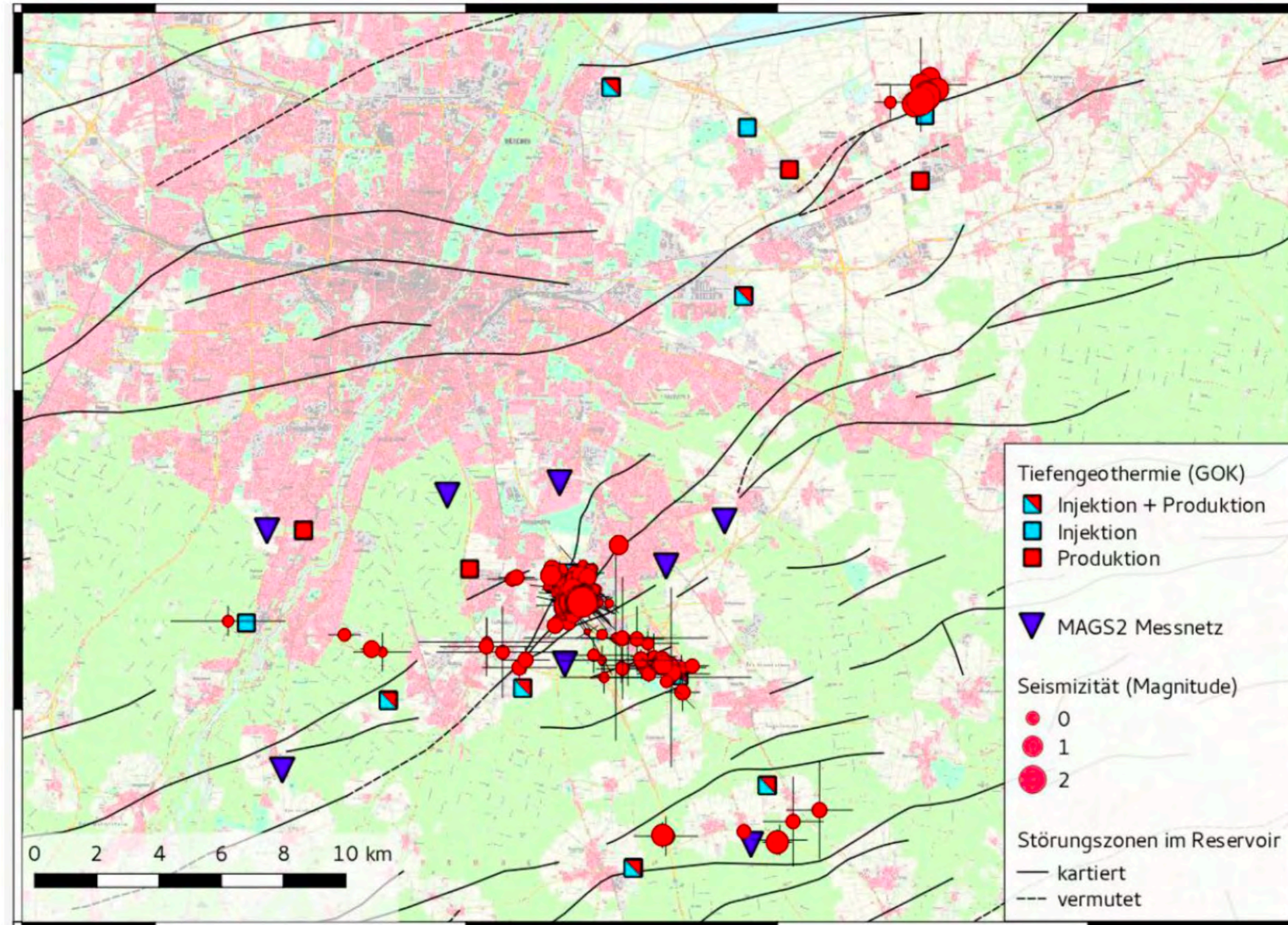


Fig. 9 Snapshots of the tsunami simulation at 20 s, 180 s and 300 s (left to right), showing only the area of Palu Bay.

Change of scales



Change of scales - Application to reservoir scales towards physics-based seismic hazard assessment (FRAGFN project)



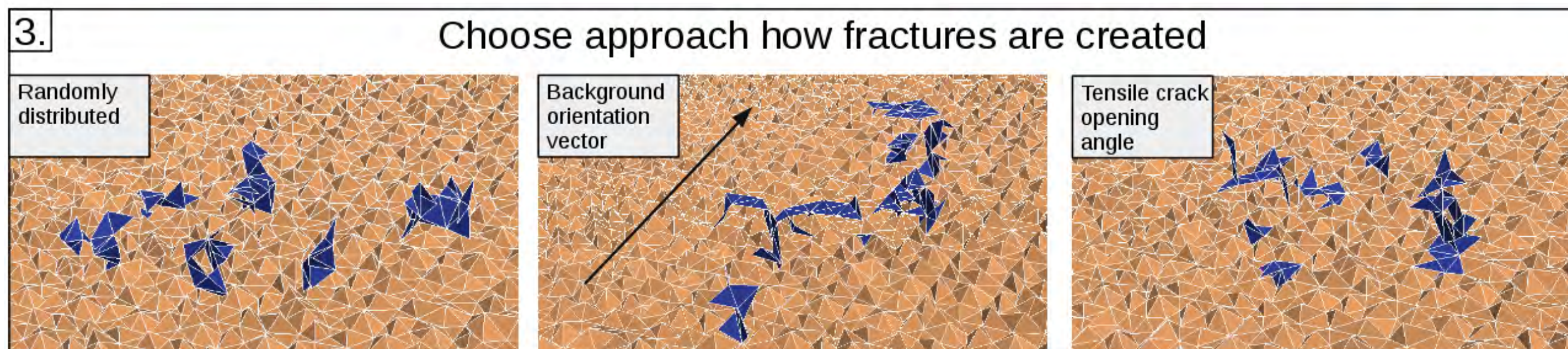
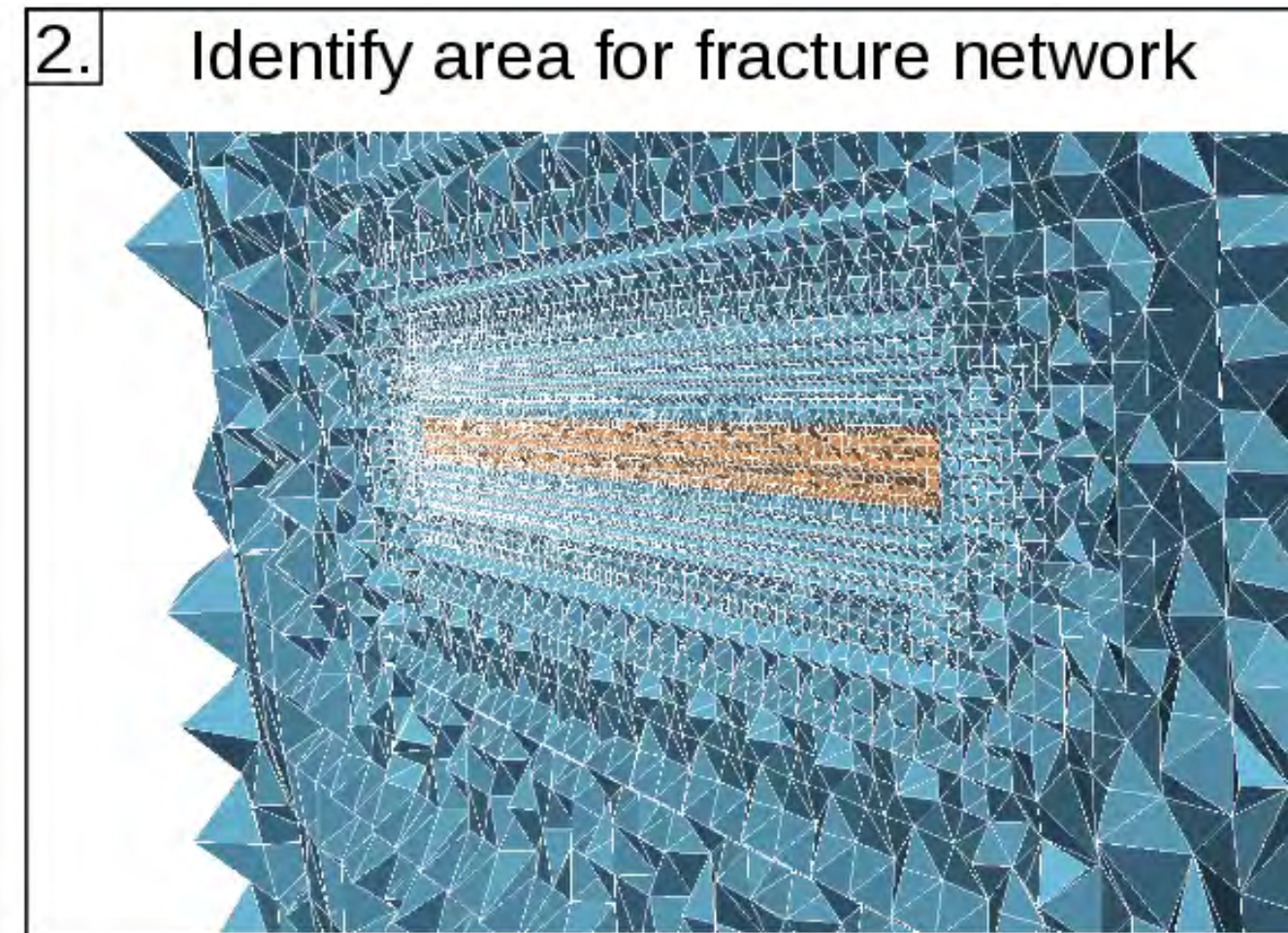
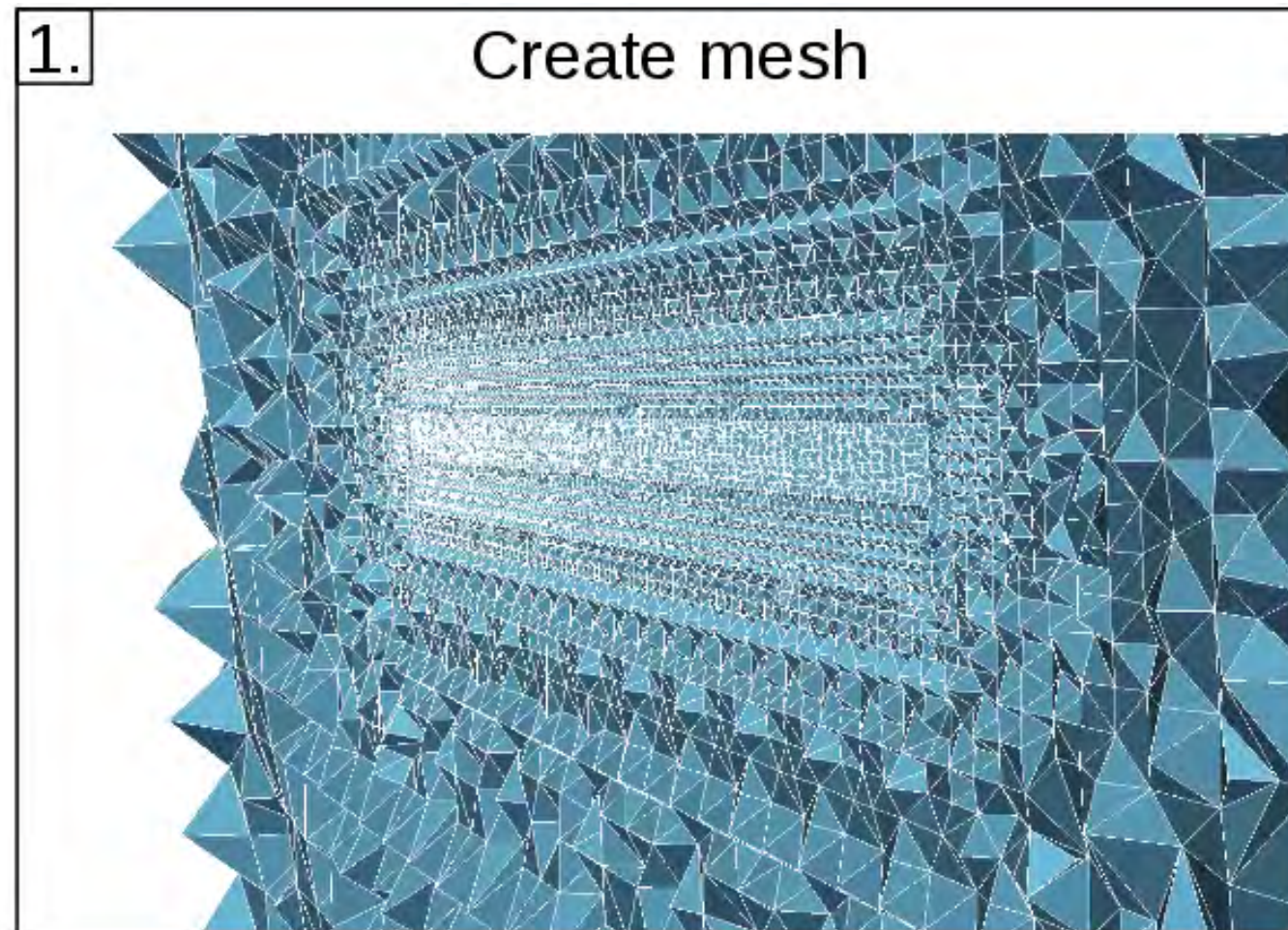
“Given the occurrence of a seismic event,
what are the driving forces for its strength?”

“How are fault- or operation-specific parameters
associated with the maximal magnitudes of
seismic events?”

Fig. 5: Megies, Wassermann, 2016, - “Praxisforum Geothermie Bayern”, Oktober 2017 pers. comm. Megies 2017. Fault traces from Bayerisches Staatsministerium für Wirtschaft, Infrastruktur, Verkehr und Technologie. 2010. Bayerischer Geothermieatlas. München

Fracture activation in geo-reservoirs

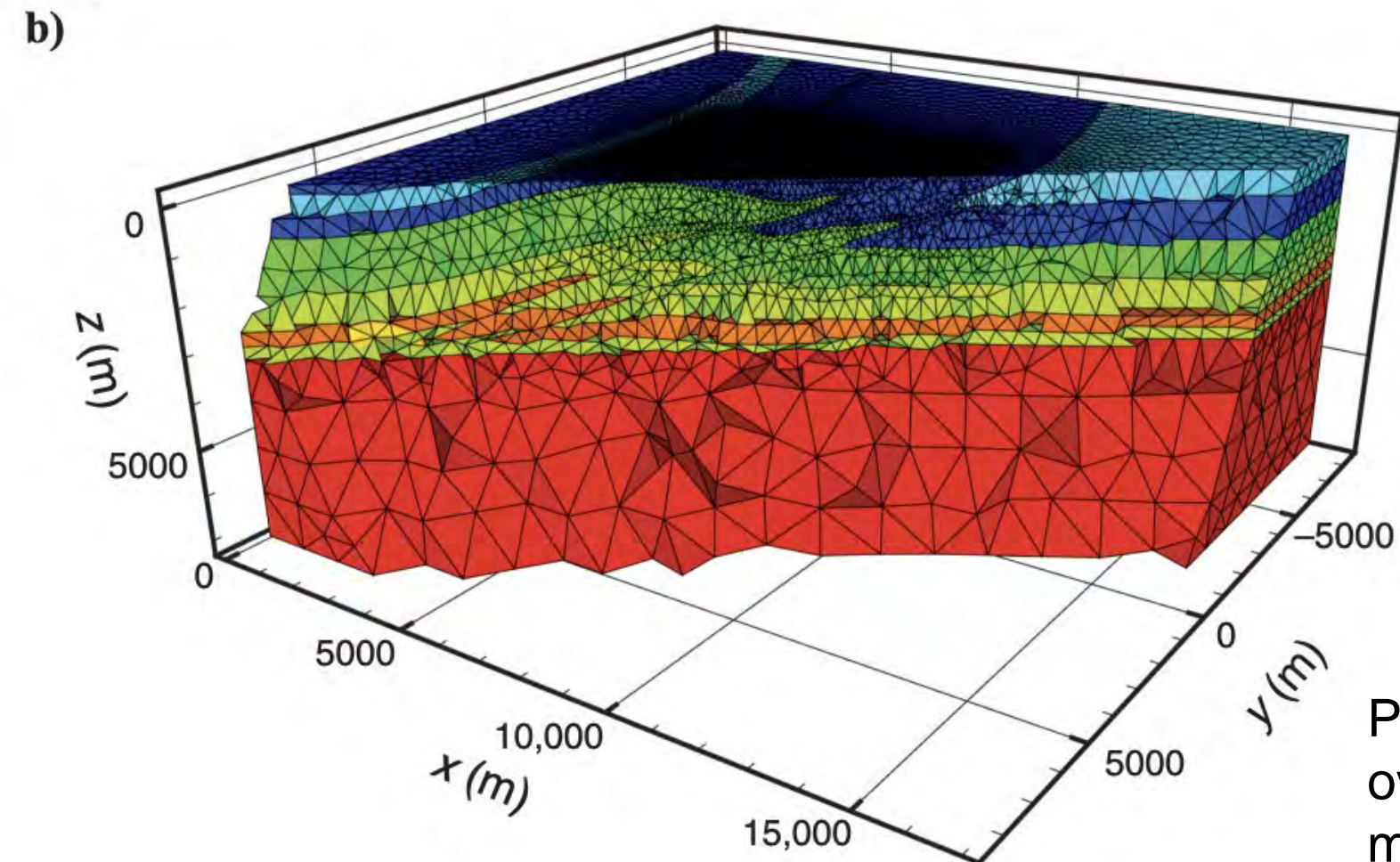
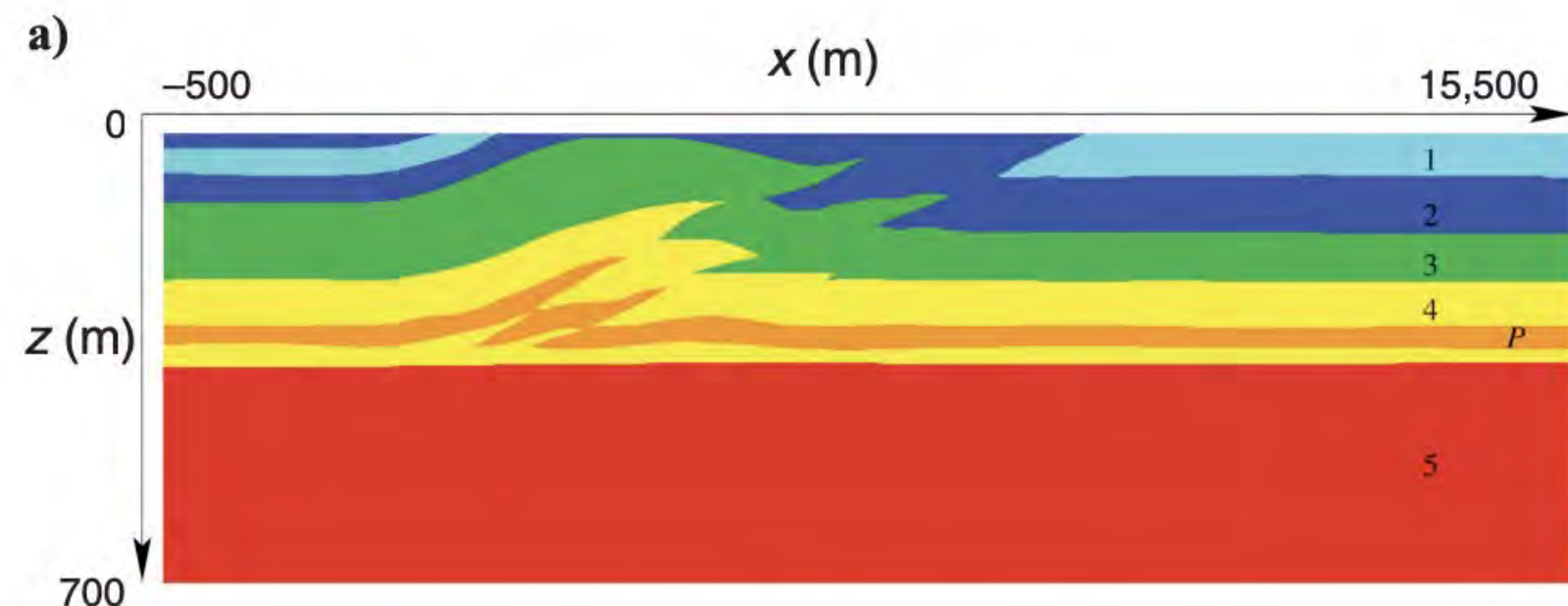
- We study the physics of (induced) earthquakes in complex fault networks which are at geo-reservoir scales inherently **geometrically complex**



Statistical fracture network for dynamic rupture simulations from physics-based Markov Chain Monte Carlo approach (Sebastian Anger, POSTER P2-10 3320)

Fracture activation in geo-reservoirs

- We develop methods to study **fault-fluid interaction on-fault and off-fault: thermal pressurisation** frictional weakening, **pressure gradients** combined with **poro-elastic wave propagation**



Poroelastic 3D wave propagation in SEG overthrust model of Aminzadeh et al., 1997 modeled with SeisSol (de la Puente et al., 2008, now work with Martin Galis)

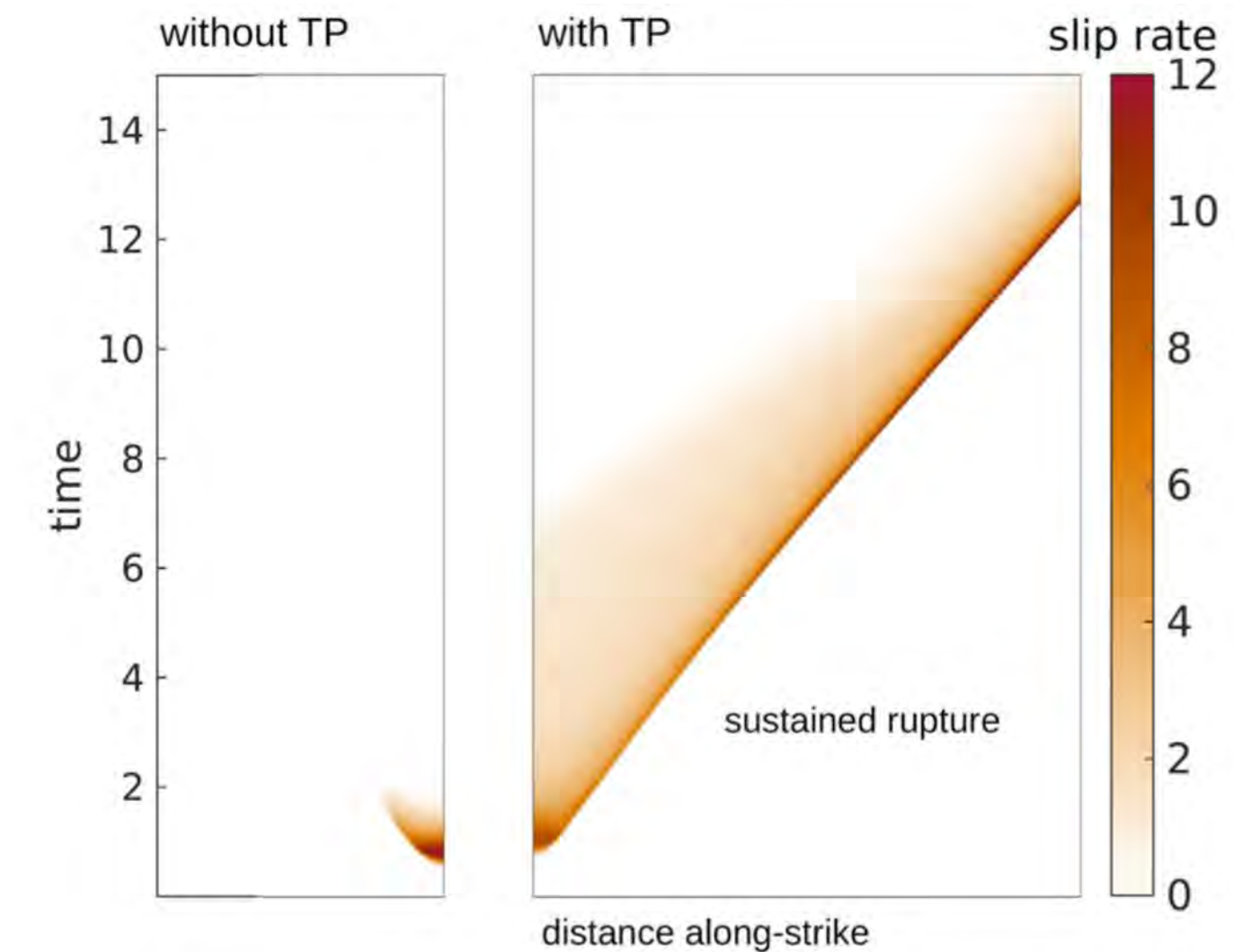
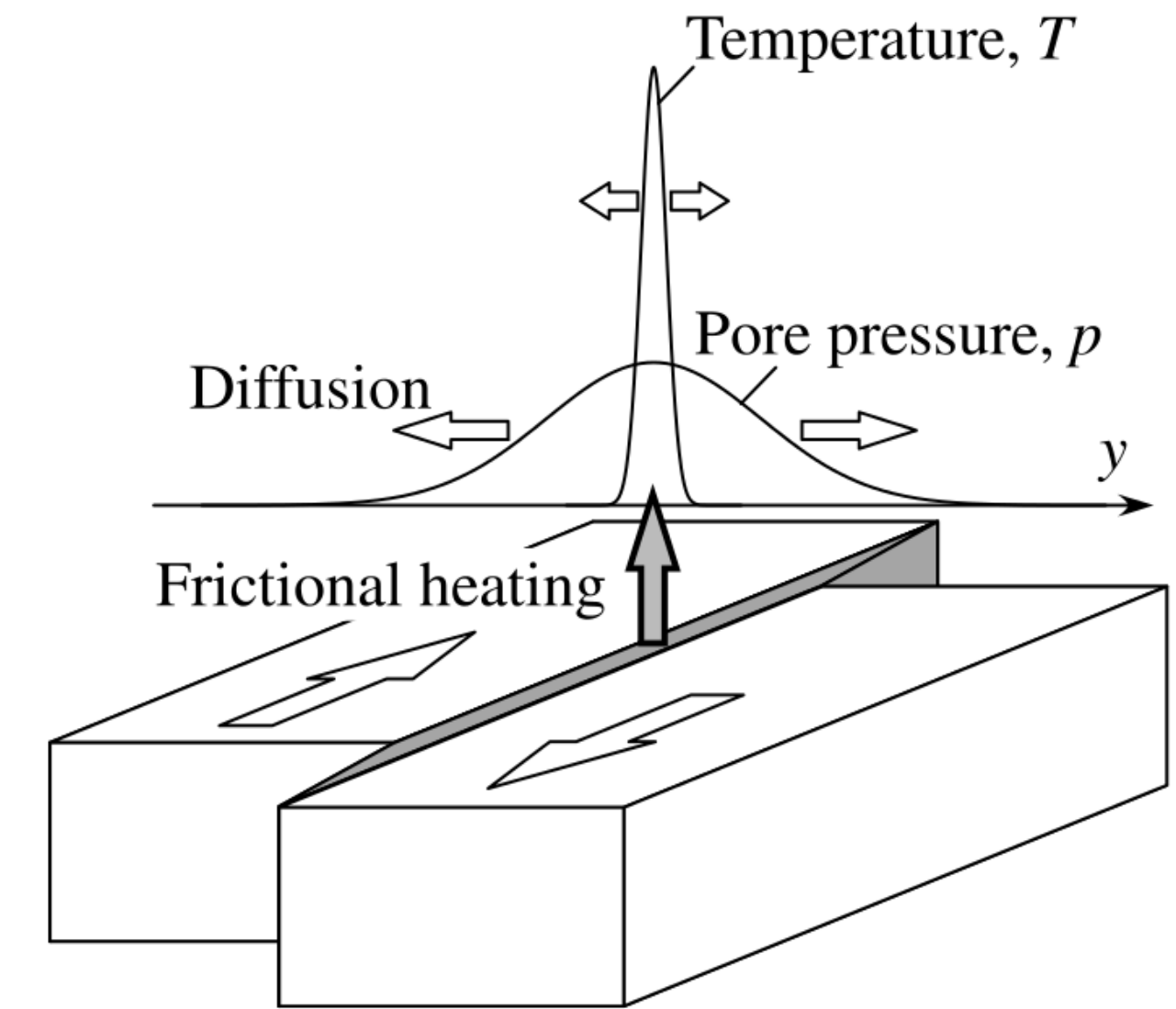
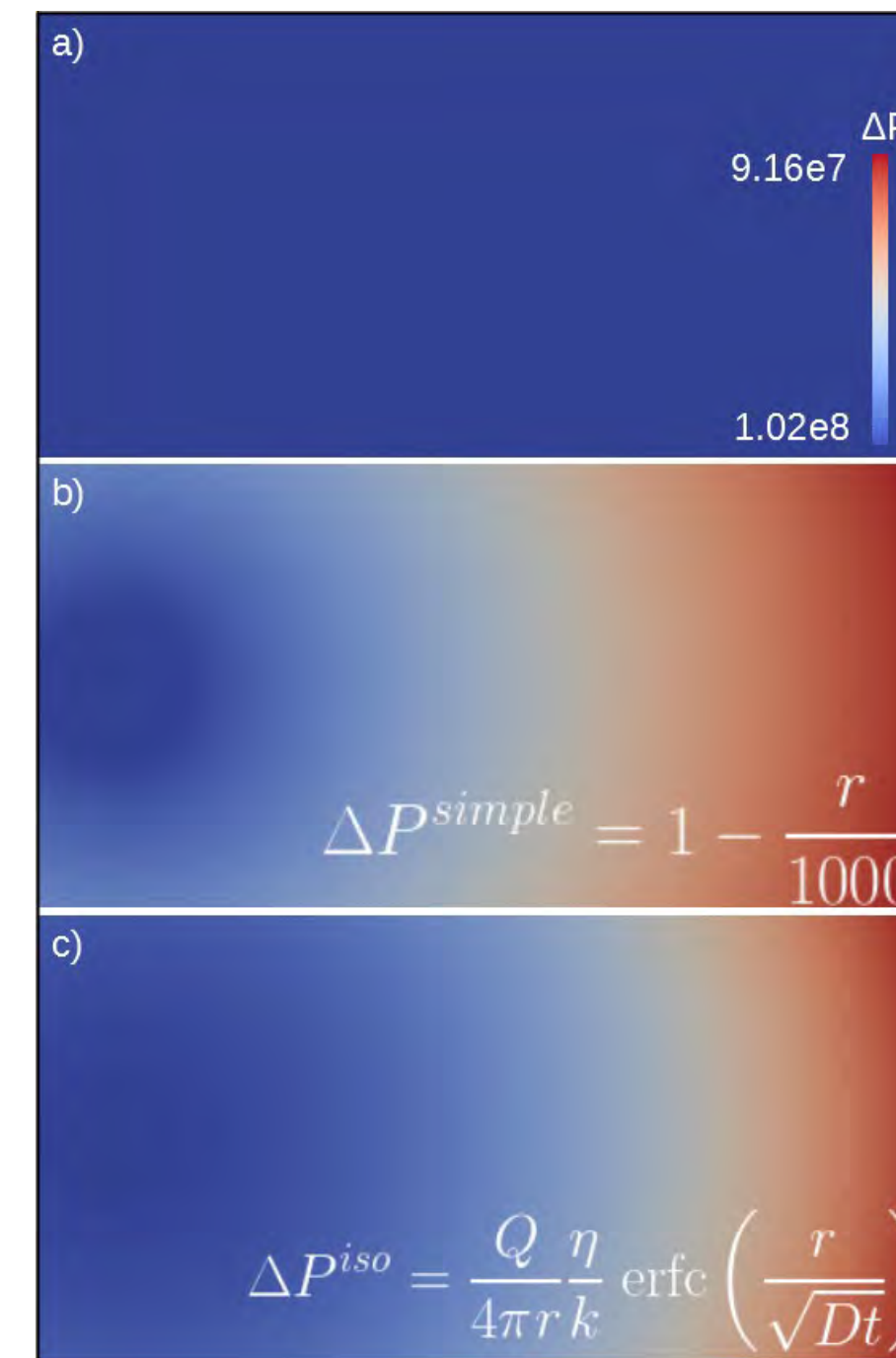


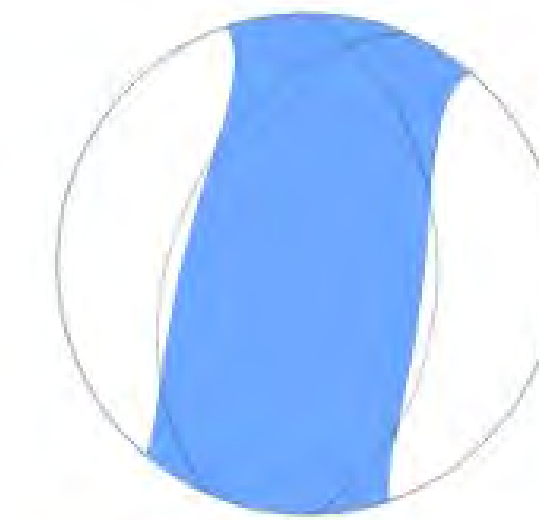
Fig 3.: Slip rate over time and along-strike for a 2D strike-slip scenario using the software SeisSol. Rupture quickly dies out without thermal pressurization (TP, left) but can be sustained for the same initial conditions when we include TP (right), taken from Wollherr et al. (2018a).

Fracture activation in geo-reservoirs

- Case-study: **The 2017 Pohang ML5.4 earthquake**
- Dynamic rupture models based on multiple faults of Kim et al., 2018; Grigoli et al., 2018
- Source complexity and strong non-DC component may be related to changes in timing/azimuth/rupture directivity of complex faults (cf. Grigoli et al., 2018)

strong non-DC component

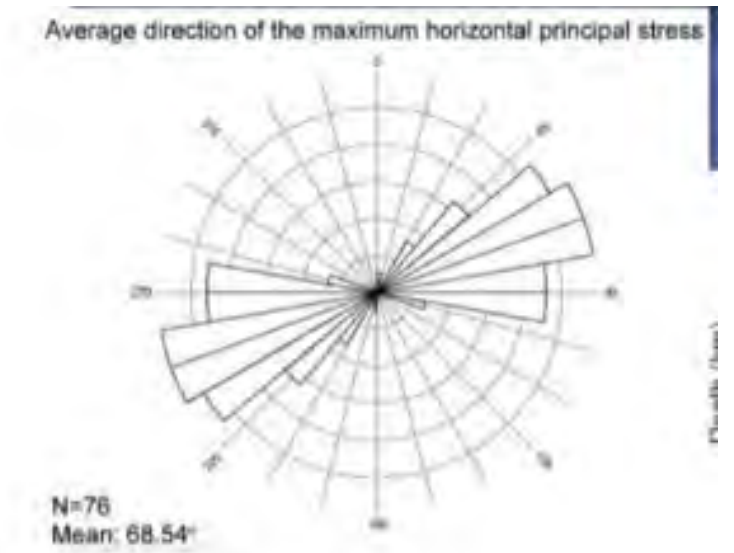
Moment Tensor



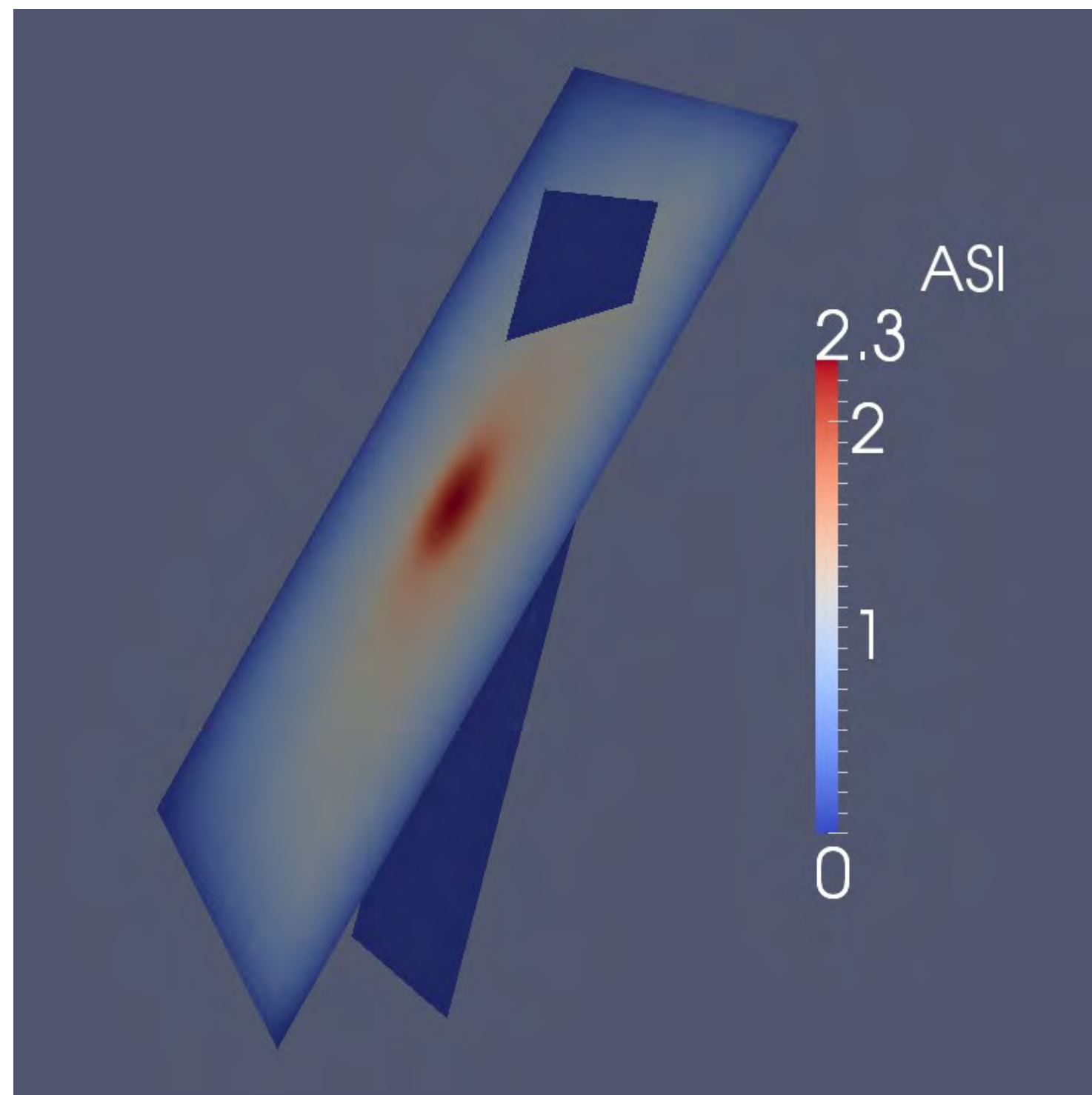
Fault Plane Solution

Grigoli et al, 2018

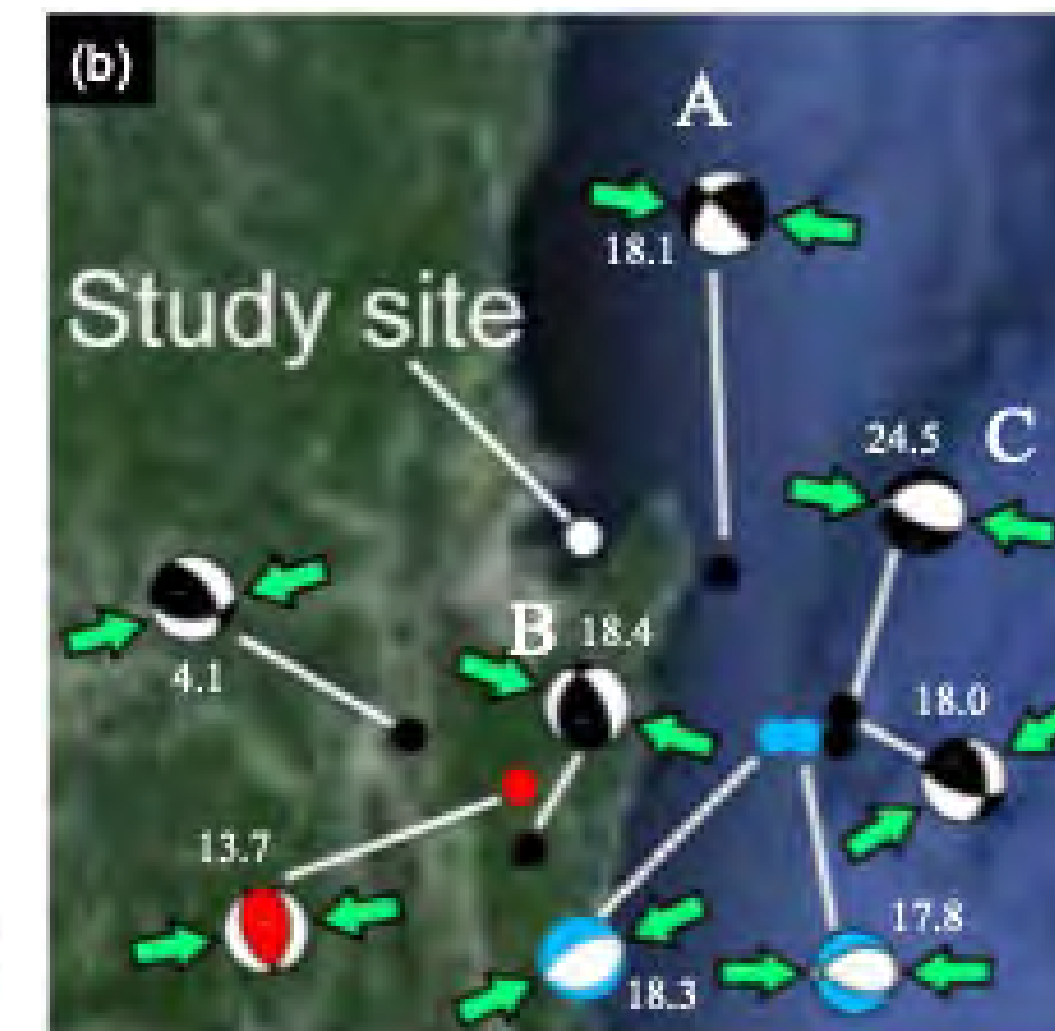
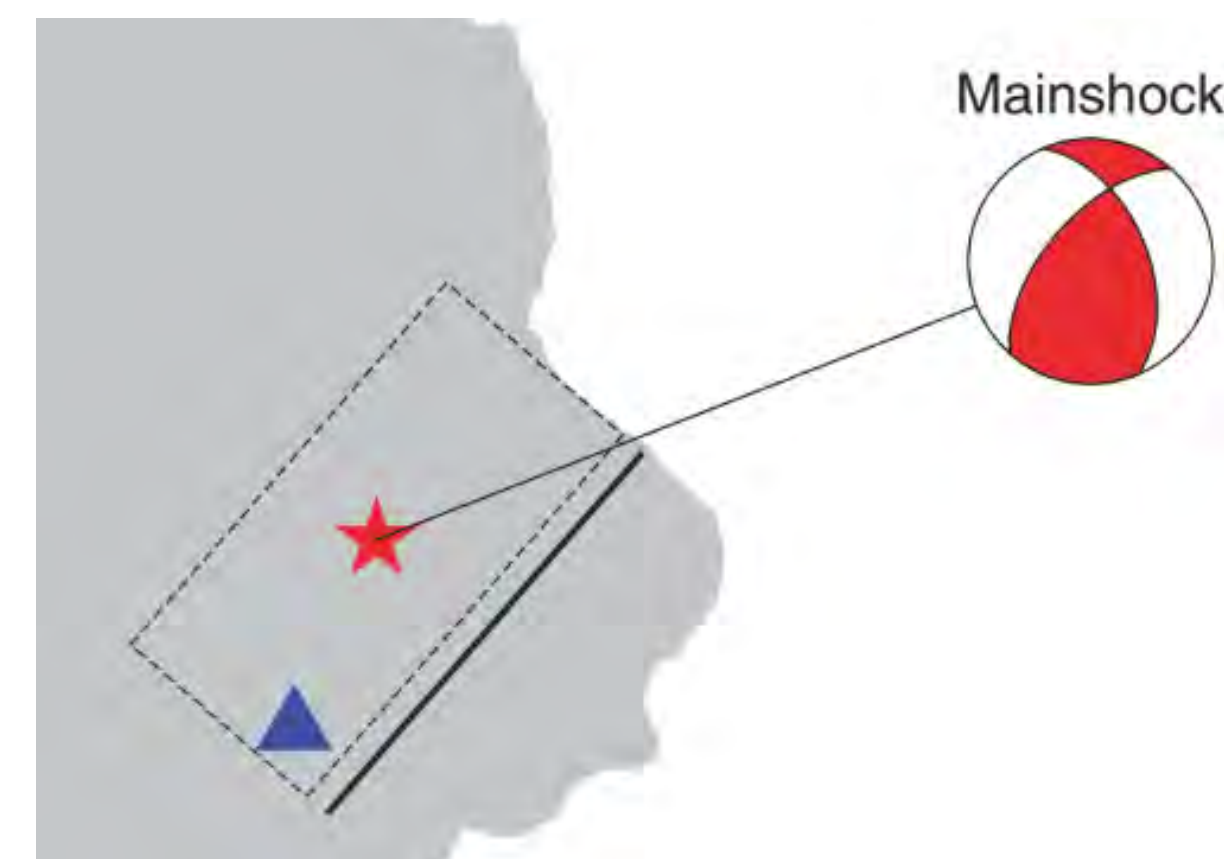
SHmax~70



Lee et al., 2017

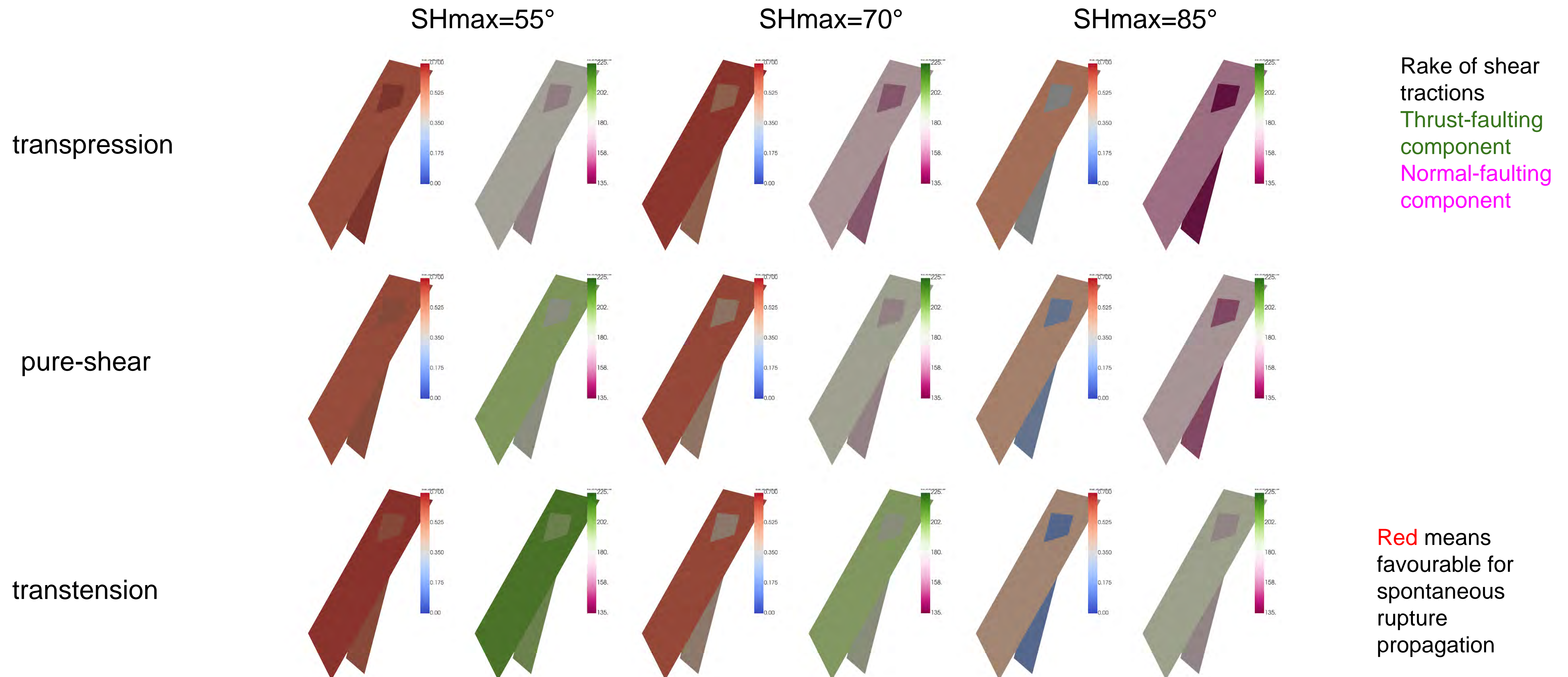


SW-NE faults dipping NW
Moment tensor suggest strike-slip/thrusting (Song and Lee, 2019)



Fracture activation in geo-reservoirs

- Assuming an Andersonian stress regime, high fluid pressure



Fracture activation in geo-reservoirs

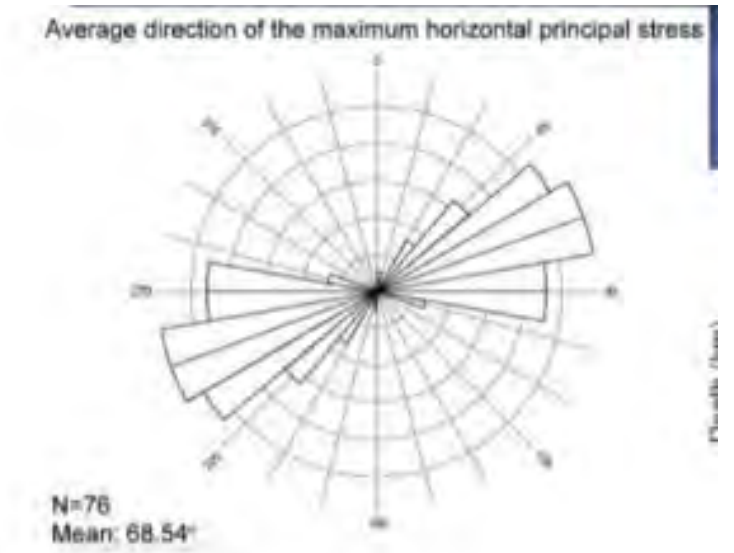
- Case-study: The 2017 Pohang ML5.4 earthquake
- A fault geometry based on Kim et al., 2018 and regional SHmax estimates seems incompatible for dynamic rupture thrust faulting
- Uniform increase in pore pressure would not change this picture (only acting on normal stresses)

Moment Tensor

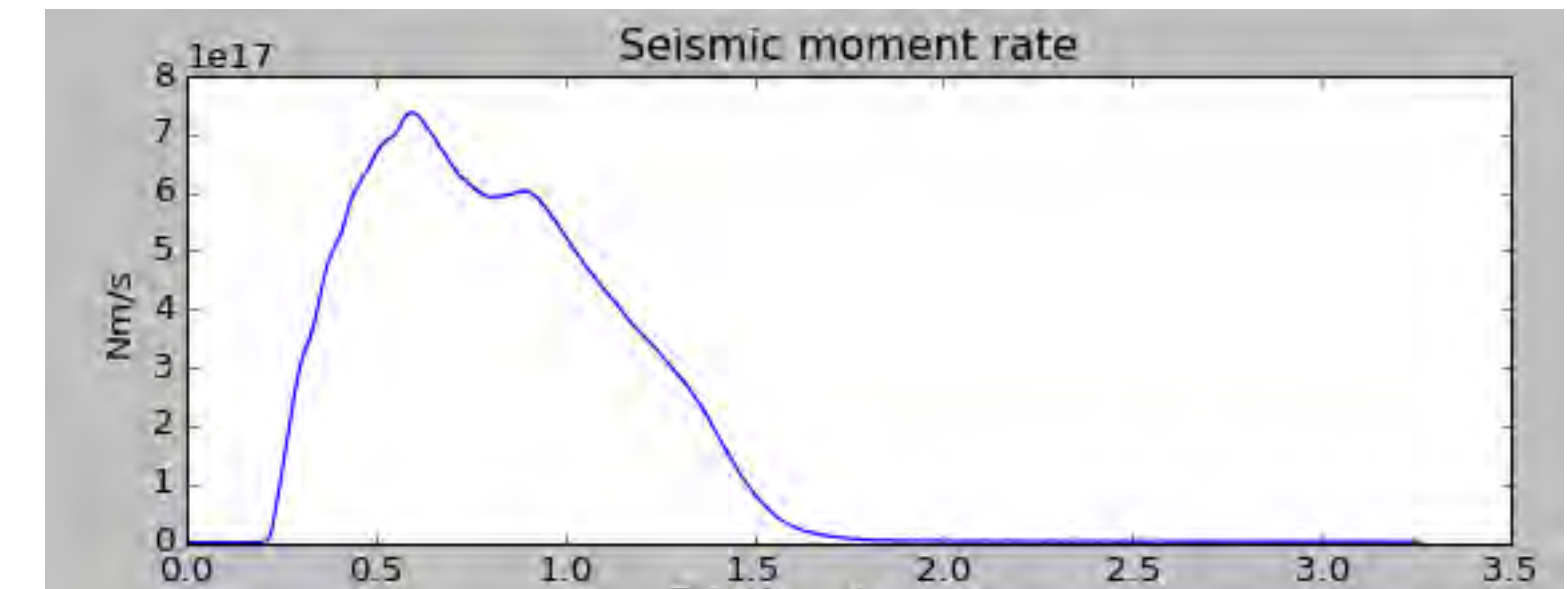
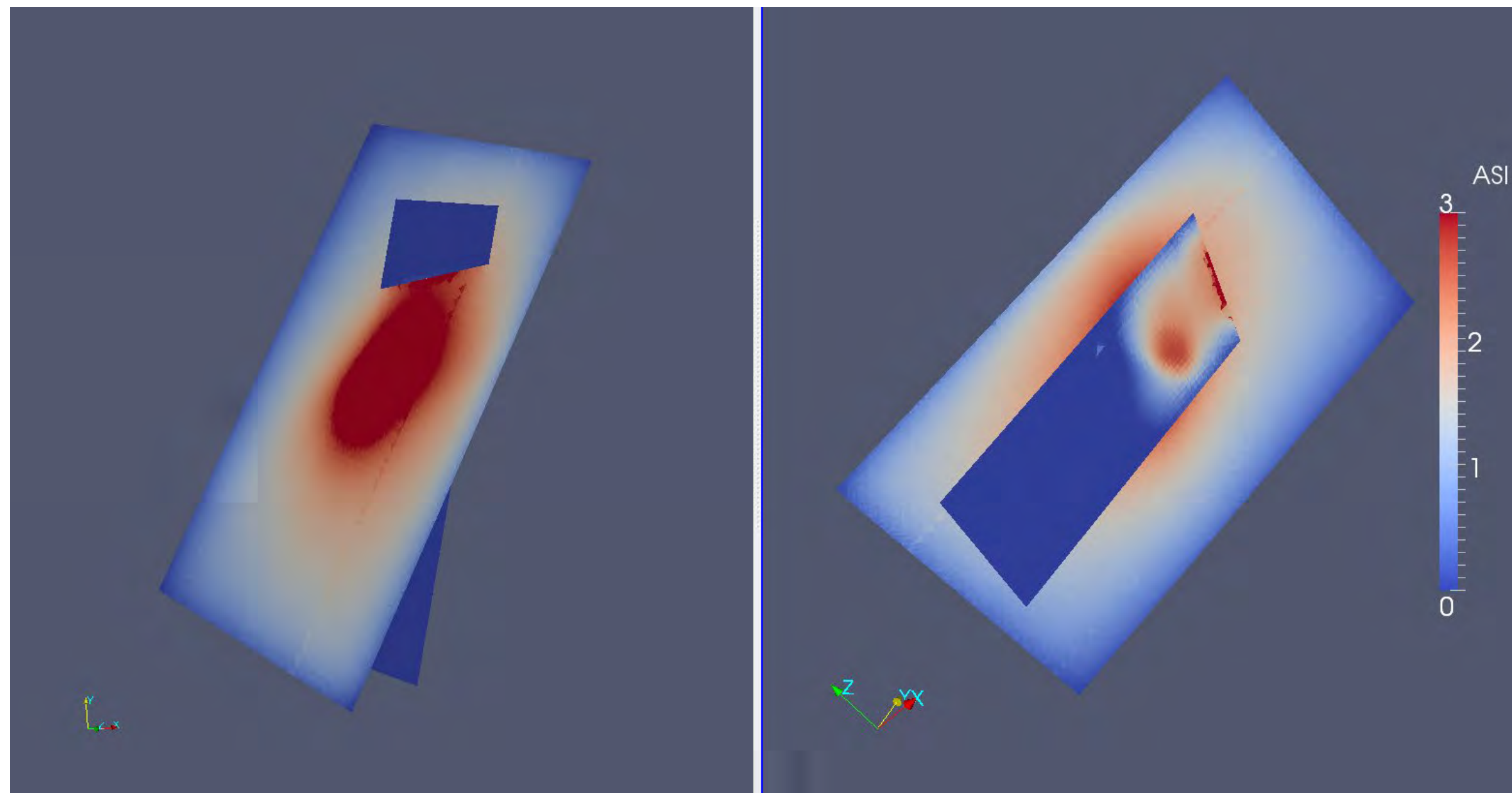


Fault Plane Solution

SHmax~70

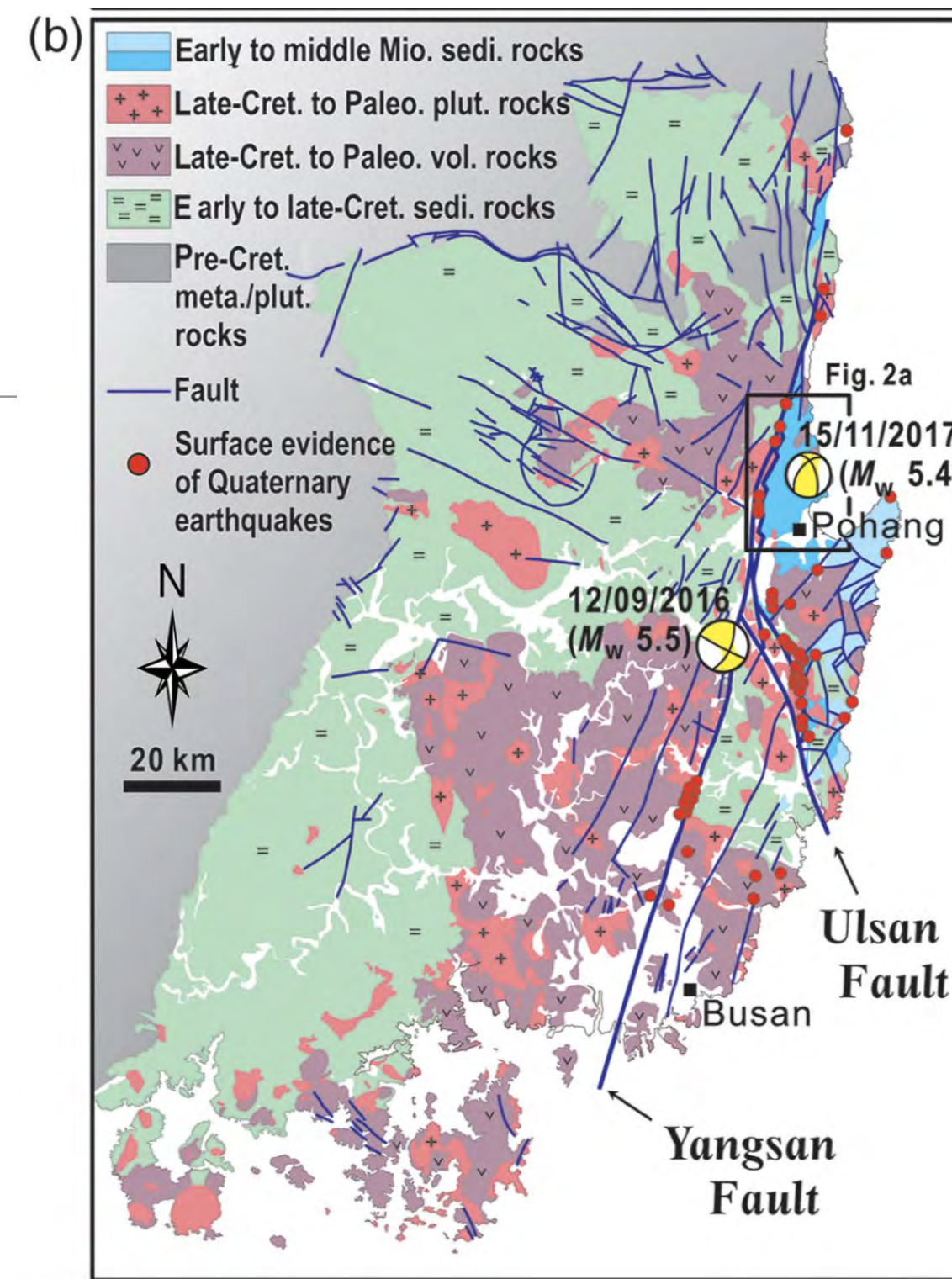


Lee et al., 2017



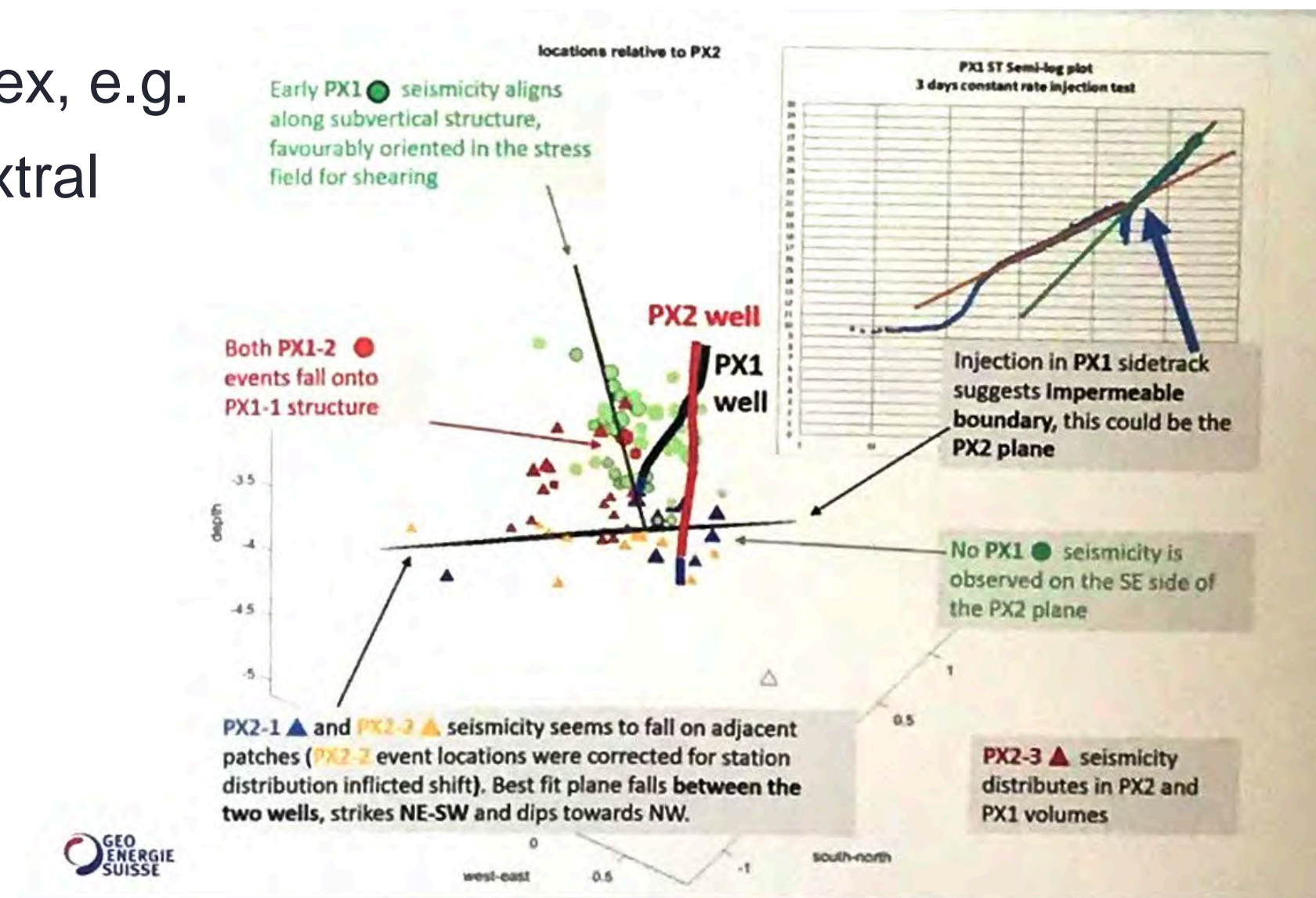
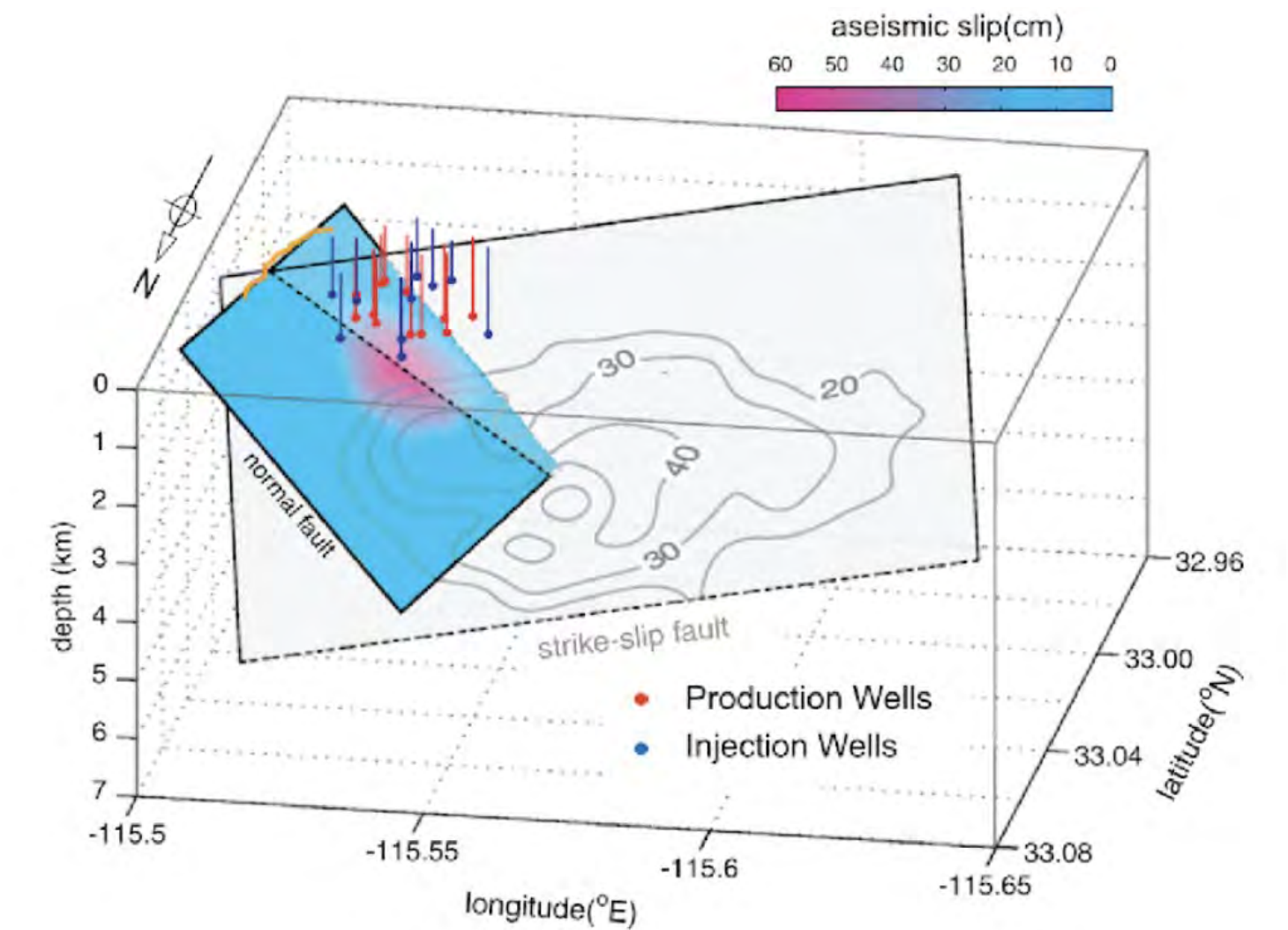
- Different fault geometry, local stress variations or stress concentrations (e.g. creep induced) will likely change rupture dynamics
- Preliminary fault reconstruction using ACLUD (Wang et al., 2013) produces two fault planes, with the secondary fault at larger strike
- Local stresses may be complex, e.g. affected by close-by large dextral strike-slip Yangsan Fault

Falko Bethmann et al., Poster yesterday

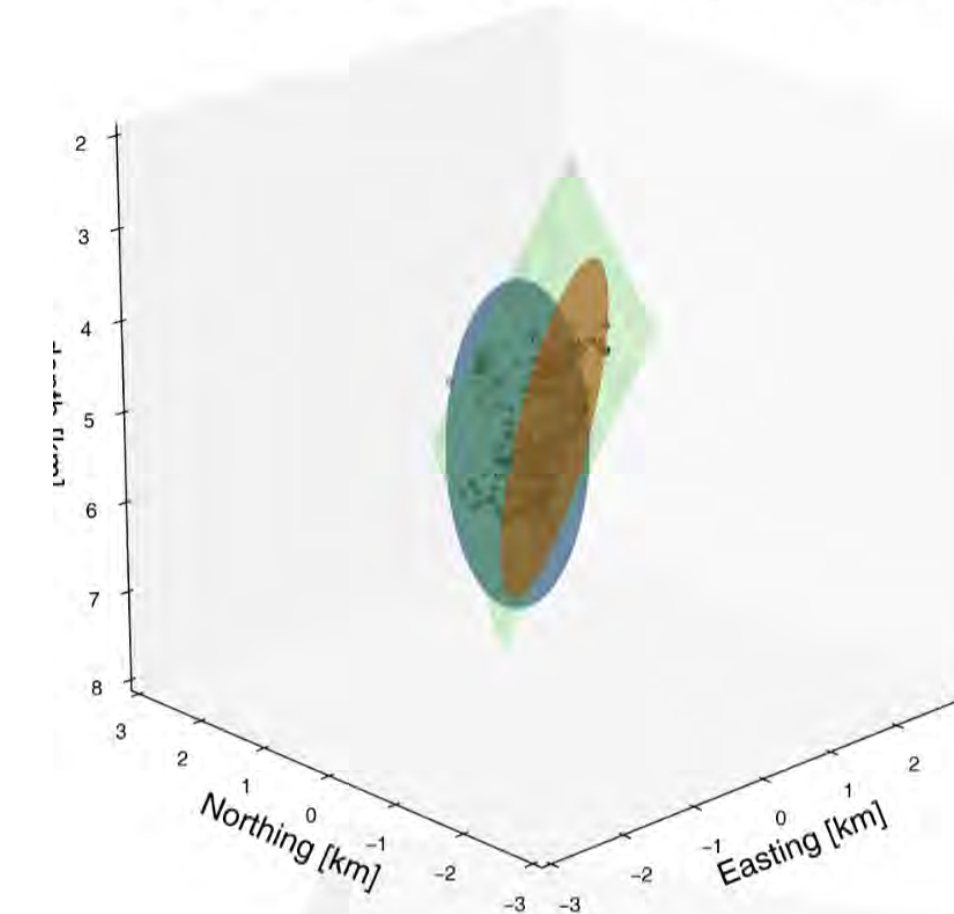


The 2012 Brawley swarm triggered by injection-induced aseismic slip

Shengji Wei ^{a, f}, Jean-Philippe Avouac ^a, Kenneth W. Hudnut ^b, Andrea Donnellan ^c, Jay W. Parker ^c, Robert W. Graves ^b, Don Helmberger ^a, Eric Fielding ^c, Zhen Liu ^c, Frederic Cappa ^{a, d}, Mariana Eneva ^e



ACLUD algorithm (Wang et al., 2013)

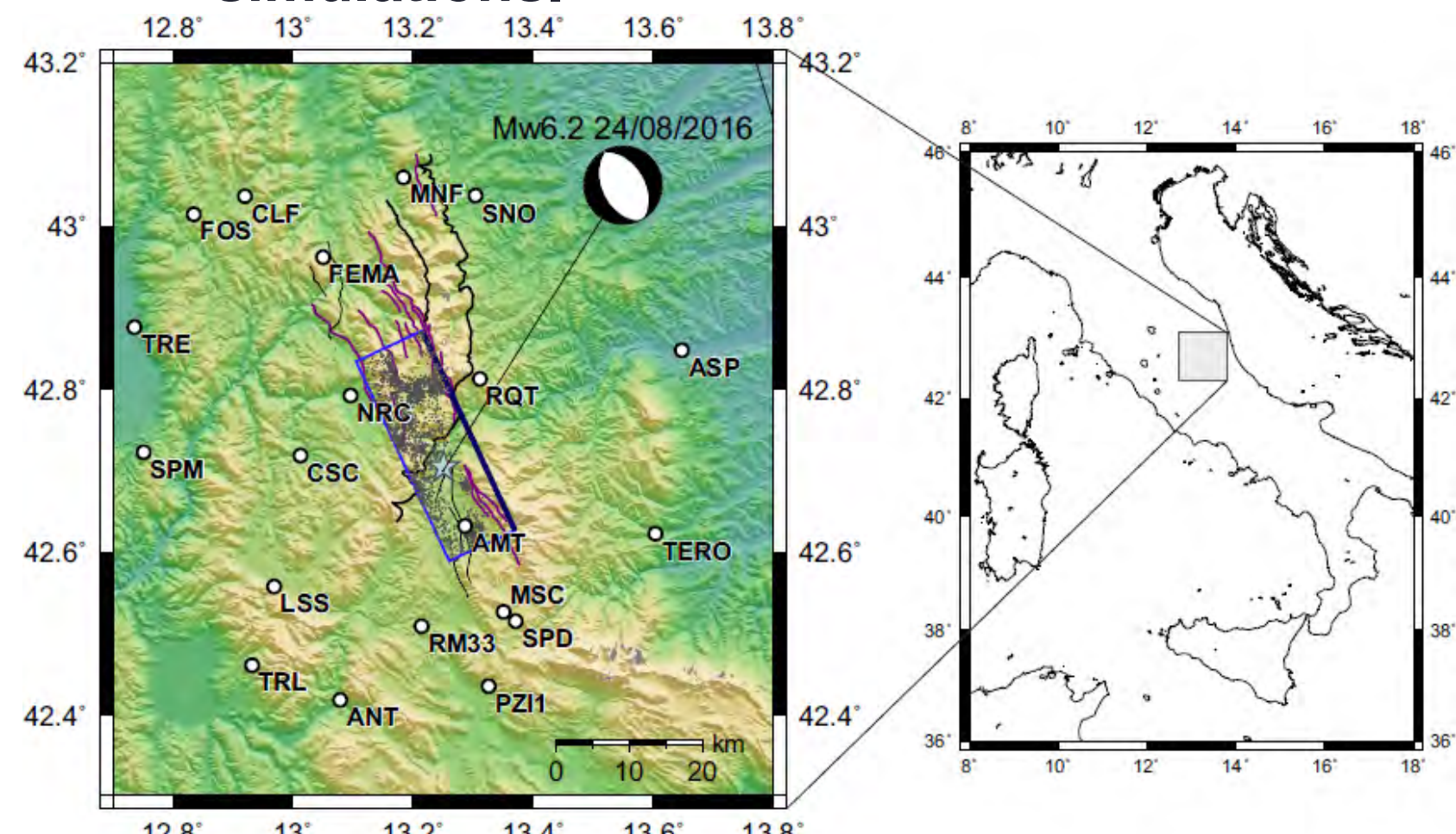


- Green plane: based on focal mechanisms
- Red and blue planes are generated from the algorithm

Preliminary fault reconstruction by Kadek Palgunadi

Fracture activation in geo-reservoirs

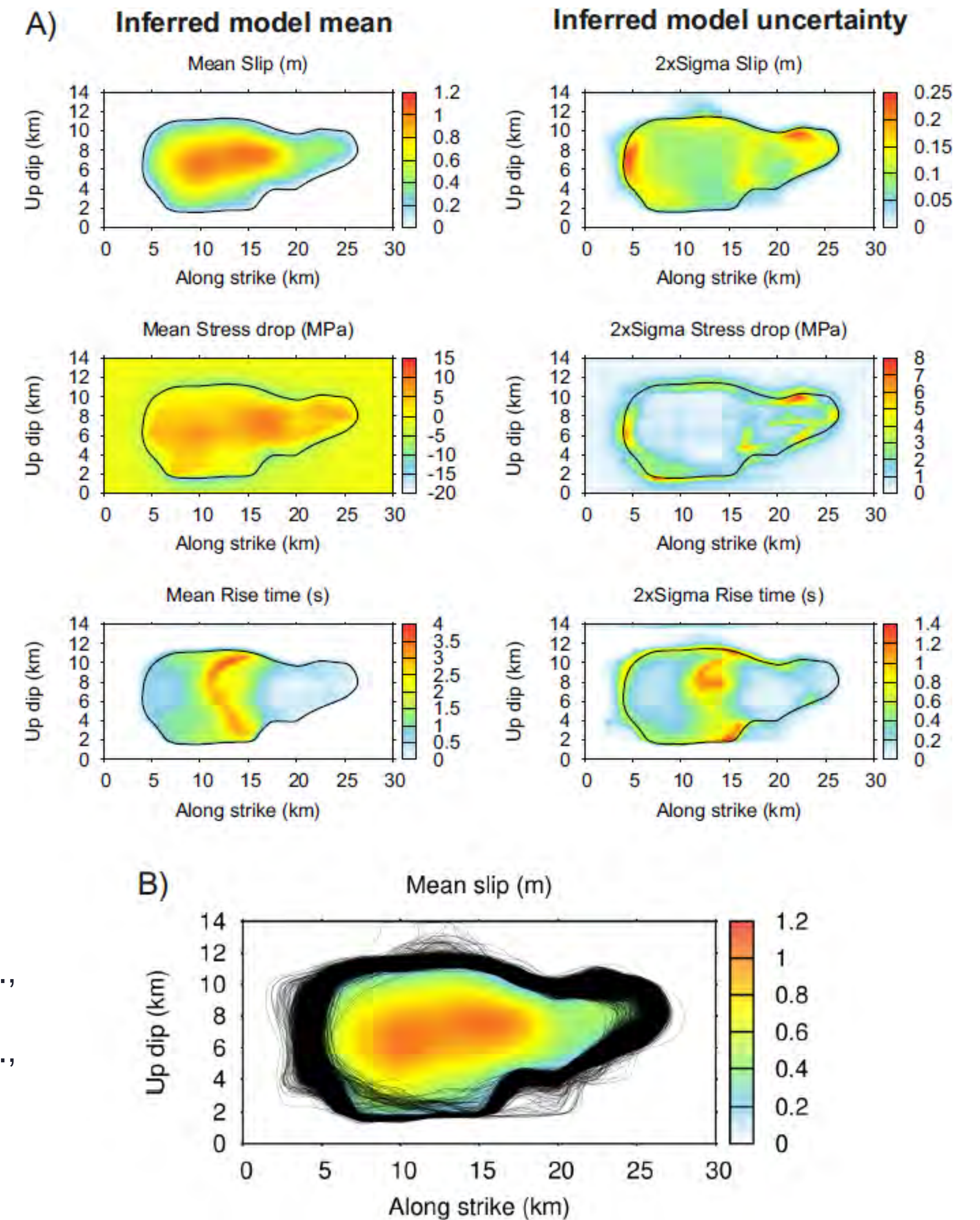
- Future directions: **Beyond scenario-based simulations**
- **Dynamic source inversion** for spatial distribution of initial stress and friction parameters
- **Bayesian framework** using Parallel Tempering Monte Carlo algorithm applied it to the 2016 Mw6.2 Amatrice, Italy event - visiting **millions** of dynamic rupture models
- Uncertainty quantification and constraining non-uniqueness in source inversions with: **Adjoint sensitivity analysis.**
Uncertainty quantification. Optimal design. Ensemble simulations.



Galovic et al., 2019a, subm.,

Galovic et al., 2019b, subm.,

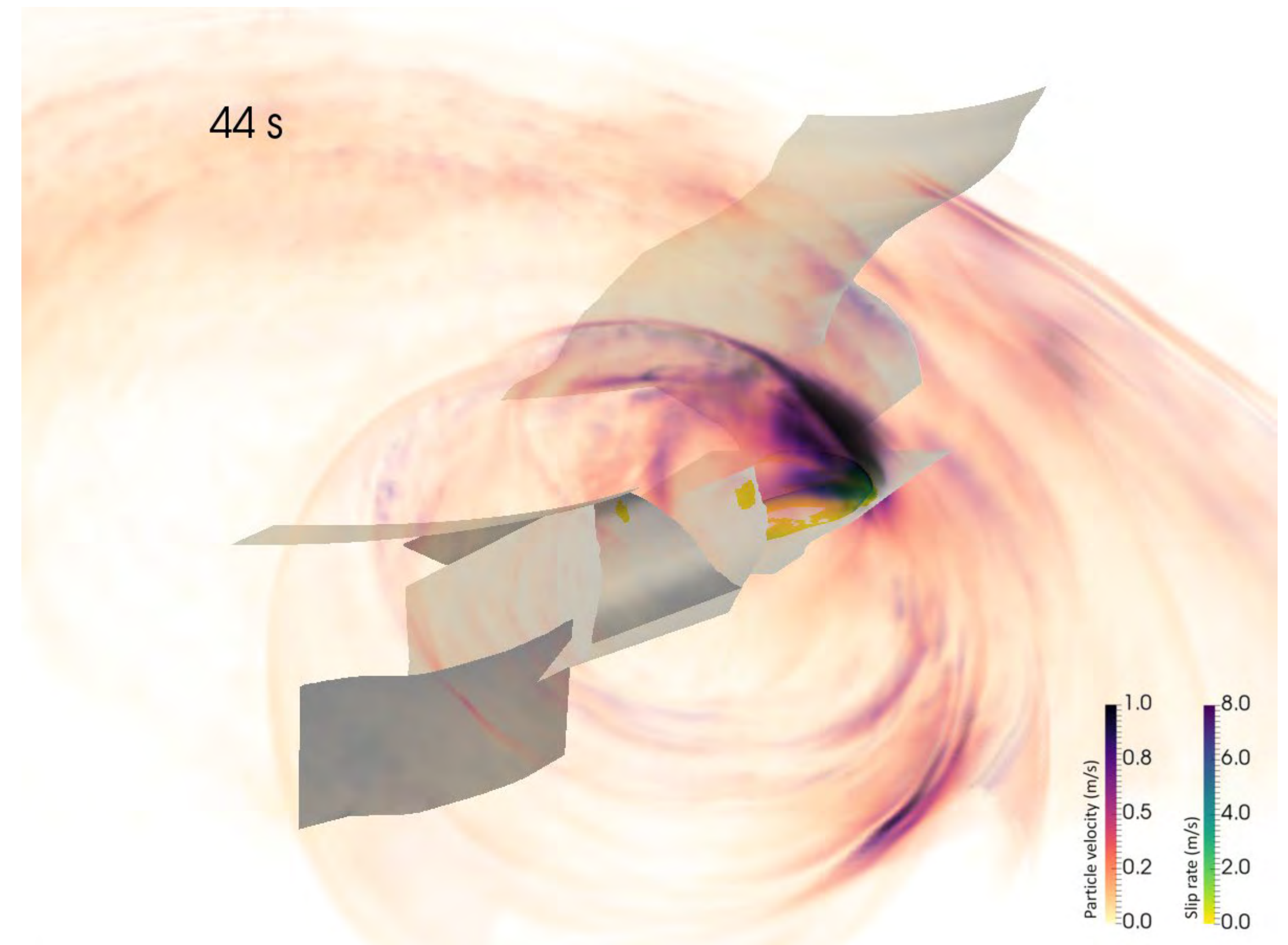
<https://eartharxiv.org/tmjv4/>



A) Rupture parameters inferred by the Bayesian dynamic inversion averaged over posterior samples (left) and the model parameters' uncertainty in terms of two sigma (right). B) Averaged model of slip (color-coded) with slip contours of all accepted posterior model samples displaying the uncertainty of the inferred spatial rupture extent.

Conclusions

- Physics-based modeling provides mechanically viable insight into the physical conditions that allow rupture on complex fault systems and helps constraining competing views on earthquake sources
- Observational constraints can be routinely included; Observational methods can themselves be constrained
- Advances in high-performance computing and dense observations allow us to go beyond scenario-based analysis, aiming for urgent response quickly after an event occurs, ensemble simulations, dynamic inversion and uncertainty quantification



A true epilogue is removed
from the story in time or space.

- *Extra Slides* -

Acknowledgements



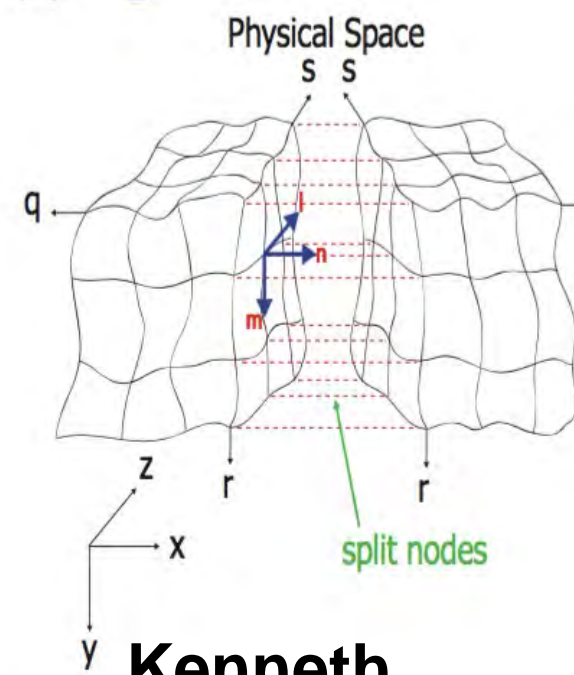
My research team at LMU Munich:



Bo Li



Duo Li



Kenneth Duru



Betsy Madden



Stephanie Wollherr



Thomas Ulrich



Sebastian Anger

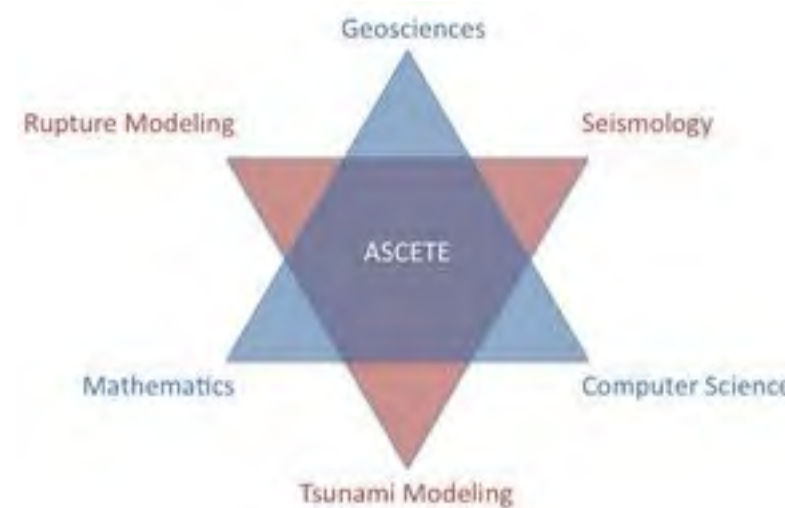


Taufiqurrahman

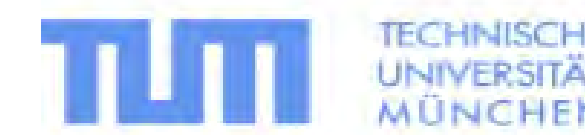


Aniko Wirp

Current projects:



Collaborators:



CoCoReCS
BAIES



Competitive Research Funds



CHARLES UNIVERSITY

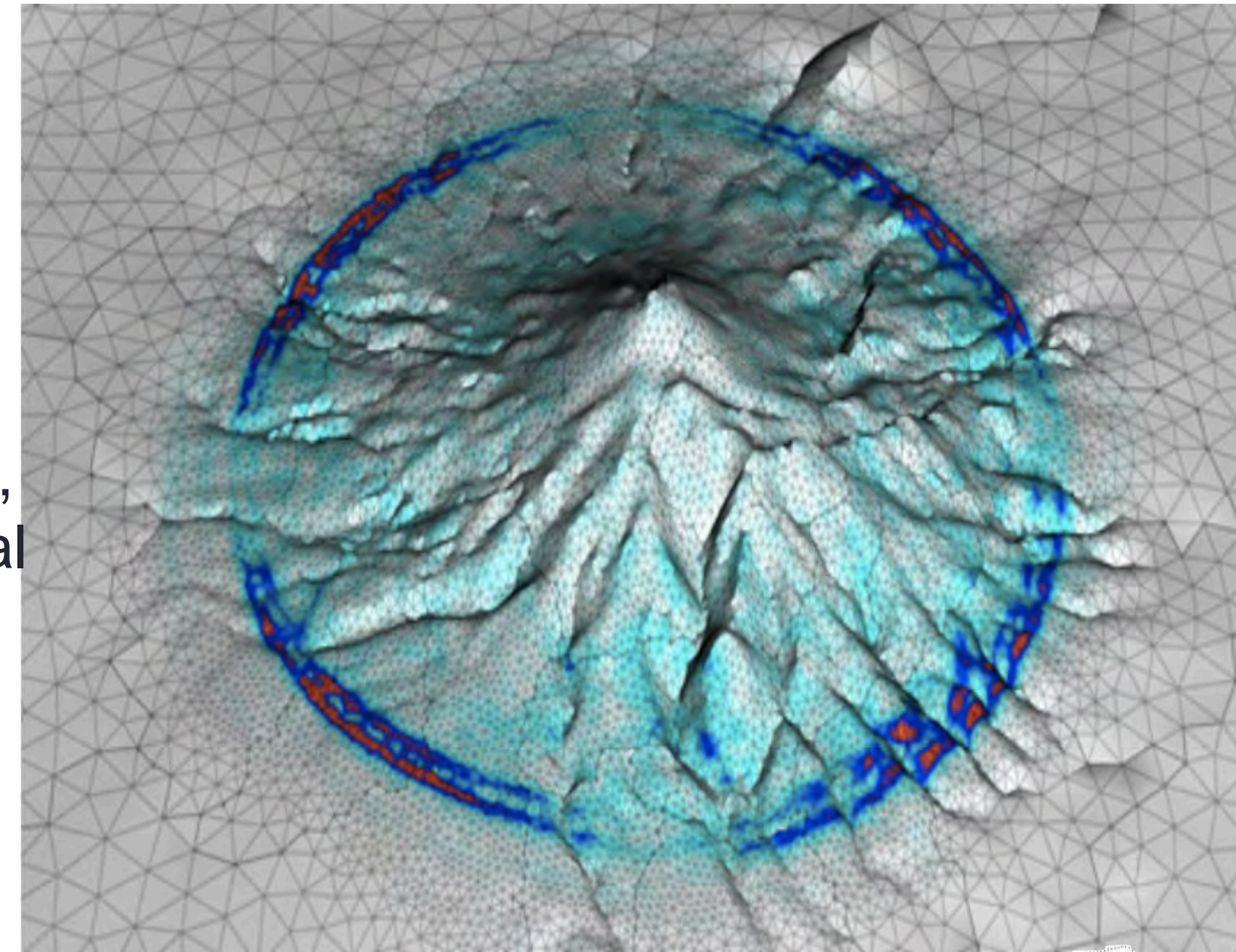
SeisSol - ADER-DG

A unique modelling framework

We develop and host an open-source Arbitrary high-order DERivative Discontinuous Galerkin (**ADER-DG**) software package. SeisSol solves the seismic wave equations in elastic, viscoelastic, and viscoplastic media on unstructured tetrahedral meshes.

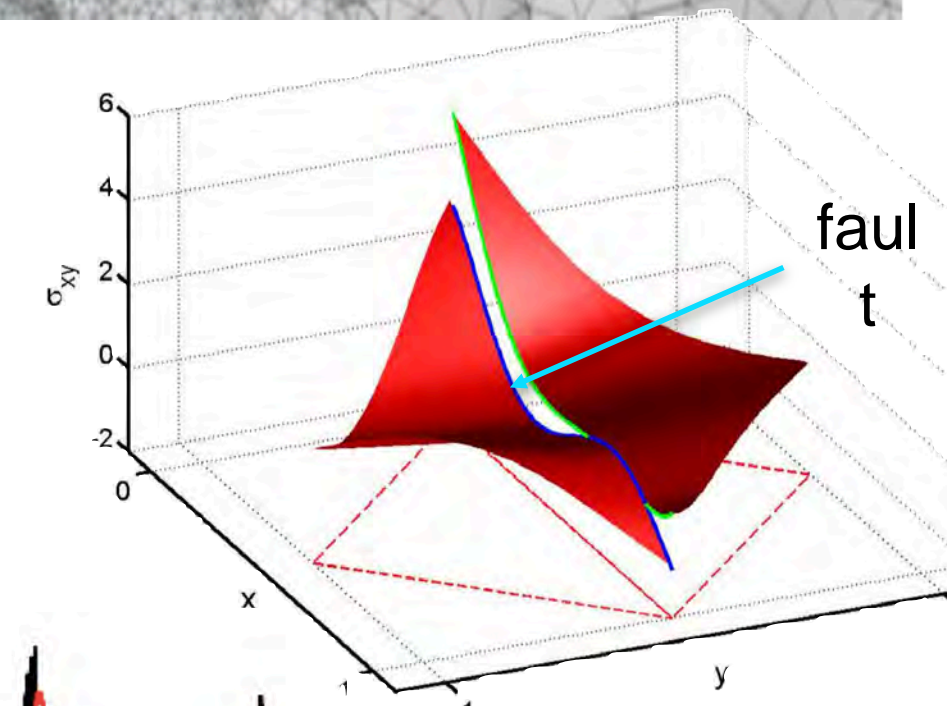
Our method, by design, permits:

- representing **complex geometries** - by discretising the volume via a tetrahedral mesh
- modelling **heterogenous media** - elastic, viscoelastic, viscoplastic, anisotropic
- **multi-physics coupling** - flux based formulation is natural for representing physics defined on interfaces
- **high accuracy** - modal flux based formulation allows us to suppress spurious (unresolved) high frequencies
- **high resolution** - suitable for parallel computing environments

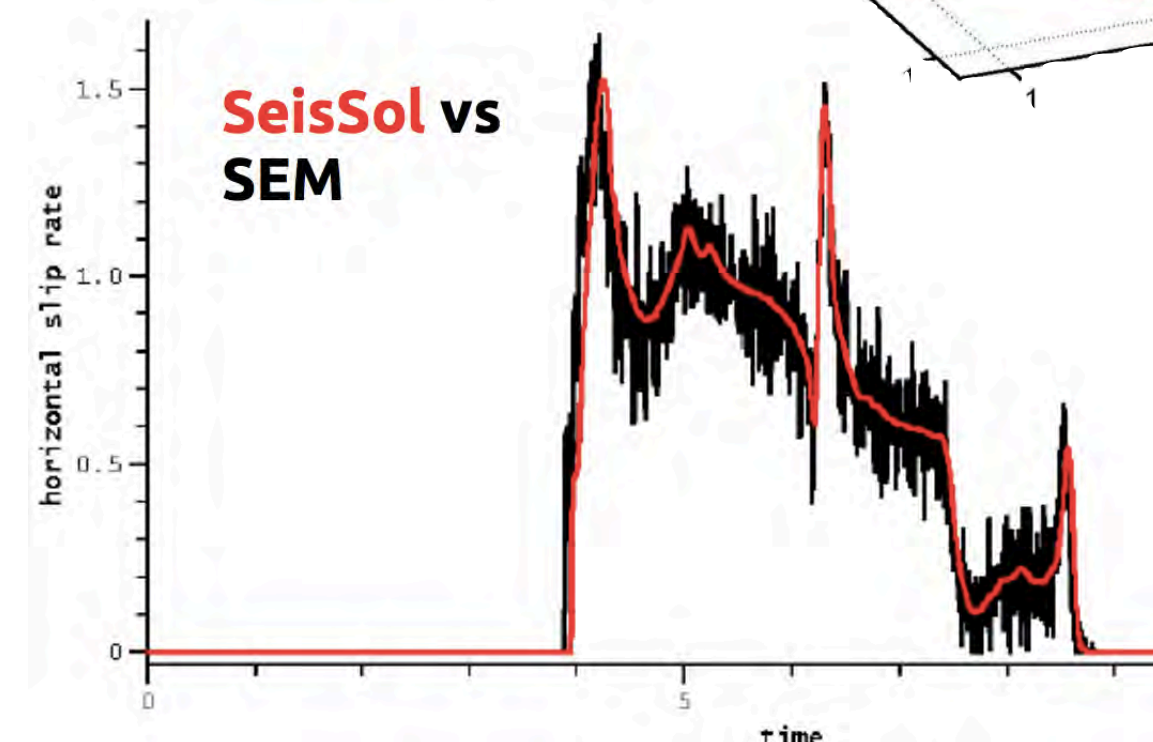


Wave field of a point source interacting with the topography of Mount Merapi Volcano.

PRACE ISC Award for producing the first simulations that obtained the “magical” performance milestone of 1 Peta-flop/s (10^{15} floating point operations per second) at the Munich Supercomputing Centre.



Representation of the shear stress discontinuity across the fault interface. Spontaneous rupture = internal boundary condition of flux term.



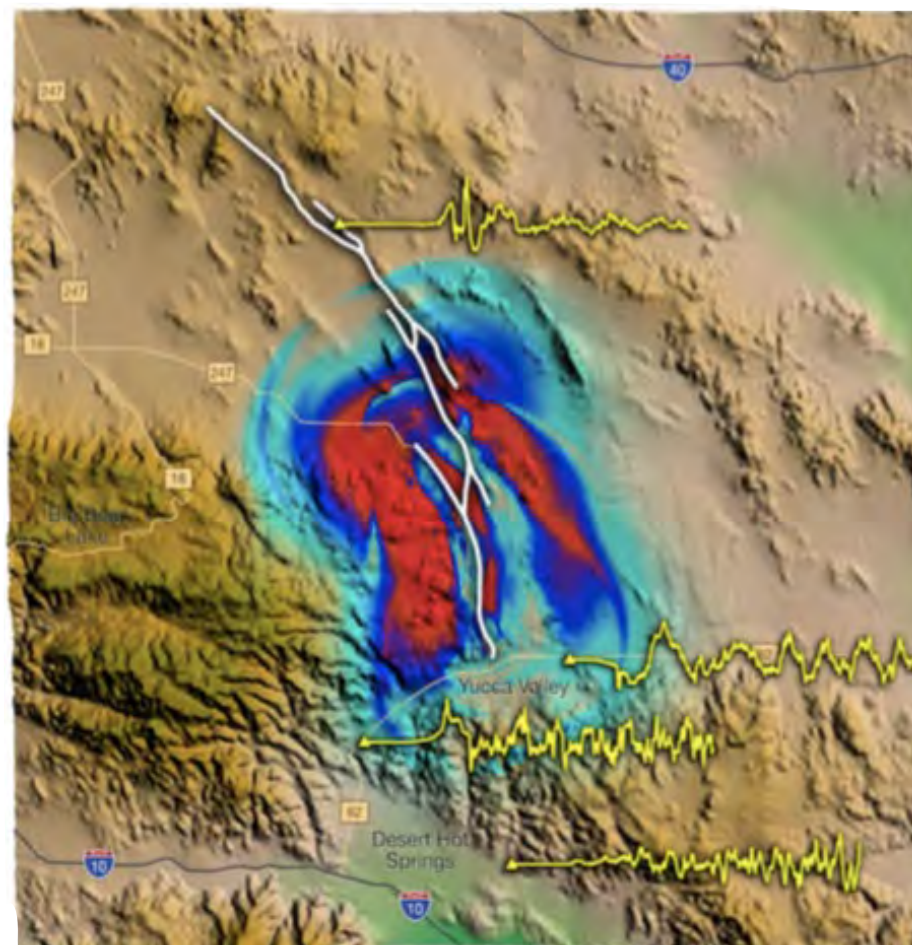
Due to the properties of the exact Riemann solver, solutions on the fault remain free of spurious oscillations

SeisSol - ADER-DG

A unique modelling framework

Breuer et al.,ISC14, Heinecke et al.,SC14
 Breuer et al.,IEEE16, Heinecke et al.,SC16
 Rettenberger et al., EASC16
 Upphoff & Bader, HPCS'16
 Upphoff et al., SC17

Gordon Bell Prize Finalist, SC14



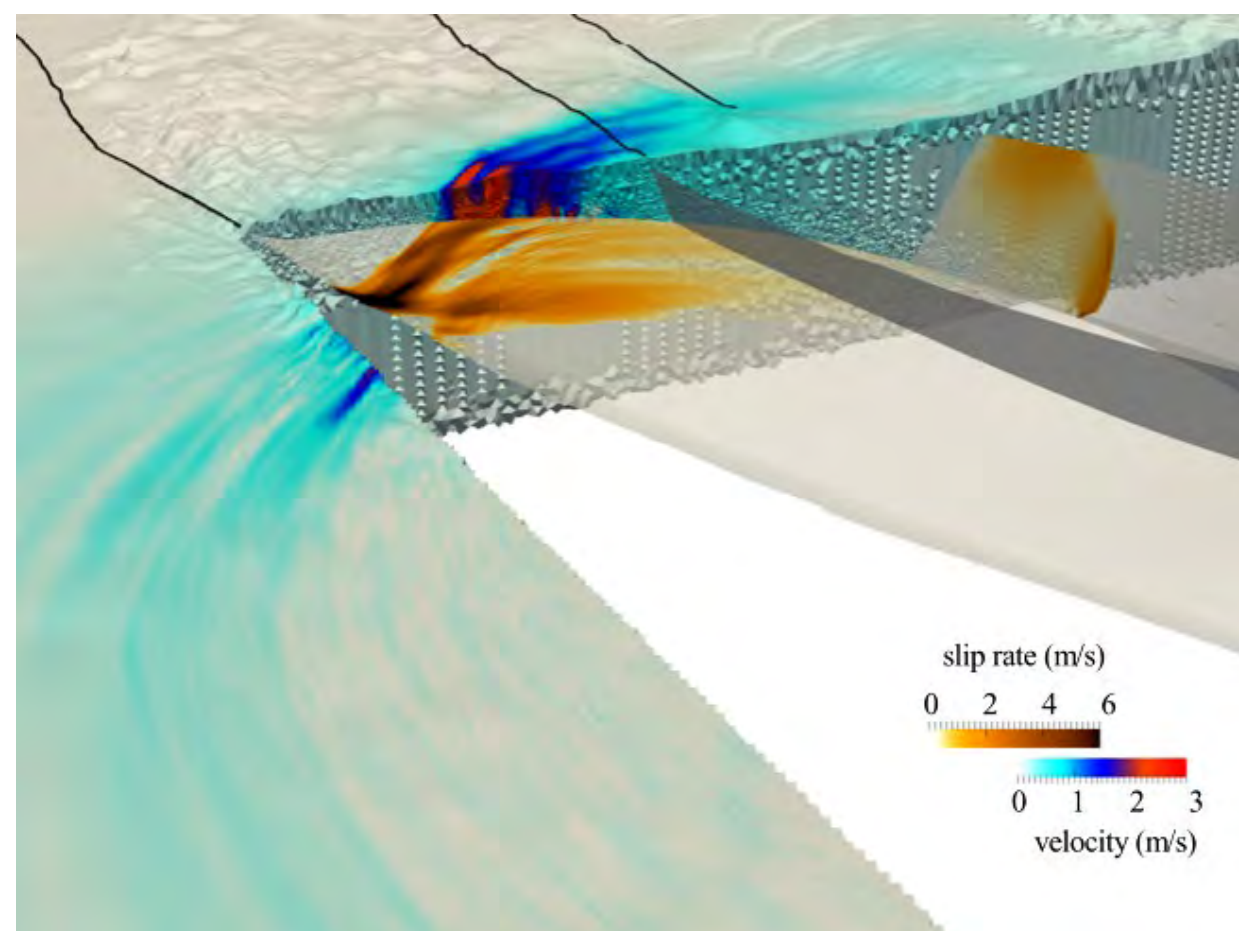
“Geophysics” Version

Landers scenario
 (96 billion DoF,
 200,000 time steps)

- Fortran 90
- MPI parallelised
- Ascii based, serial I/O

- Hybrid MPI+OpenMP parallelisation
- Parallel I/O (HDF5, inc. mesh init.)
- Assembler-level DG kernels
- multi-physics off-load scheme for many-core architectures

- > 1 PFlop/s performance
- 90% parallel efficiency
- 45% of peak performance
- 5x-10x faster time-to-solution
- 10x-100x bigger problems



Sumatra scenario
 (111 billion DoF,
 3,300,000 time steps)

- **Cluster-based local time stepping**
- Code generator also for advanced PDE's as viscoelastic attenuation
- Asagi (XDMF)-geoinformation server
- Asynchronous input/output
- Overlapping computation and communication

- Optimized for Intel KNL
- Speed up of 14x
- 14 hours compared to almost 8 days for Sumatra scenario on SuperMuc2

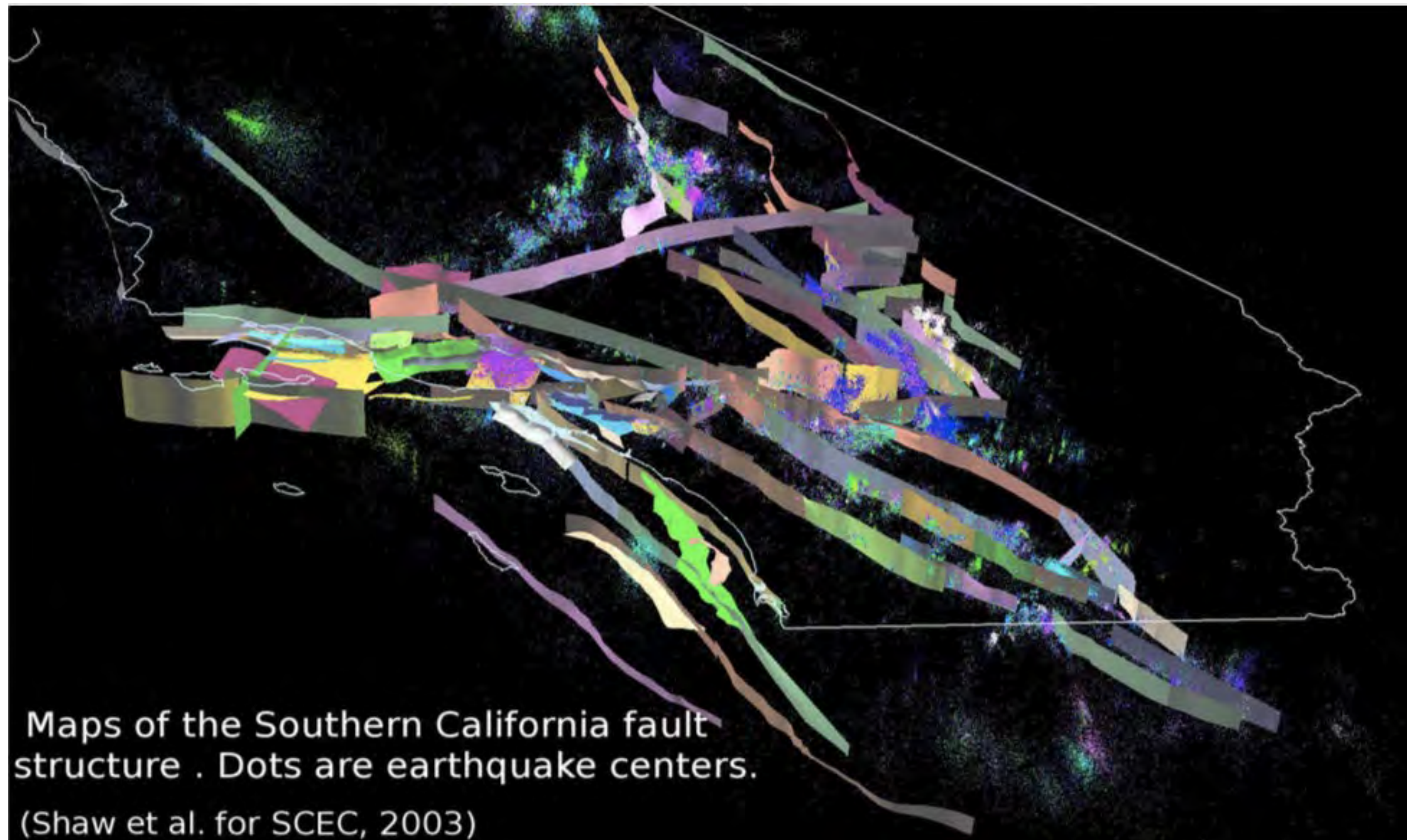
Best Paper Award, SC17

The only software that allows for rapid setup of models with realistic non-planar fault systems while exploiting the accuracy of a high-order numerical method.

Dynamic rupture earthquake simulations

the real world

→ Few methods support all modelling requirements



Multitude of spatio-temporal scales: fault geometry spans hundreds of km; frictional process zone size is m (or even cm) scale, tectonic loading (seismic cycle) 10-10000 years; rise time on second scale

- Non-planar, intersecting faults
- Non-linear friction
- Heterogeneities in stress and strength
- Dynamic damage around the fault
- Fault roughness and segmentation on all scales
- Bi-material effects
- Low velocity zones surrounding faults
- Thermal pressurization of fault zone fluids
- Thermal decomposition
- Dilatancy of the fault gouge
- Flash heating, melting, lubrication
- Feedback mechanisms across time scales

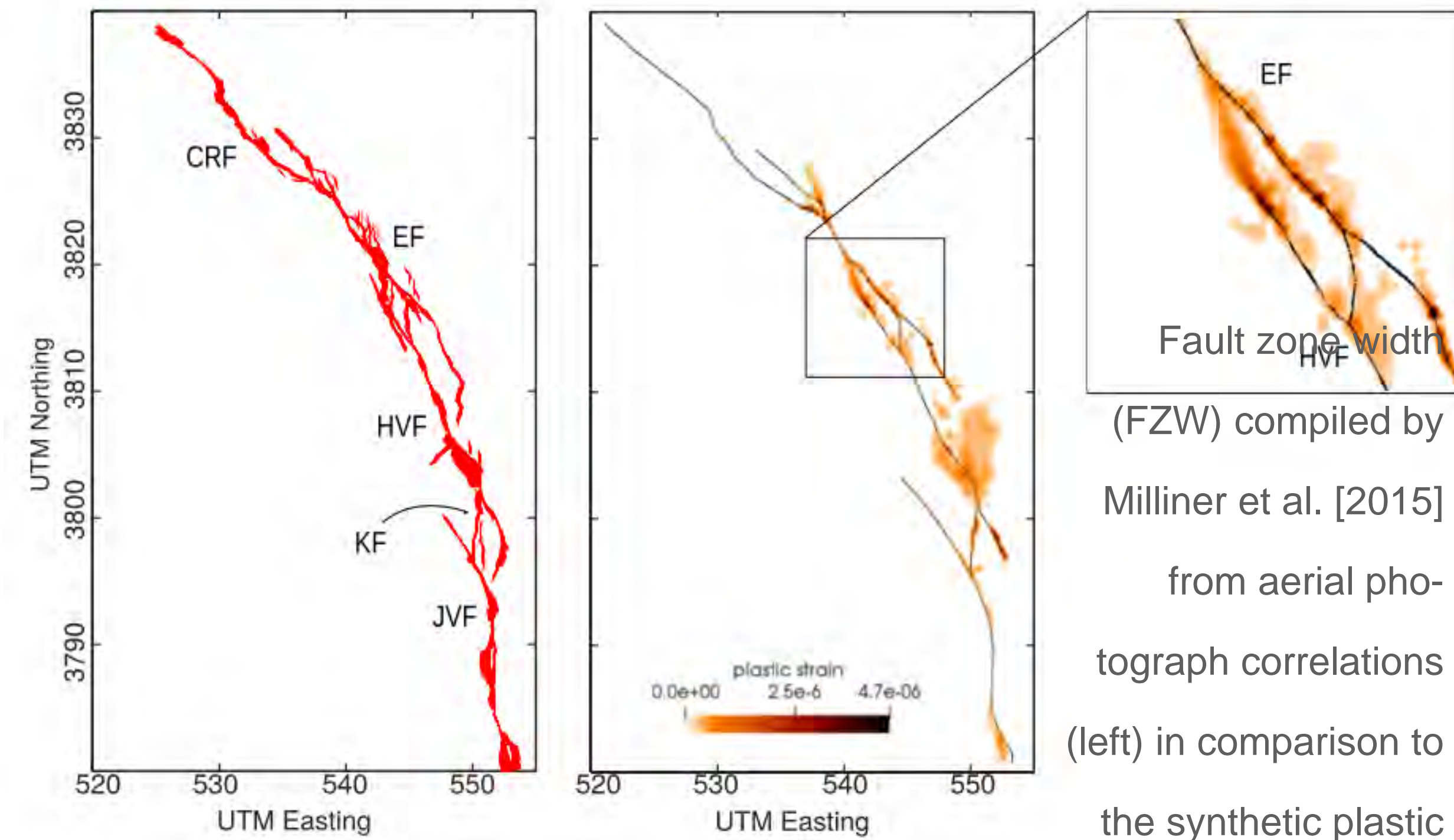
... this list grows continuously

The 1992 Mw 7.3 Landers earthquake

“reloaded” (Wollherr et al., preprint [doi:10.31223/osf.io/kh6j9](https://doi.org/10.31223/osf.io/kh6j9))

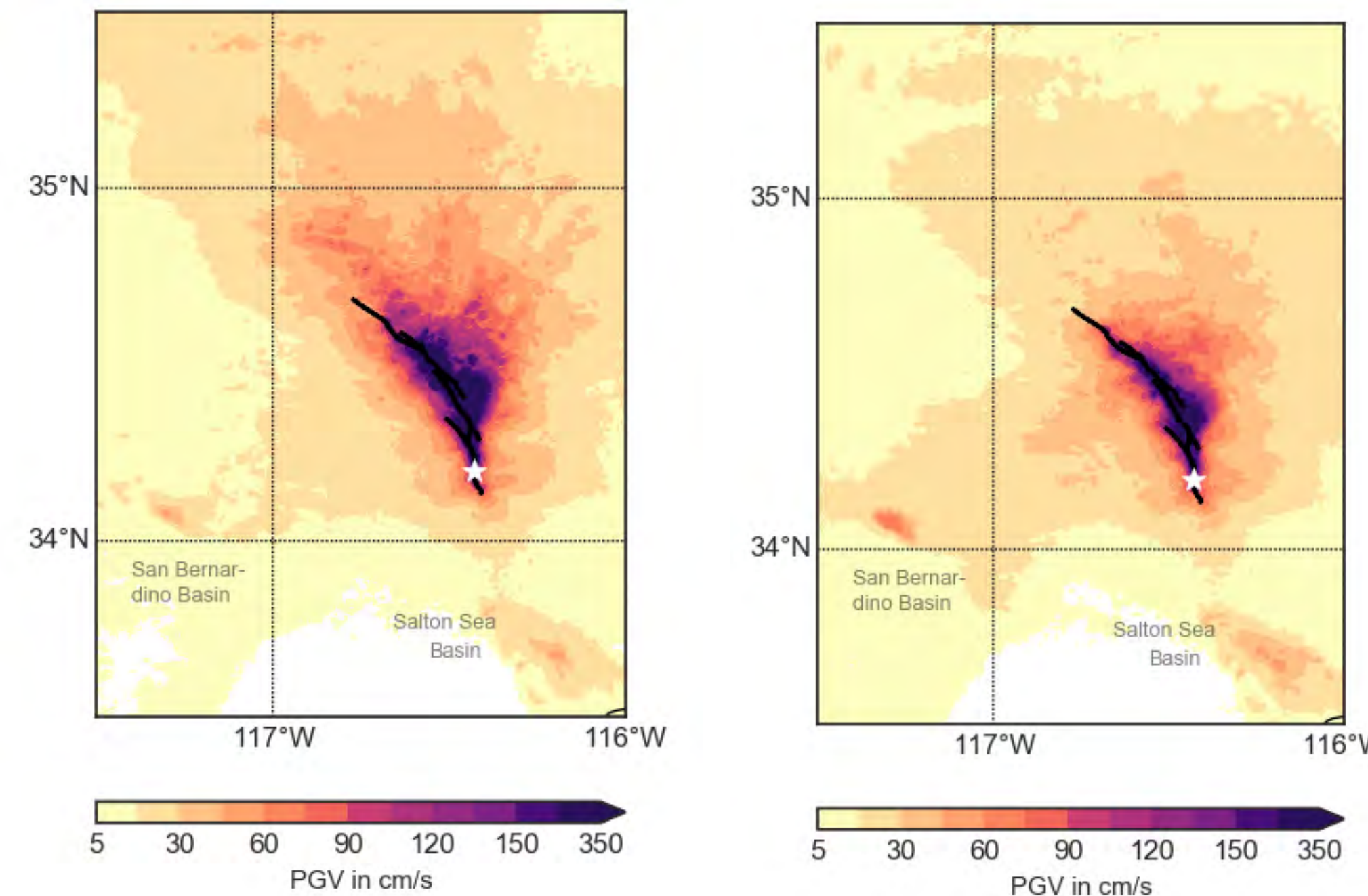
Multi-physics, such as off-fault plasticity, matters!

- **Drastic increase of off-fault deformation in geometrically complex fault regions** enhancing geometric barriers, hindering rupture transfers and matching newly available mapping
- **Strain localisation** forming non-prescribed ‘faults’
- Off-fault plasticity **reduces peak ground velocities (by 35%)** as well as ground motion **variability and directivity**



Fault zone width (FZW) compiled by Milliner et al. [2015] from aerial photograph correlations (left) in comparison to the synthetic plastic

Simulated GMRotD50 PGVs for a purely elastic simulation cf. the visco-elasto-plastic simulation

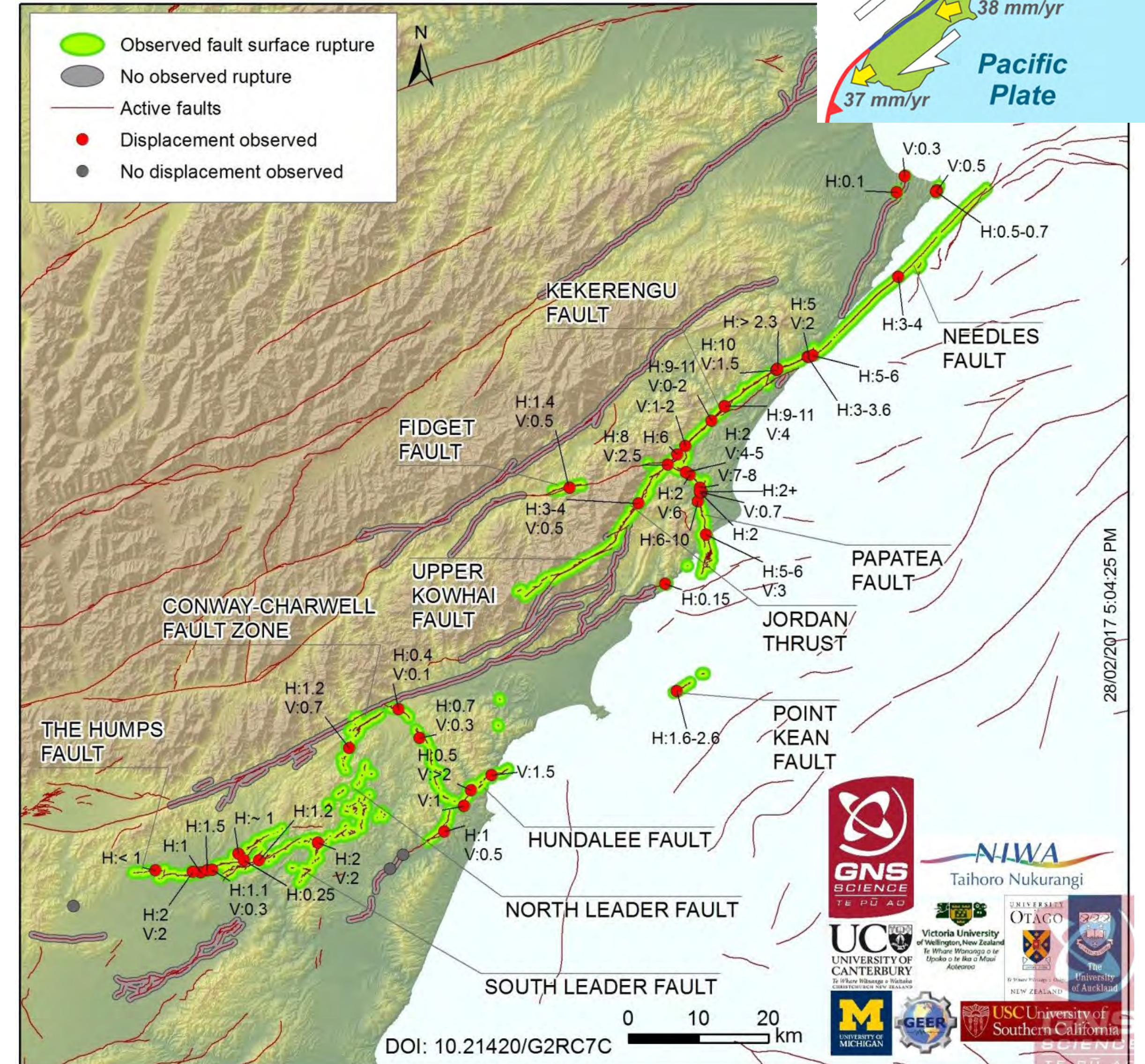


The 2016, Mw7.8 Kaikōura earthquake - a rupture cascade on weak crustal faults

- Rupture propagation across highly segmented fault system with **diverse orientations and faulting mechanisms (strike-slip, thrusting)**
- Duration of ~100s, 200km of rupture, triggered landslides, local tsunami
- 2 deaths, 57 injured, damaged infrastructure, e.g. bridges, road subsidence



Keekerengu Fault rupture displacement by ~10 meters

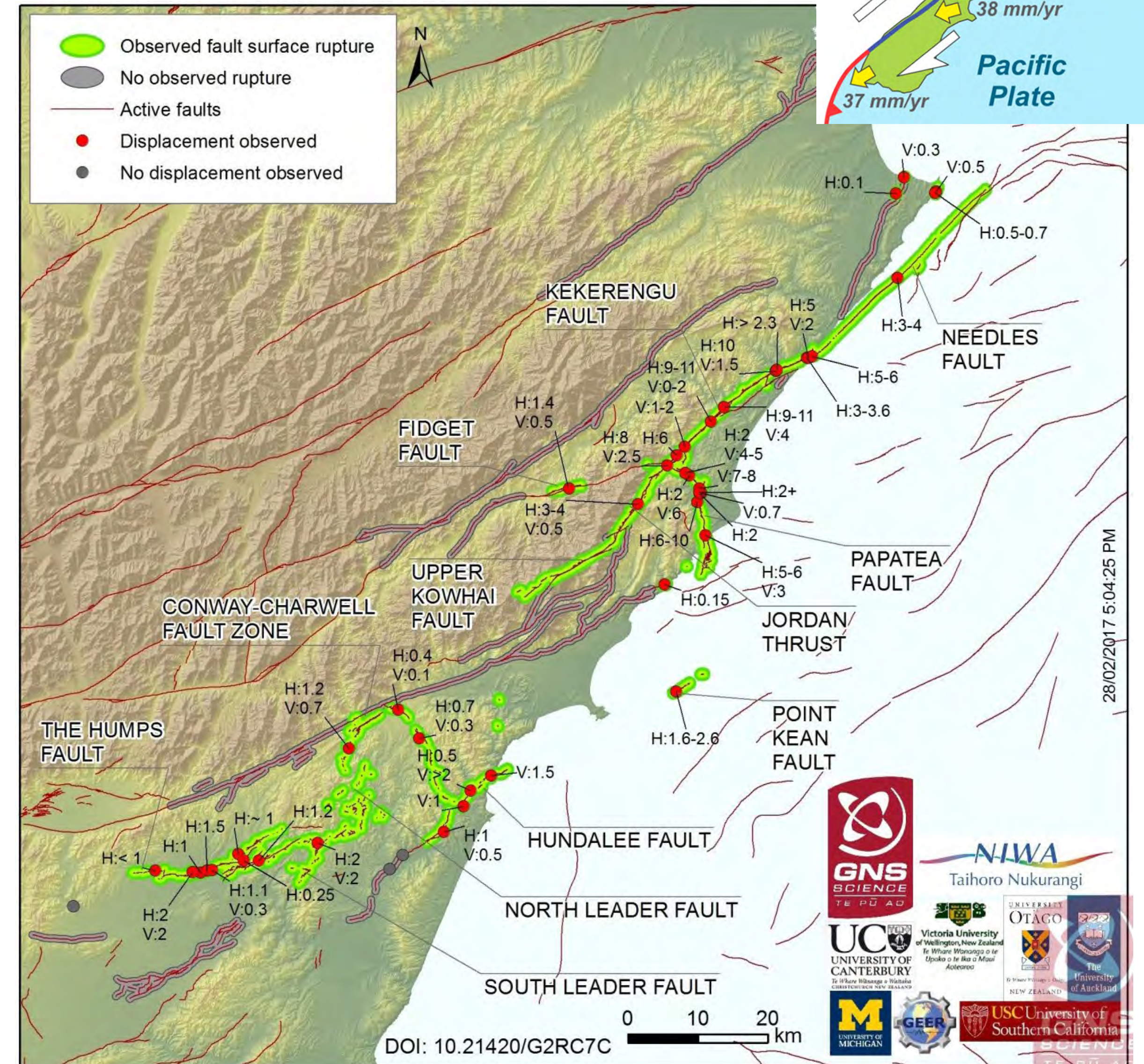


The 2016, Mw7.8 Kaikōura earthquake - a rupture cascade on weak crustal faults

Open questions:

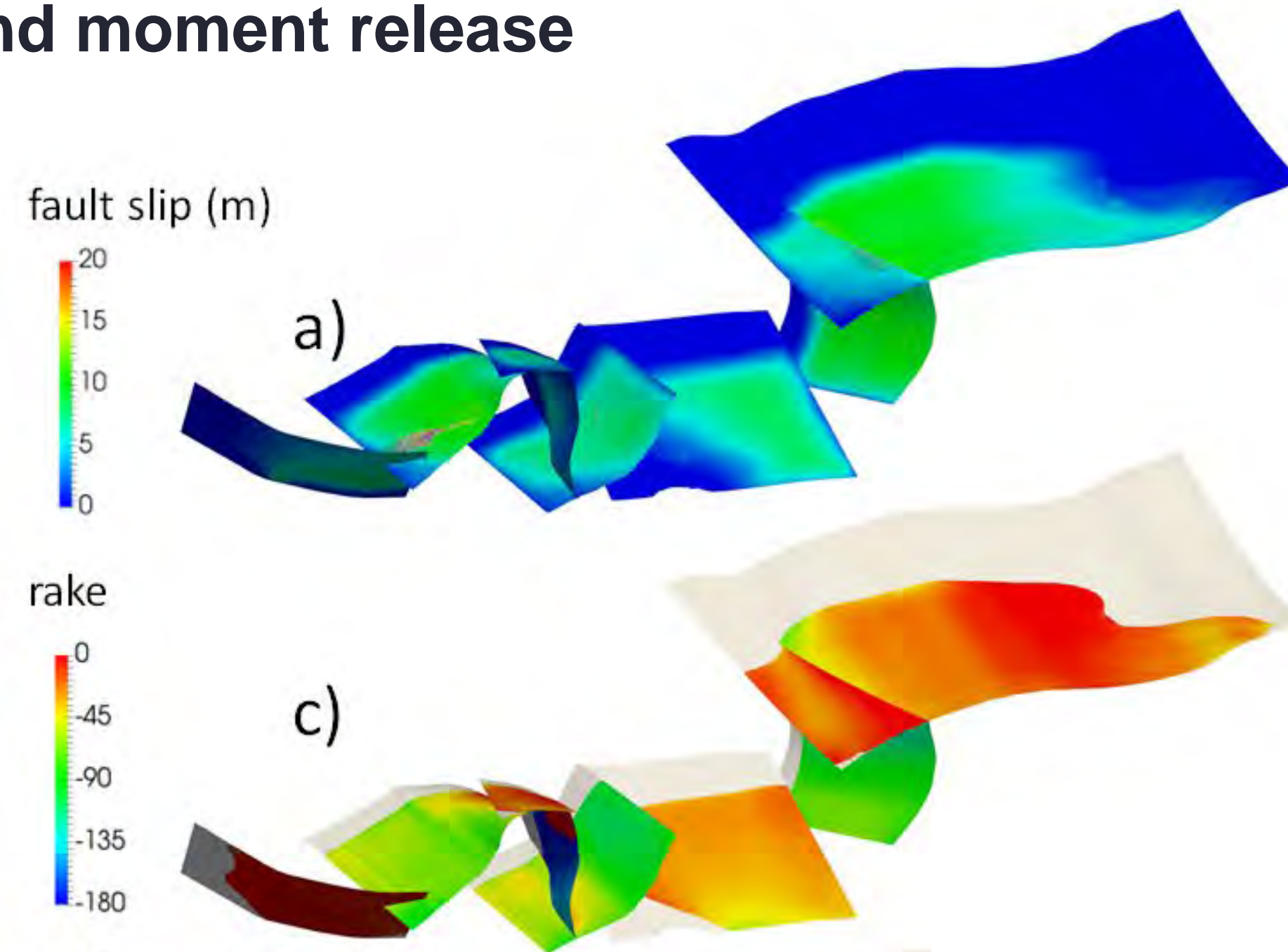
- Did the rupture of multiple crustal faults **connect via slip on a subduction interface?**
- A 15 km large gap separating the surface ruptures of the Hundalee and Upper Kowhai faults - **Can earthquake ruptures jump across wider fault gaps than previously thought?**
- Why was this earthquake **anomalously slow?**
- Why did the **Hope Fault** not rupture?
- How can such a complex cascade occur on faults that have **low apparent friction?**

Physics-based dynamic rupture simulations can help constraining those competing views and provide a self-consistent earthquake source description

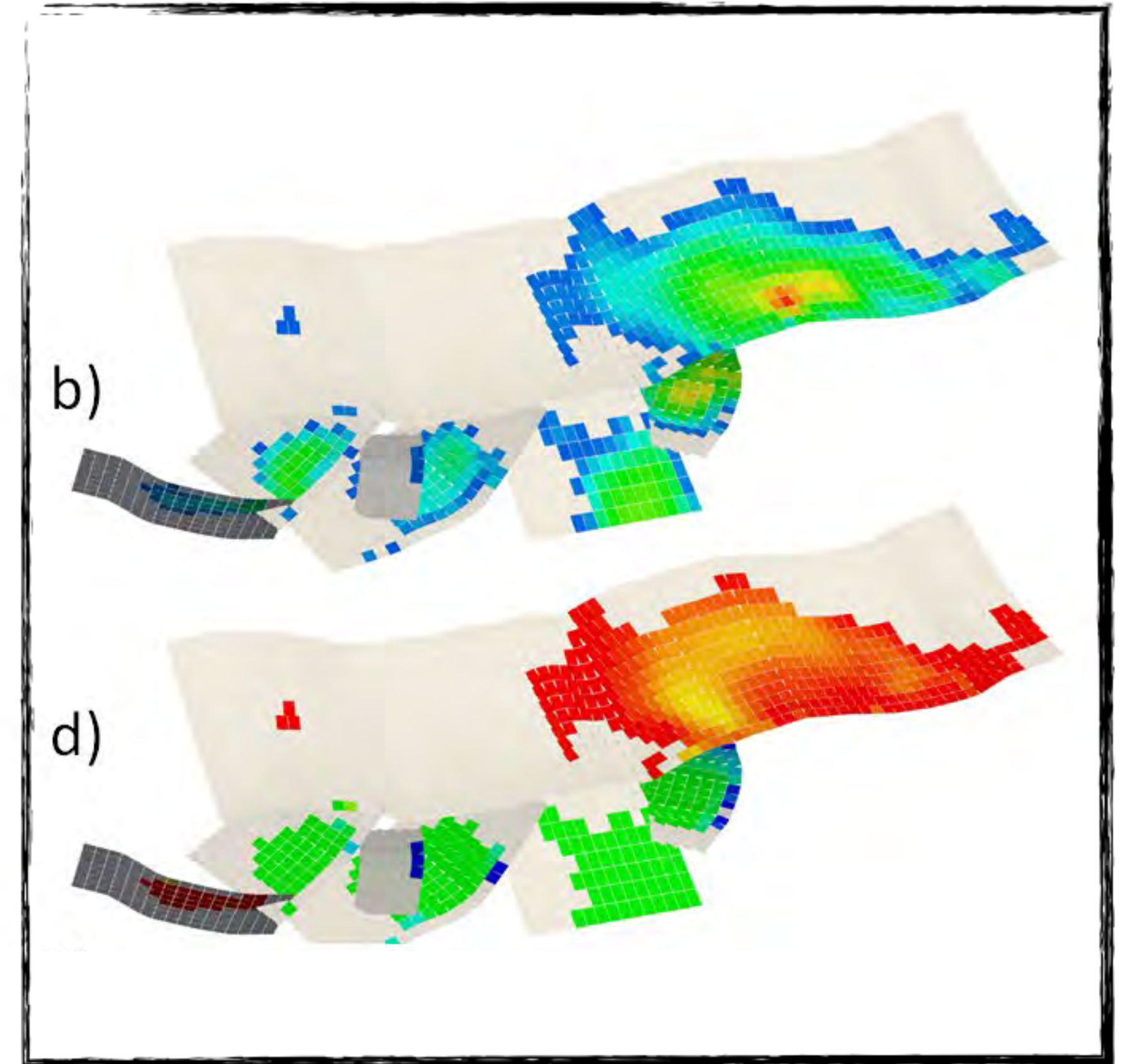


The 2016, Mw7.8 Kaikōura earthquake - **constrained by observation**

- Slip distribution and moment release

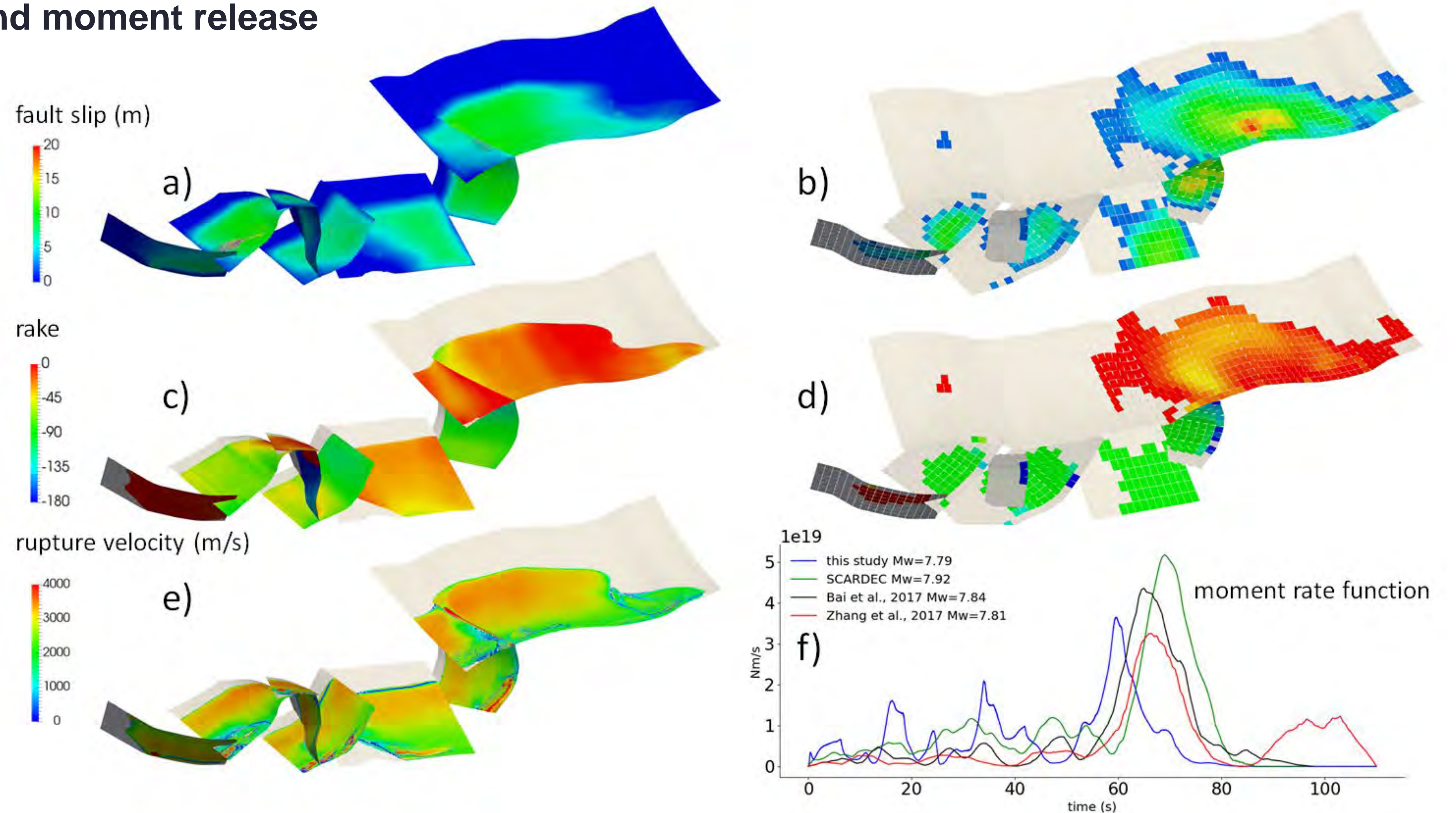


Kinematic source inversion (Xu et al., 2018)



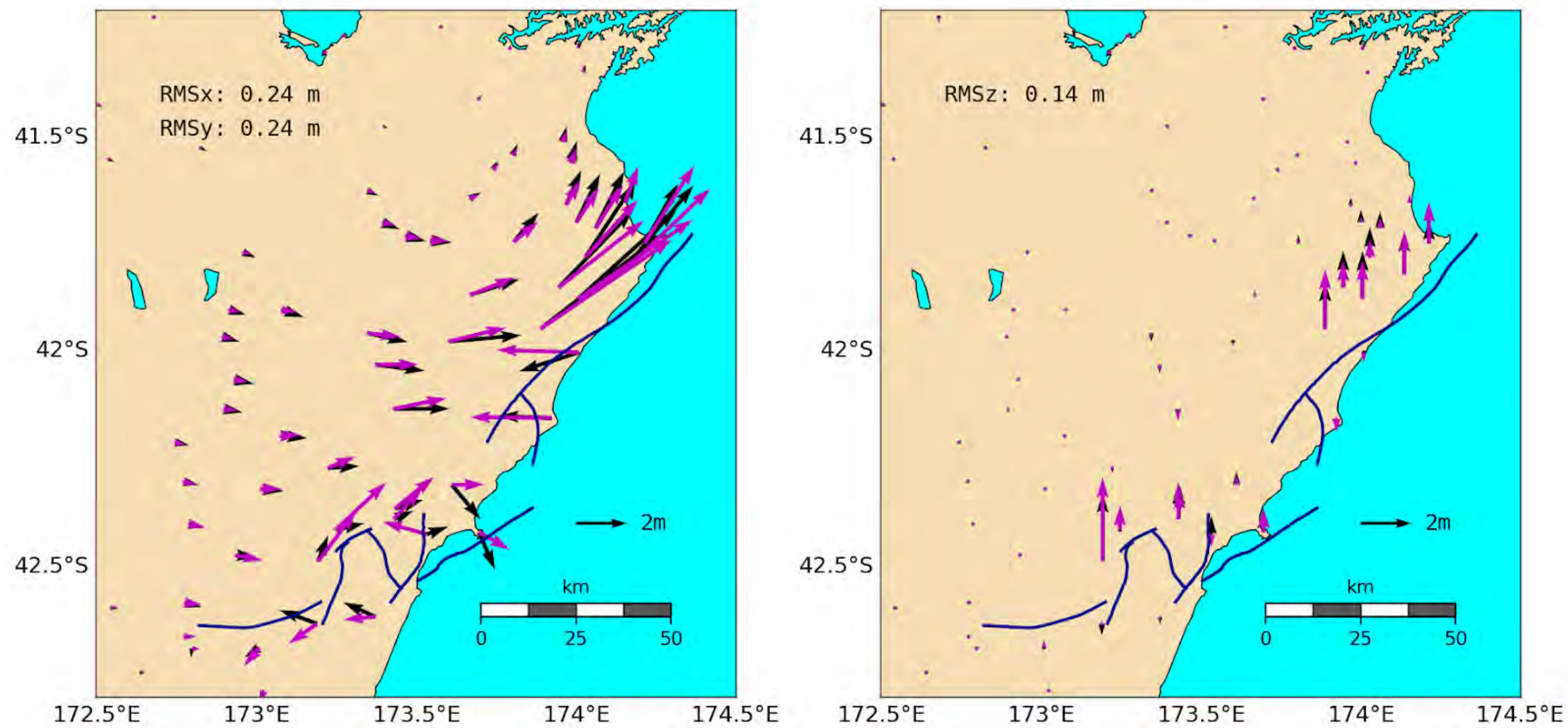
The 2016, Mw7.8 Kaikōura earthquake - constrained by observation

- Slip distribution and moment release



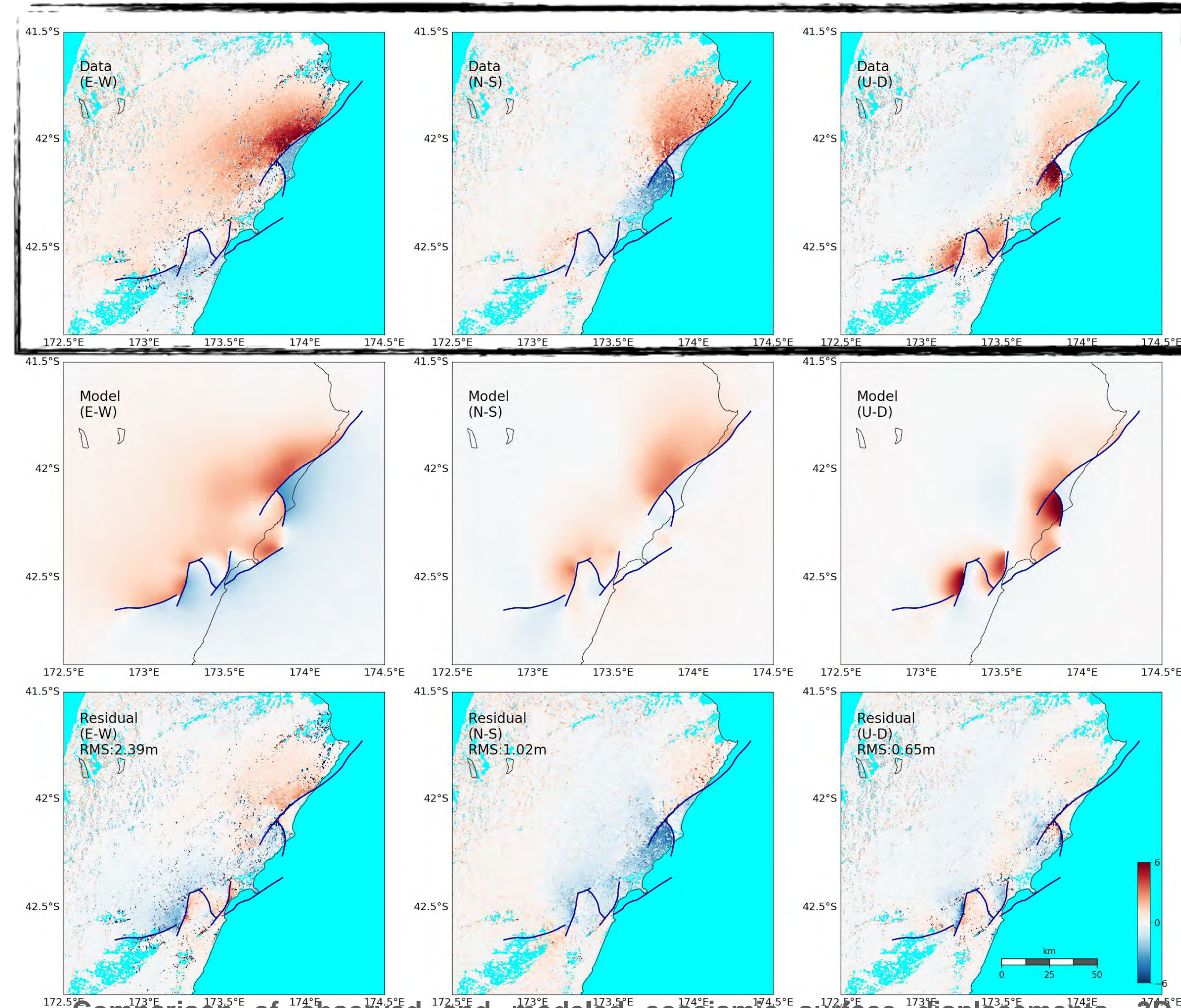
The 2016, Mw7.8 Kaikōura earthquake - constrained by observation

- Ground deformation



Comparison of observed (black, Hamling et al. 2017) and modeled (magenta) horizontal (left) and vertical (right) ground displacement at GPS stations. Root-mean-square (RMS) misfits are provided for each component.

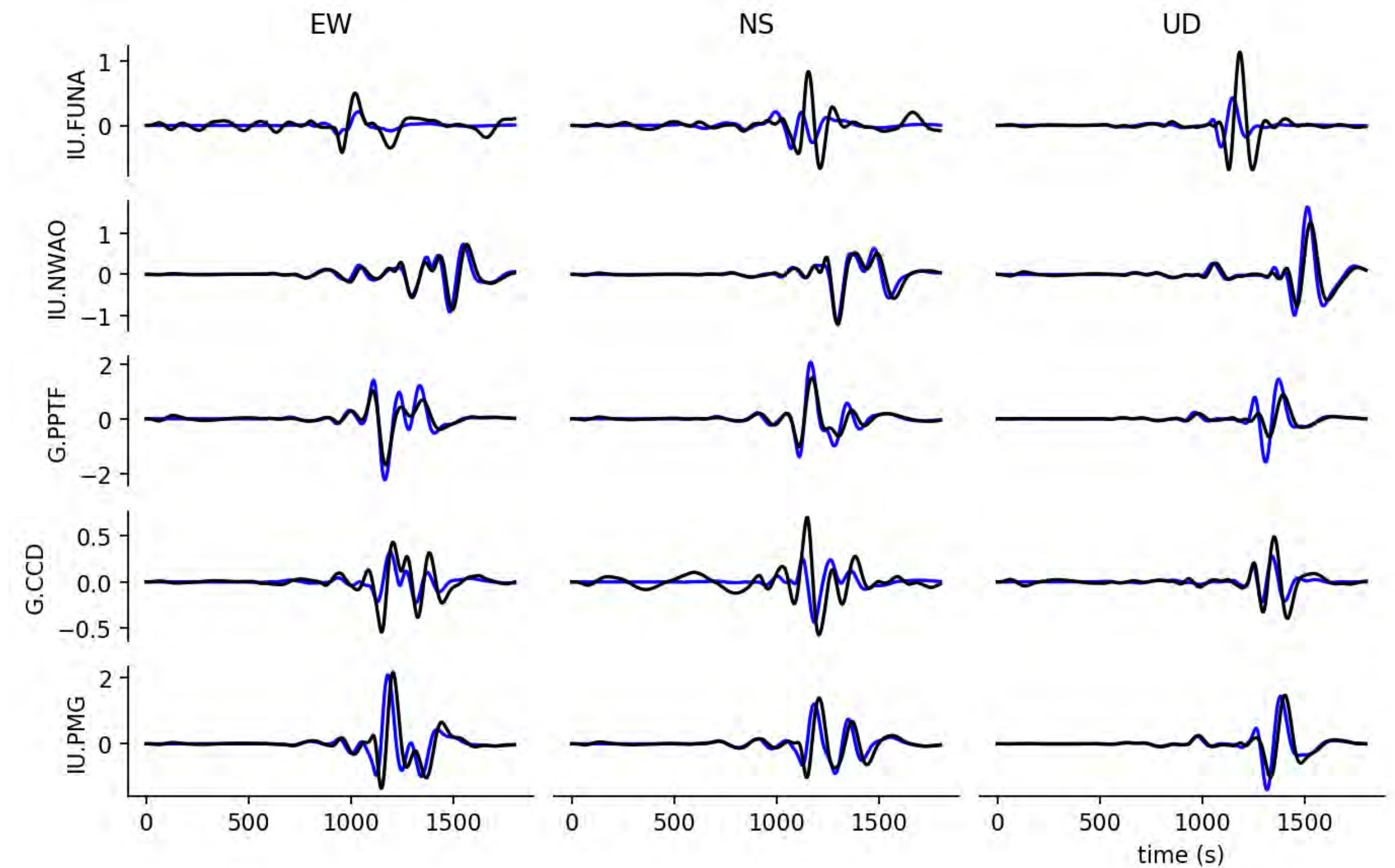
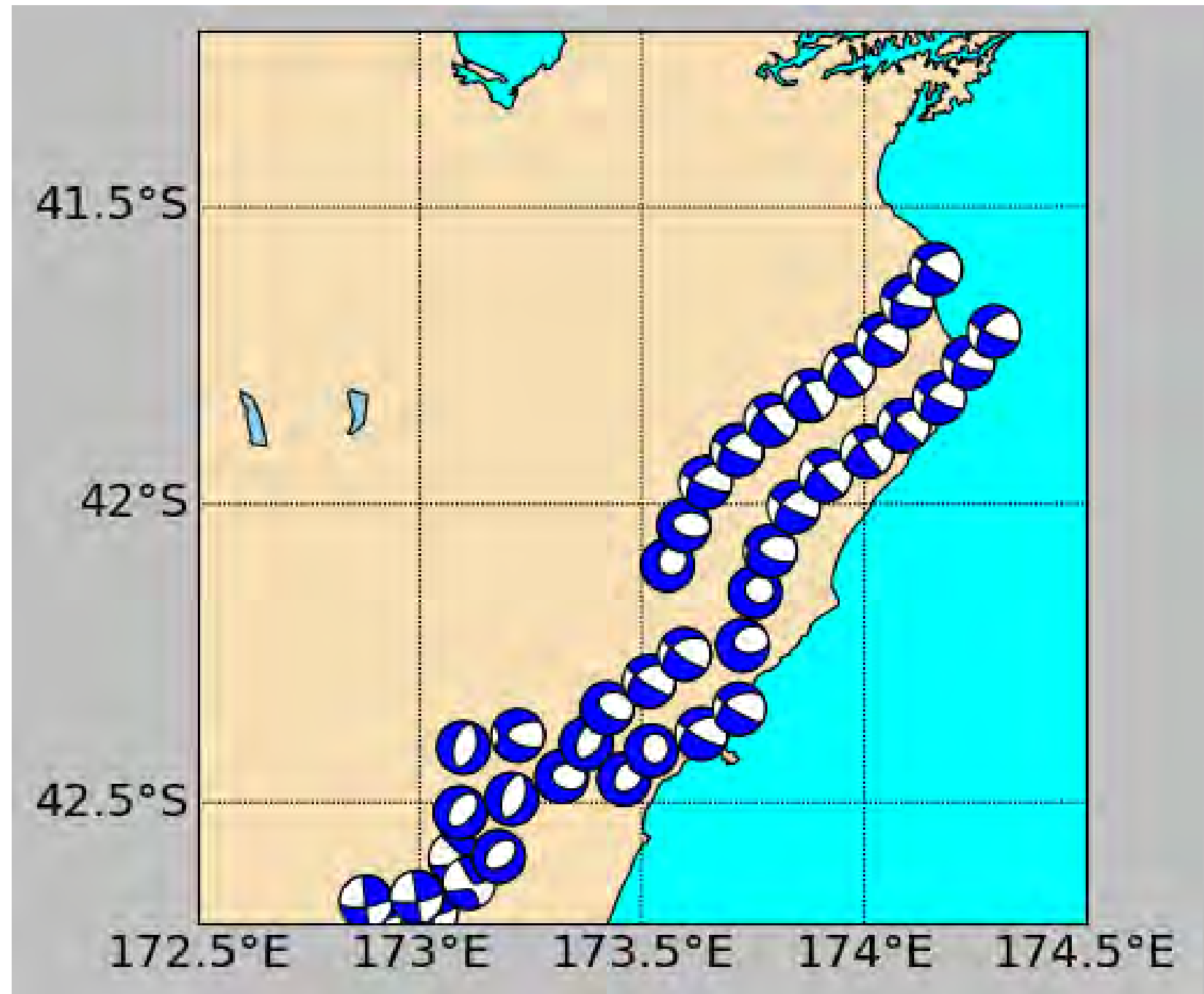
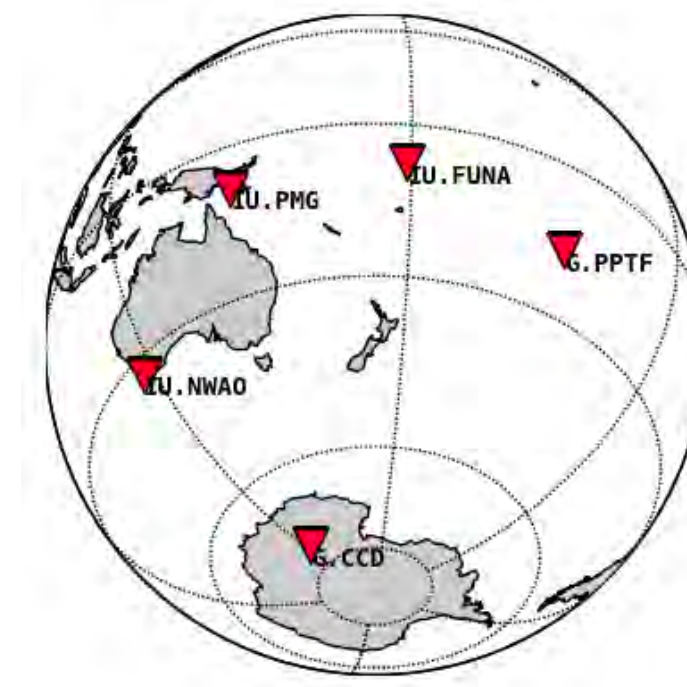
Geodetic data (Xu et al., 2018)



Comparison of observed and modeled coseismic surface displacements. 3D ground displacement (first row) inferred by space geodetic data (Xu et al. 2018), (second row) generated by the dynamic rupture model and (third row) their difference, all in meters. Columns from left to right are EW, NS and UD components. Root-mean-square (RMS) misfits are provided in the third row for each component.

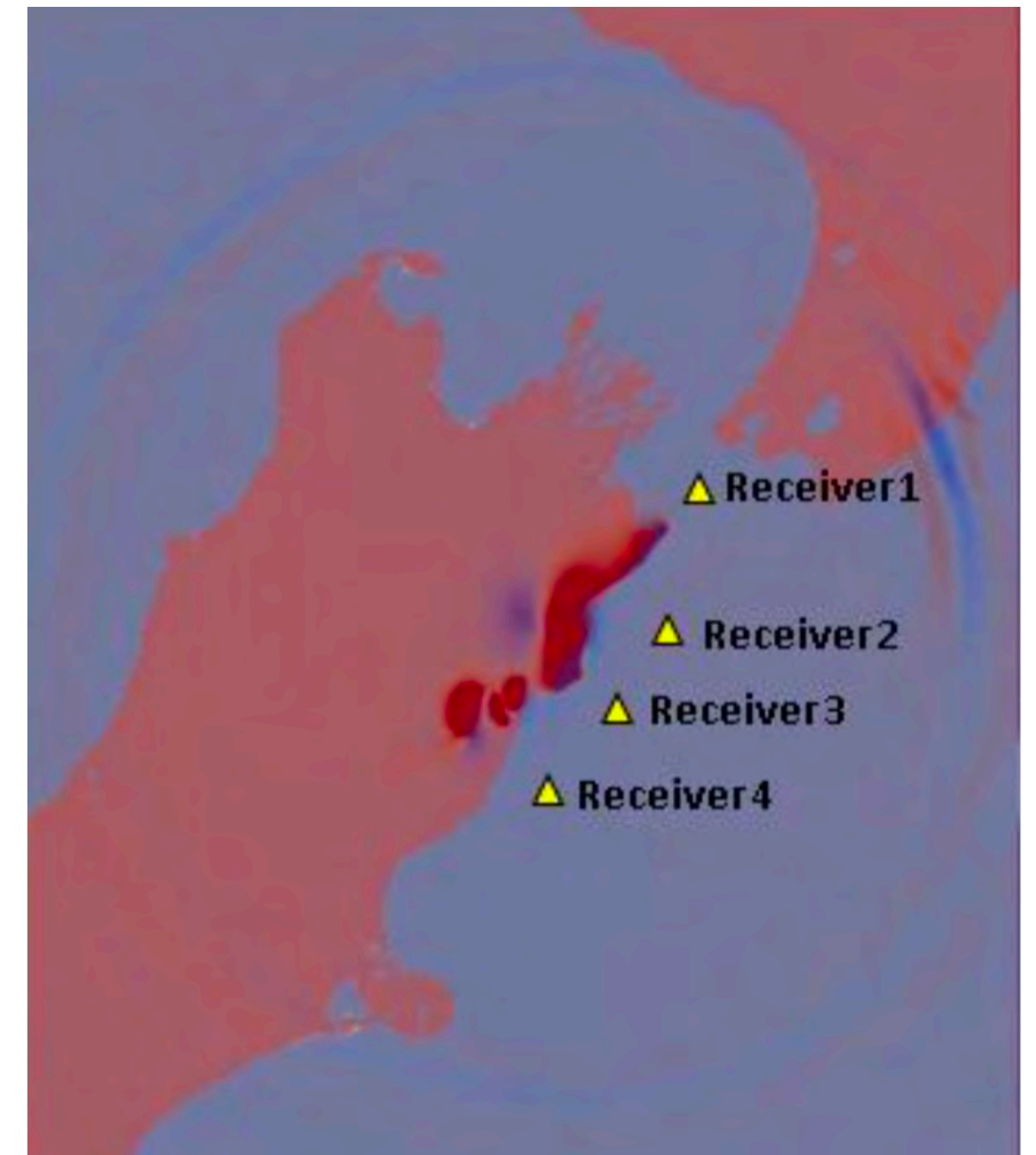
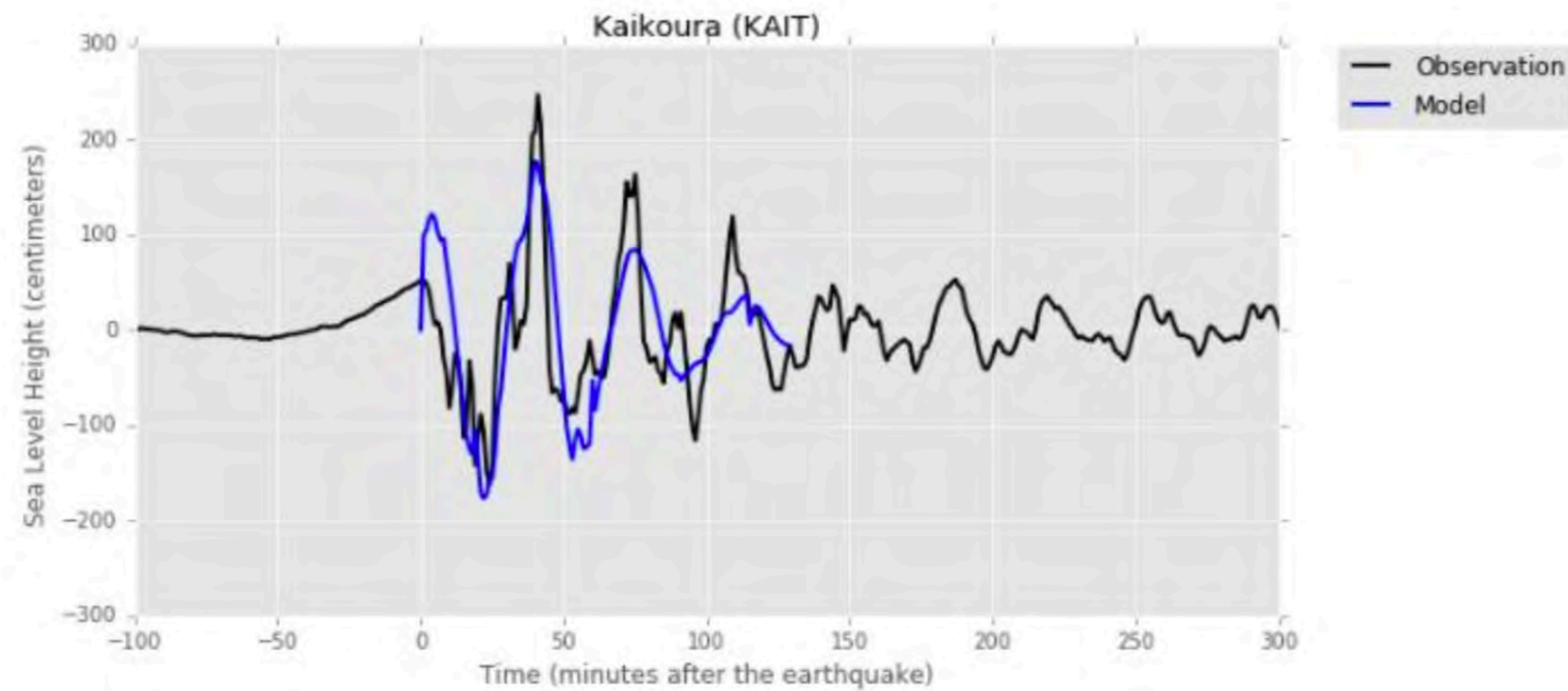
The 2016, Mw7.8 Kaikōura earthquake - constrained by observation

- **Teleseismic waveforms and tsunami data** (by off-line coupling)



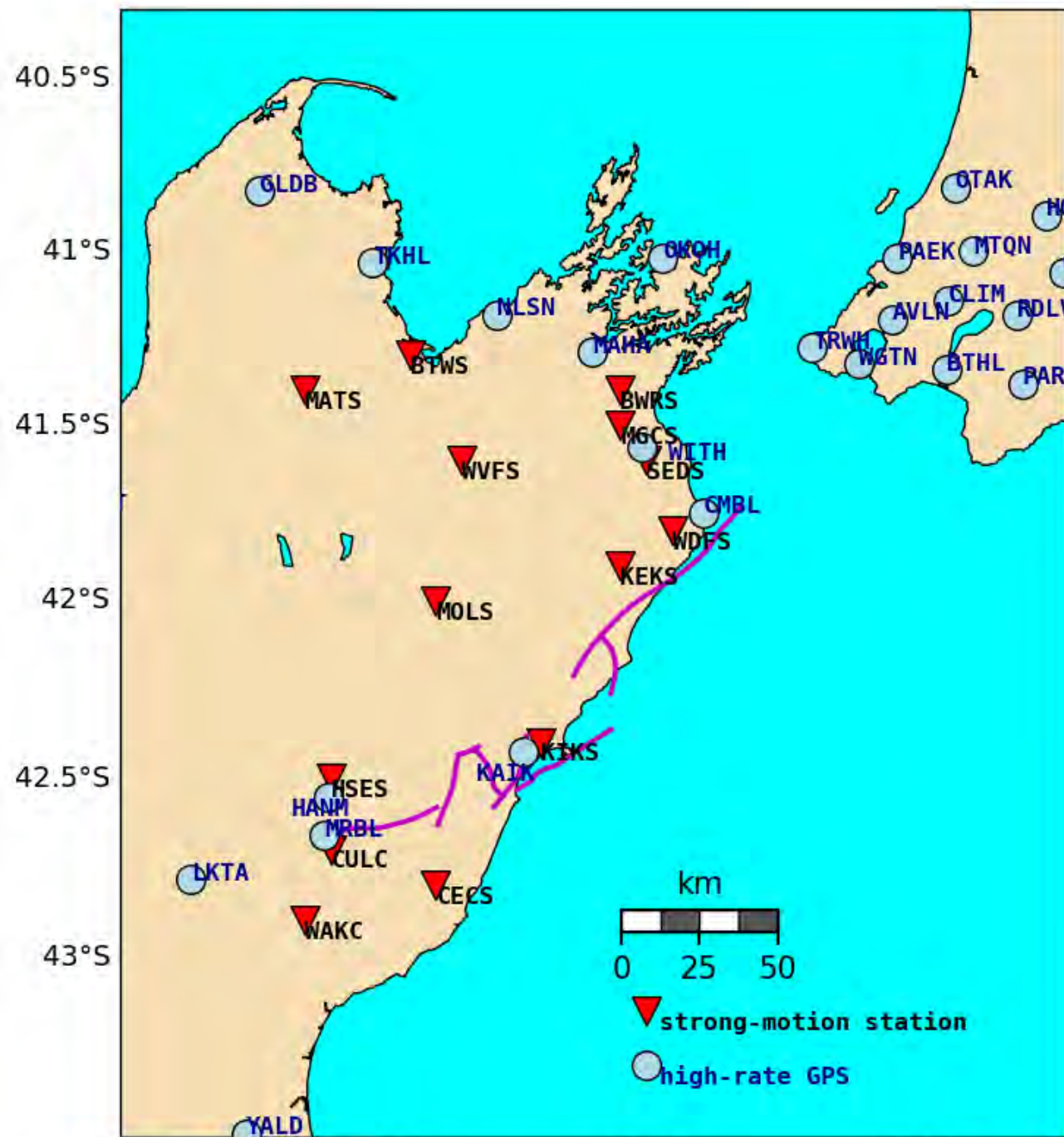
The 2016, Mw7.8 Kaikōura earthquake - constrained by observation

- **Teleseismic waveforms and tsunami data**
(by off-line coupling)

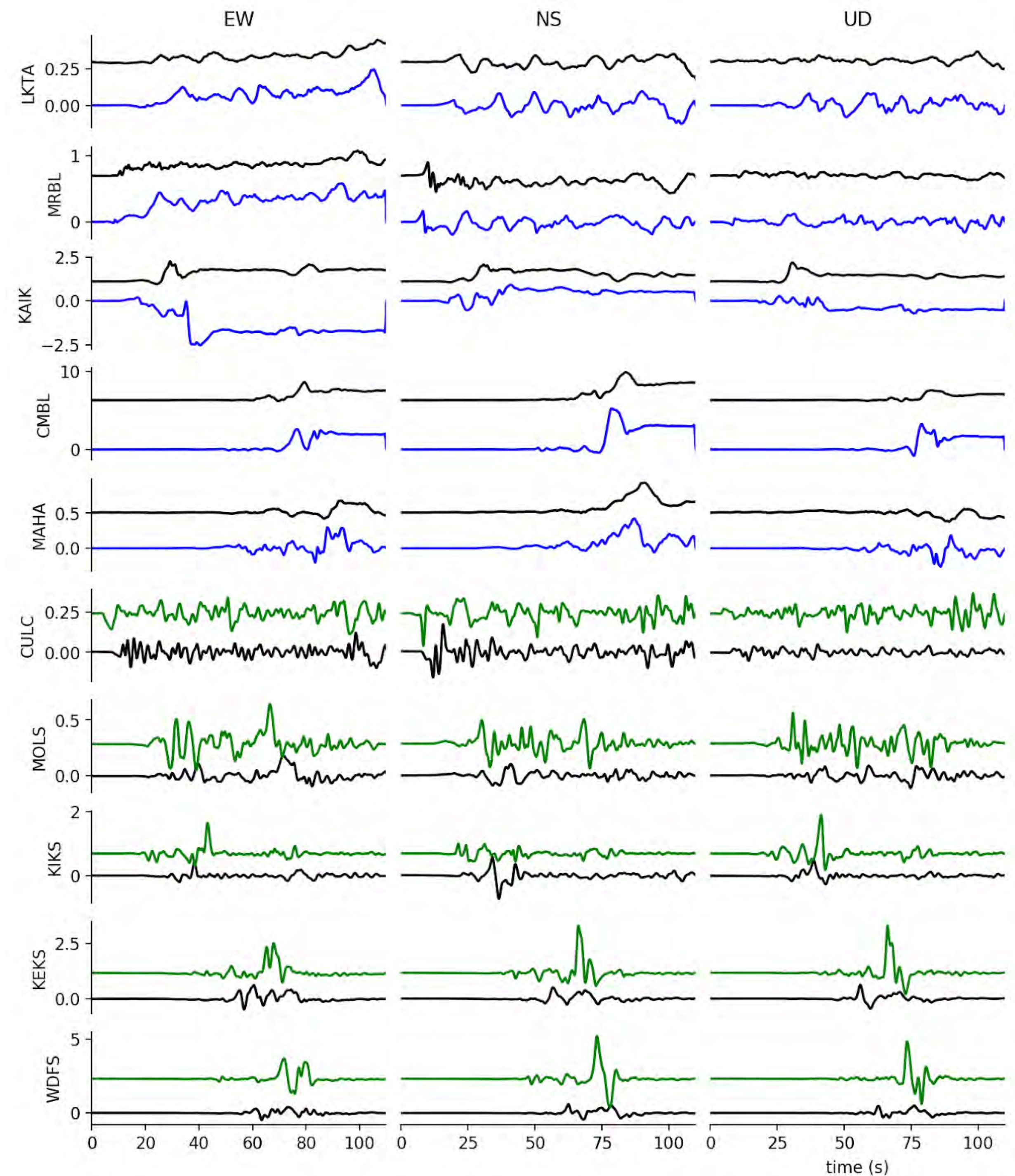


The 2016, Mw7.8 Kaikōura earthquake - (reproducing) observations

Comparison of modelled and observed ground motions. Five top rows: synthetic (blue) and observed (black) ground displacements at selected GPS stations. A 1 s low-pass filter has been applied to both signals. Five bottom rows: synthetic (green) and observed (black) ground velocities at selected strong-motion stations. A 0.005-1 s band-pass filter has been applied to both signals.



Nearest high-rate GPS and strong-motion stations (on South Island) active during the Kaikōura earthquake (left). Teleseismic stations at which synthetic data is compared with observed records (right).



Seismo-tectonic simulations: current capabilities

time-scales 

| | Dynamic simulation | Kinematic simulation | Dynamic boundary integral | Quasi-dynamic integral | Short-term tectonics, fully numerical | Long-term tectonics, fully numerical |
|-------------------------|--------------------|----------------------|---------------------------|------------------------|---------------------------------------|--------------------------------------|
| Dimension | 3D | 3D | 2D/3D | 2D/3D | 2D | 2D |
| Rupture | Spontaneous | Prescribed | Spontaneous | Spontaneous | Spontaneous | Spontaneous |
| Inertia | Yes | Yes | Yes | Radiation damping | Yes | Limited |
| Seismic cycle | Single | Single | Multiple | Multiple | Multiple | Simplified |
| Fault morphology | Complex | Complex | Planar | Fault network | Planar | Complex and emergent |
| Distributed deformation | Limited | Limited | None | Viscoelastic | Viscoplastic | Viscoplastic |
| Material heterogeneity | Fine-grain | Fine-grain | None | Simplest cases | Fine-grain | Fine-grain |
| Fault evolution | None | None | None | None | Allowed | Emergent |
| Fluid effects | Thermal Press. | None | Poroelastic | Poroelastic | Poroelastic | Poroelastic & metamorphism |
| Large strain | None | None | None | None | None | Yes |

Contribution to Modeling Earthquake Source Physics
White Paper, in prep. with Nadia Lapusta (Caltech)